UNIVERSITY OF CALGARY

Structure-function analysis of ING1

by

Michelle Scott

A THESIS
SUBMITTED TO THE FACULTY OF GRADUATE STUDIES
IN PARTIAL FULFILLMENT OF THE REQUIREMENTS FOR THE
DEGREE OF MASTER OF SCIENCE

DEPARTMENT OF BIOCHEMISTRY AND MOLECULAR BIOLOGY

CALGARY, ALBERTA
NOVEMBER, 2000

National Library of Canada
Acquisitions and Bibliographic Services
395 Wellington Street
Ottawa ON K1A 0N4
Canada

Bibliothèque nationale du Canada
Acquisitions et services bibliographiques
395, rue Wellington
Ottawa ON K1A 0N4
Canada

Your file Votre référence

Our file Notre référence

0-612-55239-X

Canada

Abstract

The ING1 candidate tumor suppressor gene encodes nuclear proteins that have been reported to be involved in apoptosis and growth control. Here, ING1 is shown to interact with PCNA shortly after cells are irradiated with low amounts of UV light and to translocate to the nucleolus several hours after cells are irradiated with high amounts of UV light. ING1 contains a nucleolar targeting sequence composed of two distinct 4 amino acid regions. ING1 proteins were also found to be tightly associated with the nuclear matrix and to play an active role in chromatin remodeling. In addition to characterizing the two major human isoforms, five mouse ING1 transcripts were also identified and cloned. Taken together, these results indicate that several ING1 isoforms exist, that they are involved in the regulation of gene expression by modifying acetylation of histones in healthy cells and that they participate in the post-UV response of cells.

Acknowledgements

My supervisor, Dr. Karl Riabowol for all his help and his guidance.

My Committee members and examiners, Dr. Phyllis LuValle, Dr. Derrick Rancourt, Dr. Steve Robbins and Dr. Manfred Lohka for their counseling and support.

Members of the lab; Rebecca Nelson, Dr. Paul Bonnefin, Phillip Berardi, Dr. Tatsuya Toyama, Dongping Ma, Dr. Ed Parr, Dr. Muthu Meyyappan, Jason Quarrie, Denise Lawless, Keith Wheaton, Donna Boland, Vanessa Olineck, Yasuo Hara, Ivan Chebib, Parneet Cheema, Harry Wu.

My parents Lise and Doug, and my sister Christianne for their love, support and encouragement.

My fiancé, Michel, for all his help and his support, love and understanding.

Mes beaux-parents, Louise et Georges Boisvert pour leur soutien.

My two cats, Bretelle and Trouser, for their unconditional love.

Anne-Julie Boivin, Tim Huang, Todd Unger, Susan Poelman, Peter Lewkonia, Knut Woltgen, Duncan Browman and all my other friends, for their support, encouragement and good ideas.

The Alberta Heritage Foundation for Medical Research and the National Science and Engineering Research Council of Canada for supporting me throughout my graduate studies.

Dedication

To Michel, for all his help, his understanding and his love.

Table of contents

Table of figures

List of abbreviations

APS	ammonium persulfate
ARF	Alternate reading frame
ATP	adenosine 5'-triphosphate
BRCA	breast carcinoma antigen
BrdU	bromo-deoxy-uridine
CBP	CREB binding protein
CCD	cooled coupled detector
cDNA	complimentary DNA
DAPI	4'-6-diamidino-2-phenylindole
DEPC	diethyl pyrocarbonate
DIC	differential interference contrast
DIG	digoxygenin
DNA	deoxyribonucleic acid
DNase	deoxyribonucleic acid nuclease
dNTP	2'-deoxynucleotide 5'-triphosphate
DRB	5,6-dichloro-β-D-ribofuranosylbenzimidazole
DTT	dithiothreitol
EDTA	ethylynediamine-tetraacetic acid
FBS	fetal bovine serum
Fen-1	Flap endonuclease-1
5-FU	5-fluorouridine
g	gram
HAT	histone acetyltransferase
HDAC	histone deacetylase
ING1	inhibitor of growth 1
JMEM	Joklik's minimal essential medium

kb	kilobase pair
kDa	kilodalton
LB	Luria-Bertani bacterial medium
L-DMEM	low Dulbecco's modified Eagle's medium
M	molar
mg	milligram
mL	milliliter
mM	millimolar
MOPS	morpholinopropane-sulfonic acid
mRNA	messenger RNA
NaCl	sodium chloride
ng	nanogram
NLS	nuclear localization signal
NTS	nucleolar targeting sequence
O.D.	optical density
PBS	phosphate buffered saline
PCNA	proliferating cell nuclear antigen
PCR	polymerase chain reaction
PIP	PCNA interacting protein
RACE-PCR	rapid amplification of cDNA ends
Rb	Retinoblastoma tumor suppressor protein
rDNA	ribosomal DNA
RNA pol	RNA polymerase
RNA	ribonucleic acid
RNase	ribonucleic acid nuclease
rpm	revolutions per minute
rRNA	ribosomal RNA
SDS	sodium dodecyl sulphate
SDS-PAGE	SDS polyacrylamide gel electrophoresis

SSC	standard saline citrate
SV40	simian virus 40
TAE	Tris-acetate EDTA buffer
TEMED	N,N,N',N'-tetramethylethyldiamine
Tris	Tris (hydroxymethyl)aminomethane
UV	ultraviolet
XPG	*Xeroderma pigmentosum* type G
µg	microgram
µL	microliter
µM	micromolar
°C	degree Celsius

CHAPTER 1:
INTRODUCTION

Discovery of the inhibitor of growth ING1

ING1b was initially identified by Karl Riabowol's group in 1995 as a growth inhibitor and candidate tumor suppressor that had minimal homology to known proteins (33, 34). It was isolated by performing a subtractive hybridization of adaptor ligated cDNAs from phenotypically normal epithelial cells which were used as testers and 4 different sets of adaptor ligated breast cancer cell cDNAs which were used in excess as drivers. These four different rounds of subtractive hybridation were performed to highly enrich for transcripts only expressed in normal cells and not in cancer cells. The resulting products were used as probes to screen a cDNA library of senescent Hs68 normal diploid fibroblasts (MPD82) to identify candidate transcripts that are overexpressed during senescence. 200 clones were selected, digested with ClaI, ligated into the retrovirus pLNCX, and packaged in Bosc23 which was then used to infect normal mouse mammary epithelial cells. These infected cells were then injected into mice and caused tumor formation (the construct was shown to be inserted in the antisense orientation). These assays had thus identified a transcript downregulated in cancer cells, overexpressed in senescent cells and able to promote tumor formation when inserted in the antisense orientation.

Several subsequent experiments demonstrated that ING1b was an inhibitor of growth that behaves in some aspects like the p53 and Rb (Retinoblastoma) tumor suppressors. Overexpression of ING1b inhibited cell growth by blocking normal diploid cells in the Go/G1 phase of the cell cycle (33). This inhibition of cell growth by ING1b is suppressed in the presence of SV40 large T antigen, similar to the inactivation of the tumor suppressors p53 and Rb by large T antigen (67). Inhibition of ING1 expression by antisense RNA also increased the occurrence of focus-formation in NIH 3T3 and promoted anchorage-independent growth of NMuMG cells in soft agar (33). Furthermore, suppression of ING1b also appeared to extend the proliferative life span of some normal diploid cells (34), approximately to the same extent as inactivation of p53 by its mutant form (13).

Structure of the ING1 gene

The ING1 gene is found on the long arm of chromosome 13 at 13q33-34 (31). Loss of heterozygosity has been observed at sites close to this region on chromosome 13q in head and neck squamous cell carcinomas (74) as well as gastric adenocarcinomas (81) and breast cancers (24, 59). The ING1 gene is believed to contain several large introns although the genomic sequence is presently incomplete. Western blots using polyclonal antibodies raised against the conserved region of the ING1 proteins show many different bands of various sizes in different tissues. This is particularly well illustrated in epithelial cells, testis and brain.

Presently, the sequences of three different human ING1 isoforms have been well characterized: ING1a, which has a predicted mass of 47 kDa (73, 94), ING1b, which has a predicted mass of 33 kDa (which has been used for most functional experiments to date)(33) and ING1c, which has a predicted mass of 24 kDa (73, 94). Both ING1a and ING1b possess a 742 bp (approximately 27kDa) identical 3' region encoded by a shared 3' exon (referred to as the common region, shown in bold in figure 1, page 14) which is believed to be common to all the isoforms of the ING1 gene (Fig.1). ING1c results from an internal initiation in this exon and thus is lacking approximately 3 kDa from the 5' region of this exon (Fig.1). It is not presently known which human transcripts generate this 24 kDa protein or whether it is encoded by its own separate transcript (both the ING1a and the ING1b transcripts could potentially generate the smaller protein by internal initiation although preliminary data suggests that only the ING1a transcript does). One report also suggests the existence of two other different human isoforms of the ING1 gene: a 27 kDa protein (called here ING1e) and a 34 kDa protein (referred to here as ING1d) (51) (also illustrated in Fig.1). It is very probable that other isoforms also exist, especially larger ones, considering all the different bands seen on western blots by using both polyclonal and monoclonal antibodies against the common region of the ING1 proteins.

ING1 is also well conserved throughout evolution. Mice, rats, *Xenopus*, *Drosophila* as well as *Saccharomyces cerevisiae* and *Saccharomyces pombe* all have proteins that possess regions of high homology to the conserved region of the human ING1 proteins. Three distinct ING1 transcripts have been reported to exist in mice (122). However, two of these transcripts generate the same protein, which is the mouse orthologue of human ING1c. The other protein identified in mouse is the orthologue of human ING1b. Interestingly, these proteins have been reported to interact with and regulate murine p53 differently. Mouse ING1b was reported to interact with p53 and inhibit its transcription transactivation function, in contrast to human ING1b, which has been reported by the same group to be necessary for p53 function (32). Mouse ING1c, on the other hand, was suggested to enhance the p53-dependent transcriptional activation but does not directly interact with p53 (122). More studies are clearly necessary to address this question.

It is also interesting to note that very recently, several other human ING1 family members have been identified. These proteins bear regions of high homology to parts of the ING1 gene and thus could potentially compete with ING1 proteins for the same binding partners. One of these proteins, ING1L (ING1 like), localizes to chromosome 4q35 and has been found to be overexpressed in several colon cancers compared to normal colon tissue from the same patient (99). Another family member, ING2, was reported to be expressed in all normal tissues tested but was not expressed in one out of 8 melanoma and two out of 6 breast cancer cell lines tested (51). This protein, however, is very small and has recently been taken out of the GenBank database. Very recently, a third ING1 family member (referred to as ING1 homologue gene) has been reported in GenBank. Nothing has been published on this protein. All three proteins might be recognized by the antibodies raised against the common region of the ING1 proteins. Figure 2 (page 16) compares some of the ING1 family members.

Consensus and targeting sequences of the ING1 isoforms

Very few protein motifs and consensus targeting sequences have been identified in the ING1 isoforms. The conserved region of the ING1 gene possesses a nuclear localization signal (NLS) and all known human isoforms of the ING1 gene examined to date localize to the nucleus. This subcellular localization of the isoforms has been shown by immunofluorescence with ING1 specific antibodies. However, since no isoform specific antibodies exist yet, it is not possible to differentiate between the different isoforms.

The common region also possesses a plant homeo domain (PHD), which is found in transcription factors and in proteins involved in chromatin-mediated transcriptional control (2). PHD motifs are a specific type of zinc finger domain (Cys_4-His-Cys_3) that have been suggested to be implicated in the regulation of chromatin structure (2). The NLS and the PHD motif of the ING1 proteins are shown in figure 3 (page 18).

Decreased expression of ING1 in many cancers

A deregulation of the expression of the ING1 gene seems to be involved in some tumorigenic processes. Though mutations in the ING1 gene do not seem frequent in the primary tumors examined, the expression of ING1 is significantly decreased in many breast cancer cell lines and primary tumors (33, 109). Additionally, it has recently been shown that the decreased expression of ING1 in breast cancer highly correlates with metastasis (109). Another study has reported that in 73% of breast cancers that tested negative for p53 by immunostaining, ING1 expression was very low, on average showing only 20% of the level seen in normal tissue and as low as approximately 5% of the level seen in normal tissue (108). ING1 expression is also decreased in other tumor types including human gastric cancer and lymphoid malignancies (83, 84). Thus, altered expression of the ING1 gene, rather than mutation of key residues, seems to be involved in tumorigenic processes, defining it as a class II cancer gene (93).

Functional roles of ING1 in the cell:

-During apoptosis

ING1b has been strongly implicated as a regulator of apoptosis. Levels of ING1 were seen to increase in the teratocarcinoma cell line P19 when these cells were induced to enter apoptosis by serum starvation (48). Furthermore, it was seen that ING1 is involved in the regulation of apoptosis caused by overexpression of c-myc (48). To demonstrate this, rat fibroblast cells containing a tetracycline inducible c-myc gene were microinjected with GST-ING1b protein in the presence of tetracycline. Uninjected cells overexpressing the c-myc protein showed a low percentage of survival compared with cells not expressing c-myc. However, microinjected cells that were also overexpressing c-myc showed an even more dramatic decrease in cell survival. This suggested that ING1b might act in the c-myc apoptotic pathway and that perhaps suppression of ING1 could allow cellular transformation by deregulating this apoptotic pathway.

Additionally, it has recently been reported that p53 and ING1b are both required for the promotion of growth suppression in one assay system: colony formation was shown to be inhibited by ING1b only in cells expressing wild-type p53 (32). Similarly, the same group has reported that inhibition of growth by p53 requires the presence of ING1. They also reported that ING1b and p53 physically interact and that transcriptional activation of the p21 promoter by p53 requires the presence of ING1b. This suggests that p53 and ING1b cooperate to inhibit cell growth and are part of the same, or a closely related, signaling pathway.

ING1b and p53 were also reported to cooperate in causing an increase of apoptosis in glioma cells (100), though it was not shown whether physical interaction of the proteins was required to do so. This apoptotic pathway was shown to cause mitochondrial damage but does not up-regulate the expression of Bax and Fas.

Because of its functions as a growth inhibitor and apoptosis regulator and its altered expression pattern in many cancer cell lines and tissues, ING1 fulfills many of the criteria of a tumor suppressor.

-Cell cycle control

When ING1 was first discovered, its expression was shown to be cell cycle controlled and to reach maximal levels in S phase (34). Overexpression of ING1 was also demonstrated to cause a Go/G1 arrest in the cell cycle, consistent with a role in regulating cell growth (33). The expression pattern of ING1 closely follows that of PCNA (proliferating cell nuclear antigen), which was initially identified as a protein called cyclin whose expression peaked during S-phase (58). Both ING1 and PCNA are involved in cell cycle control but also play roles in cells that have been stressed by different DNA damaging agents. It has been therefore hypothesized that ING1 and PCNA might be involved in some common cellular pathways.

PCNA has been shown to be essential for DNA replication (58) but is also involved in DNA repair, recombination and possibly in chromatin assembly and RNA transcription (55, 110). It functions as a homotrimeric ring around DNA and has been shown to interact with many different proteins including both enzymes involved in nucleic acid metabolism and regulatory proteins (55, 58). PCNA binds many different proteins by interacting with their PIP motif (PCNA interacting protein motif). These proteins include cell cycle regulatory proteins such as p21 (116), proteins involved in DNA replication including Fen-1 (115) and DNA ligase I (66) as well as DNA repair proteins including XPG (36, 91). PCNA is required for nucleotide excision repair and base excision repair in mammalian cells (115) and the different PCNA interacting proteins are suggested to compete for binding to PCNA. This competition has been suggested to regulate the switch between PCNA-dependent DNA replication/RNA transcription and DNA repair (114).

-Chromatin remodeling

Several lines of evidence indicate that the different isoforms of the ING1 gene interact with proteins involved in chromatin remodeling. ING1 is thought to bind TRRAP, which is a new member of the PI3-kinase/ATM-related family of proteins. TRRAP (transformation/transcription domain-associated protein) has been shown to be essential for oncogenic transformation in the c-myc and the E2F pathways in mammalian cells (78). The cellular function of TRRAP in mammalian cells is not known but this protein has been seen in the PCAF histone acetyl transferase complex (112) and has recently been shown to recruit hGCN5, another histone acetyltransferase, to c-myc complexes (79).

TRRAP is well conserved throughout evolution and Tra1, a *Saccharomyces cerevisiae* homolog of TRRAP has also been shown to be part of HAT complexes (40). Three *Saccharomyces cerevisiae* homologs of the ING1 proteins have been identified, one (Yng2) of which interacts with Tra1 (69). Further experiments have demonstrated that Yng2 is associated with HAT activity in yeast and that it binds the yeast HAT Esa1, a gene required for cell cycle progression (20). Thus Yng2 is part of the yeast NuA4 complex, an essential transcription adaptor/histone H4 acetyltransferase complex (3).

More recently, it has been shown that ING1 antibodies can immunoprecipitate histone acetyltransferase (HAT) activity in mammalian cells indicating that ING1 proteins interact with at least one functional HAT. Histone acetylation is a reversible process that is considered important in the regulation of gene transcription. It has been shown that transcription of tightly compacted nucleosomal DNA is severely inhibited because of limited access of the transcription machinery to the template (86). To allow transcription to proceed, histone acetyltransferases add acetyl groups to specific lysines on specific histones. This neutralizes the positive charge of the lysines and thus increases the

hydrophobicity of the complex, creating a less compact structure of chromatin, which is more accessible to transcription factors and to the transcription machinery (43, 63). Histones are deacetylated by HDACs (histone deacetylases) and this causes a compaction of DNA and generally a repression of transcription. The most well characterized HDACs are HDACs 1, 2 and 3 (28, 106). Some transcriptional repressors are thought to recruit HDACs to specific promotors to inhibit gene expression (88).

Several transcriptional regulators possessing intrinsic HAT activity have been identified. These include the Gcn5p family, PCAF, the p300/CBP family and the $TAF_{II}250$ family, which all have different specificities and different suggested functions in the cell (reviewed in (63)). It is interesting to note that some of the HATs have been shown to acetylate non-histone proteins and acetylation has been proposed to be a post-translational modification regulating protein function to the same extent as phosphorylation (61). ING1 proteins can be shown to interact with CBP (CREB binding protein) but not hGCN5, indicating a possible role for ING1 in the regulation of chromatin remodeling through this complex.

Interestingly, several known tumor suppressors have been associated with chromatin remodeling proteins. The retinoblastoma tumor suppressor protein (Rb) physically interacts with HDAC1 and HDAC2 and is thought to recruit these histone deacetylases to E2F1 when it is bound on S-phase promoters (14), which are promoters from which transcription is activated specifically during S-phase. This would be one mechanism regulating how Rb inhibits cell-cycle progression through E2F. Rb interacts with these HDACs through its pocket domain and this interaction is inhibited by viral oncoproteins that also bind this region of Rb (15). The HDACs and the viral oncoproteins are thought to bind Rb by using the same LXCXE motif (75). p53 has been demonstrated to interact with p300 (44) and CBP/p300 is thought to act as a coactivator for p53 and to enhance its transcriptional activity

(45). BRCA1 also interacts with CBP and BRCA2 itself has intrinsic HAT activity (101).

-The nuclear matrix

Because the ING1 proteins appear to be very insoluble when overexpressed in bacteria and possibly in mammalian cells, it has been proposed that they can be tightly associated with the nuclear matrix. The nuclear matrix was first discovered during the 1970s when Berezney and Coffey established that it is possible to treat nuclei with DNase I and 2M NaCl to isolate an insoluble component of the nucleus which was later called the nuclear matrix (7). The isolation procedure was subsequently improved and many different groups have focused on the structural aspects of the nuclear matrix and its associated functions. It is composed of the lamina-pore complexes and of an intranuclear fibrogranular structure (47). It has been shown to harbor many diverse processes (reviewed in (9, 90, 105)) including DNA replication (8), gene localization (121), post-translational modification of chromosomal proteins and higher order chromatin structure (22), targeting of many transcription factors and control of gene expression (27, 111), pre-mRNA splicing activity and RNA processing (75, 113) and transport of transcripts (16, 65).

Matrix-attachment regions (MARs), which allow binding of specific sequences of DNA to the nuclear matrix have been found throughout the genome (21, 35). These MARs are postulated to organize the chromosomes in the nucleus. Because these regions of DNA are attached to the nuclear matrix, it has been suggested that they are not protected by as many layers of organization as other regions of DNA and thus they are more exposed and more susceptible to DNA-damaging agents such as UV or ionizing radiation (5, 18, 85). This could be one explanation why some regions of DNA are more prone to mutations than others. The nuclear matrix is also considered a major site for nucleotide excision

repair after UV irradiation (60). The damaged DNA is thought to be brought to the nuclear matrix, which contains many repair enzymes, including XPG endonuclease (87). However, the DNA regions bound to the matrix might be more susceptible to damage and thus might need more repairing, which could explain why the enzymes localize to these regions. Furthermore, the nuclear matrix has been shown to be altered in cells undergoing apoptosis (76, 77) and in transformed cells (105).

Research hypothesis

Work described in this research thesis was designed to test the following hypothesis: first, because ING proteins have been implicated in some forms of apoptosis, it was suspected that they would behave differently, localize to different compartments and play a different role in cells in response to DNA damaging agents such as UV irradiation when compared to untreated cells. Second, with the ING1 proteins believed to be relatively insoluble, we hypothesized that they might bind the nuclear matrix and associate with its major components during different phases of the cell cycle. Third, because preliminary evidence suggested that yeast and mammalian ING1 were thought to interact with proteins involved in chromatin remodeling, it was proposed that when ING1 protein levels change in the cell, the patterns of histone acetylation would also be modified. Finally, we also suspected that many unidentified ING1 isoforms exist the cell because of all the bands present on western blots probed with antibodies that recognize the conserved region of the ING1 gene.

The ING1 proteins appear to be involved in the regulation of several different cellular processes including cell growth, chromatin remodeling and gene transcription, DNA repair and apoptosis and might serve as links between a few of these cellular functions. Only very recently have the ING1 proteins been

discovered to be involved in most of these pathways. This thesis presents some of the first evidence of ING1's role in chromatin remodeling as well as post-UV responses of cells including DNA repair.

Figure 1: The different known isoforms of the human ING1 gene

Five different isoforms of the human ING1 gene have been reported to date and are compared here. All five proteins contain a common 3' exon (233 amino acids) which is indicated in bold. ING1c is initiated at an internal ATG in this common exon and thus only possesses 210 amino acids of this exon. The four other isoforms each contain a 5' unique region although some of this region is common between isoforms ING1a and ING1d (shown in italic).

Figure 1: The different known isoforms of the human ING1 gene

ING1a	MSFVECPYHSPAERLVAEADEGGPSAITGMGLCFRCLLFSFSGRS	45
ING1a	GVEGGRVDLNVFGSLGLQPWIGSSRCWGGPCSSALRCGWFSSP	88
ING1a	PPSKSAIPIGGGSRGAGRVSRWPPPHWLEAWRVSPRPLSPLSPAT	133
ING1d	MPLCTA	6
ING1a	FGRGFIAVAVIPGLW*ARGRGCSSDRLPRPAGPARRQFQAASLLTR*	178
ING1d	TRIPRYSSSSDPGPV*ARGRGCSSDRLPRPAGPARRQFQAASLLTR*	51
ING1b	MLSPANGEQLHLVNYVEDYLDSIESPFDLQRNV	33
ING1a	*GWGRAWPWKQ***ILKELDECYERFSRETDGAQKRRMLHCVQRALIR**	222
ING1d	*GWGRAWPWKQ***ILKELDECYERFSRETDGAQKRRMLHCVQRALIR**	95
ING1b	SLMREIDAKYQE**ILKELDECYERFSRETDGAQKRRMLHCVQRALIR**	77
ING1e	ME**ILKELDECYERFSRETDGAQKRRMLHCVQRALIR**	36
ING1c	**MLHCVQRALIR**	11
ING1a	**SQELGDEKIQIVSQMVELVENRTRQVDSHVELFEAQQELGDTAGN**	267
ING1d	**SQELGDEKIQIVSQMVELVENRTRQVDSHVELFEAQQELGDTAGN**	140
ING1b	**SQELGDEKIQIVSQMVELVENRTRQVDSHVELFEAQQELGDTAGN**	122
ING1e	**SQELGDEKIQIVSQMVELVENRTRQVDSHVELFEAQQELGDTAGN**	81
ING1c	**SQELGDEKIQIVSQMVELVENRTRQVDSHVELFEAQQELGDTAGN**	56
ING1a	**SGKAGADRPKGEAAAQADKPNSKRSRRQRNNENRENASSNHDH**	310
ING1d	**SGKAGADRPKGEAAAQADKPNSKRSRRQRNNENRENASSNHDH**	183
ING1b	**SGKAGADRPKGEAAAQADKPNSKRSRRQRNNENRENASSNHDH**	165
ING1e	**SGKAGADRPKGEAAAQADKPNSKRSRRQRNNENRENASSNHDH**	124
ING1c	**SGKAGADRPKGEAAAQADKPNSKRSRRQRNNENRENASSNHDH**	99
ING1a	**DDGASGTPKEKKAKTSKKKKRSKAKAEREASPADLPIDPNEPTYC**	355
ING1d	**DDGASGTPKEKKAKTSKKKKRSKAKAEREASPADLPIDPNEPTYC**	228
ING1b	**DDGASGTPKEKKAKTSKKKKRSKAKAEREASPADLPIDPNEPTYC**	210
ING1e	**DDGASGTPKEKKAKTSKKKKRSKAKAEREASPADLPIDPNEPTYC**	169
ING1c	**DDGASGTPKEKKAKTSKKKKRSKAKAEREASPADLPIDPNEPTYC**	144
ING1a	**LCNQVSYGEMIGCDNDECPIEWFHFSCVGLNHKPKGKWYCPKCR**	399
ING1d	**LCNQVSYGEMIGCDNDECPIEWFHFSCVGLNHKPKGKWYCPKCR**	272
ING1b	**LCNQVSYGEMIGCDNDECPIEWFHFSCVGLNHKPKGKWYCPKCR**	254
ING1e	**LCNQVSYGEMIGCDNDECPIEWFHFSCVGLNHKPKGKWYCPKCR**	213
ING1c	**LCNQVSYGEMIGCDNDECPIEWFHFSCVGLNHKPKGKWYCPKCR**	188
ING1a	**GENEKTMDKALEKSKKERAYNR**	421
ING1d	**GENEKTMDKALEKSKKERAYNR**	294
ING1b	**GENEKTMDKALEKSKKERAYNR**	276
ING1e	**GENEKTMDKALEKSKKERAYNR**	235
ING1c	**GENEKTMDKALEKSKKERAYNR**	210

Figure 2: The ING1 family members

Three of the ING1 family members encoded by different genes are compared here. b represents the ING1b isoform of the ING1 gene, L stands for the ING1L protein (for ING1 like) and H is the protein encoded by the ING1 Homologous gene. All three proteins have approximately the same size and share many residues (bold). The PHD domain (italic) is particularly well conserved. The accession numbers of the proteins are ING1b: BAA82889, ING1L: NM001564, ING1 homologous gene: NM016162.

Figure 2: The ING1 family members

b	MLSPANGEQLHLVN- YVEDYLDS I ESLPFD	29
L	MLGQQQQQLYSSAALLTGERSRLLTCYVQDYLECVESLPHD	41
H	MAAGMYLEH YLDSI ENLPFE	20
b	L QRNVSLMREI D AKYQE ILK - ELDECYERFSRETDGAQKR	68
L	MQRNVSVL RELD NKYQETLK - EIDDVYEKYKK EDDLNQKK	80
H	L QRNFQLMRDLDQRT - EDLKAEIDKL ATEYMSSARS LSS E	59
b	RMLHCV- Q- -RAL I RSQELGDEKI Q I VSQMVELVENRT RQ	105
L	RLQQLL - Q- -RAL I NSQELGDEKI Q I VTQMLEL VENRARQ	117
H	EK LALLKQIQEAYGKCK EFGDDKVQLAMQTYEMVDKH I RR	99
b	VDSHVEL FEA -QQELGDTAGNSGKAGADRPKGEAAAQADK	144
L	MELHSQCFQ -DPAE- S ERASDKAKMDSSQP- - - - - - - - - - E	146
H	LDT DLAR FEADLKEKQ IES SDYDSSS SKGKKK- - - - - - - -	131
b	PNSKRSRRQRNNENRENASSNHDHDDGASGTPKEKKAKTS	184
L	RSSRRPRRQRTSES RDLCHMANGI EDCDDQPPKEKKSKSA	186
H	- GRTQKEKKAARA	143
b	KKKKR- SKAKAEREA- -	198
L	KKKKR- SKAKQEREA- -	200
H	RSKGKNSDEEAPKTAQKKLKLVRTSPEYGMPSVTFGSVHPS	184
b	SPADLP I DPNEP*TYCLCNQVSYGEMIGCDNDECPIEWFHFS*	239
L	SPVEFA I DPNEP*TYCLCNQVSYGEMIGCDNEQCPIEWFHFS*	241
H	DVLDMPVDPNEP*TYCLCHQVSYGEMIGCDNPDCSIEWFHFA*	225
b	*CVGLNHKPKGKW- CPKCRG*ENEKTMDKAL EKSKKERAYNR	279
L	*CVSLT YKPKGKWYCPKCRG*DNEKTMDKSTEKTKKDRRSR	280
H	*CVGLTT KPRGKWFCPRCS*QERKKK	249

Figure 3: The functional motifs of three ING1 isoforms

The structure and as well as the functional motifs of some of the ING1 isoforms are compared here. All known ING1 isoforms possess a common 3' region (though it is slightly truncated in the ING1c isoform) which contains the PHD motif and the nuclear-nucleolar localization sequences (N). Therefore, it can be presumed that all the ING1 isoforms localize to the nucleus and possess the PHD motif. The ING1a and ING1b isoforms contain their own unique 5' region.

Figure 3: The functional motifs of three ING1 isoforms

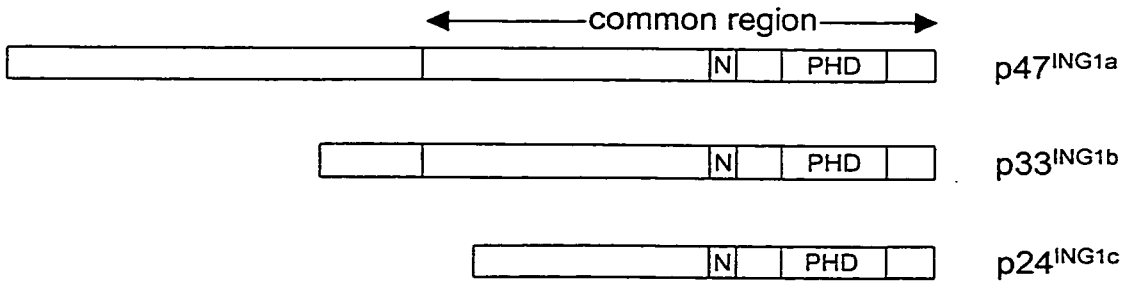

CHAPTER 2:
MATERIALS AND METHODS

Cell Culture Procedures

Cell Lines

Two different cell types have been used. The Hs68 (ATCC, CRL-1635) primary diploid fibroblast strain is a human skin fibroblast culture from the foreskin of a newborn. SK-N-SH (ATCC, HTB-11) is an established aneuploid human neuroblastoma line of the brain and the metastatic site where it was collected is the bone marrow.

Culture Media

Cells were grown in either Dulbecco's modification of Eagle's minimal essential medium (DMEM), for Hs68 cells, or Joklik's modification of Eagle's minimal essential medium (JMEM), for SK-N-SH cells (Gibco BRL). The medium was supplemented with 10% fetal bovine serum (FBS, Gibco BRL), as well as penicillin G (75 units/mL) and streptomycin (50 μg/mL). The medium was then sterilized by filtration. For transfection using Lipofectamine, the serum-free medium Opti-MEM (Gibco BRL) was used. However, for transfection with Lipofectamine 2000, only antibiotic-free JMEM or DMEM was used, supplemented with 10% FBS. For transfection by electroporation, serum-free and antibiotic-free DMEM was used.

Plating

The cells were maintained as monolayers in 5% carbon dioxide at 37°C, and split before they reached confluence, using trypsin-EDTA (Gibco BRL, 0.05% trypsin (1:250), and 5 mM EDTA). For immunofluorescence, glass coverslips were sterilized by bathing in ethanol, and allowed to dry under UV light for at least 15 minutes. The coverslips were then placed into 8-well dishes, and 2 mL of pre-warmed medium was added. Cells were then placed into the medium and allowed to adhere for at least 12 hours before use.

Cell cycle analysis

Normal diploid fibroblasts were put in presence of serum free media to obtain a majority of cells in the Go phase of the cell cycle. To synchronize cells in the S phase of the cell cycle, cells were then allowed to grow in presence of media containing 10% fetal bovine serum for 20 hours, which is when the largest percentage of cells can be found in S phase.

Transfection of Mammalian Cells

Cells were transfected by lipofectamine 2000 for immunofluorescence studies. As recommended by Gibco BRL for the Lipofectamine 2000 kit, 2 μg of DNA was diluted in 100 μL of OptiMEM (Gibco BRL) and 5 μL of Lipofectamine 2000 (Gibco BRL) was also diluted in 100 μL of OptiMEM, in separate polypropylene tubes. After 5 minutes at room temperature, the two solutions were mixed and incubated for 20 minutes to allow complex formation. The mixture was then directly added to the 2 mL of antibiotic free medium on the cells plated on glass coverslips. The medium was changed for serum and antibiotic supplemented medium 5 hours later, and the cells were allowed to grow for an additional 19 hours before fixation.

Microinjection of human diploid fibroblasts

Microinjection into the nuclei of Hs68 cells plated on glass coverslips was done as previously described (92) using a mixture of 0.01 μg/μL of GFP construct and 0.1 μg/μL of either ING1a or ING1b constructs under the control of the CMV promoter (73).

Irradiation studies

Primary normal human diploid fibroblasts (Hs68; ATCC CRL#1635) were used for all the irradiation studies since these cells could normally be irradiated when part of a living organism is exposed to sunlight and should, therefore, retain

normal patterns of UV-induced DNA repair. For the studies of localization of ING1 and transcription after ultraviolet (UV) irradiation, cells plated on glass coverslips were irradiated with ultraviolet light (25 or 60 J/m^2) in the absence of media and then left for from 10 minutes to 48 hours in complete medium at 37 °C to recover, before harvesting or labeling.

Transcription studies and inhibition of RNA polymerases

To study transcription, the cells were irradiated as described previously and left to recover for 47.5 hours. They were then incubated with 2 mM 5-fluorouridine (5-FU) in complete medium for 30 minutes at 37 °C prior to labeling, then were fixed and labeled with antibodies specific for ING1 protein or 5-FU as described in the immunofluorescence section. In order to determine which RNA polymerases were active in irradiated cells, cells were irradiated as described previously and allowed to recover for 45 hours. They were treated with RNA polymerase inhibitors, for 2.5 hours before fixation, as follows: 0.5 μg/ml of actinomycin D (from a 2 mg/ml stock solution in methanol), 75 μg/ml of DRB (from a 25 mg/ml stock solution in DMSO) and 3 μg/ml of α-amanitin (from a 2 mg/ml stock solution in water). 2.5 hours later, 5-FU was added to the media as described above, for 30 minutes before fixation.

Indirect immunofluorescence and confocal microscopy

Hs68 and SK-N-SH cells were analyzed as described previously (11). Briefly, cells were fixed for 5 minutes in 0.1% paraformaldehyde in PBS (pH 7.5) and then permeabilized for 5 minutes in 0.5% Triton X-100 in PBS. ING1 proteins were labeled with a cocktail of 4 mouse monoclonal antibodies (CAb1-4, (12)) or a rabbit polyclonal anti-ING1 antibody. Tat proteins were labeled with a rabbit polyclonal anti-FLAG antibody and 5-FU was visualized by incubating cells with a mouse monoclonal anti-bromodeoxyuridine antibody (Sigma # B-2531). p53 was labeled with a rabbit polyclonal antibody (Santa Cruz, FL-393). PCNA was labeled

with an anti-PCNA human antiserum (from Dr.. M. Fritzler). Acetylated histones were visualized using antibodies recognizing either diacetylated histone H3 (acetylated on lysines 9 and 14, Upstate #06-599) or histone H4 acetylated on lysine 5 (Upstate #06-759). All primary antibodies were left on cells for at least 30 minutes at room temperature. Cells were then washed with 0.1% Triton X-100 in PBS, followed by PBS alone and were then incubated with secondary antibodies: goat anti-rabbit Cy3 (Chemicon), goat anti-mouse Cy3 (Chemicon), goat anti-mouse Alexa 488 (Cederlane), goat anti-mouse Cy5 (Amersham) or goat anti-human Cy3 (Jackson). The secondary antibodies were left on the cells for at least 30 minutes. Cells were then rinsed with 0.1% Triton X-100 in PBS, in PBS alone and then mounted in 1 mg/ml paraphenylenediamine in PBS/90% glycerol that also contained DAPI at 1 μg/ml. Digital imaging was performed using a 14-bit cooled CCD camera (Princeton Instruments) mounted on a Leica DMRE immunofluorescence microscope. VayTek Microtome digital deconvolution software was used to remove out of focus contributions and image stacks were projected into a one image plane using Scion Image software. For quantitative analysis of colocalization, raw images were analyzed before deconvolution. The signal representing 10% of the nucleus for each labeling was thresholded to a value of 1, the rest becoming 0. The two images were then subjected to a Boolean AND using ERGOvista software v4.4. The resulting number of pixels with a value of 1 was divided by the number of pixels representing 10% of the nucleus. This value represents the percentage of colocalization between the two proteins. For signal density quantitation, the nuclear signal of acetylated histones was integrated for injected and non-injected cells, using ERGOvista v4.4.

Image Processing

For false coloring, level adjustment and creation of panels, images were imported in Adobe Photoshop v5.0 or v5.5, converted from 12 bit images (in a 16 bit format) to 8 bit images. False colors were added by changing the image mode to indexed color, and the color mode to the desired RGB (red-green-blue) mixture.

Typically, DAPI was shown as cyan (red = 100, green = 200, blue = 255), GFP and Alexa488 as green (red = 0, green = 255, blue = 0), Cy3 as red (red = 255, green = 0, blue = 0) and Cy5 as purple (red = 255, green = 0, blue = 255). For superimposition, the recipient image was converted to a RGB mode, and the second image was pasted over. The blending mode used to see two color channels is "screen". The resulting colored images were then copied into a larger RGB file and saved in a TIFF format.

Protein harvesting and nuclear fractionation

Transfected cells were harvested for SDS-PAGE as follows. Cells were washed twice with 1X ice-cold PBS, then scraped in 1 mL of PBS with a rubber policeman. Cells were then pelleted by centrifugation for 1 minute at 5000xrpm and the pellet was resuspended in Laemmli sample buffer. The samples were boiled for 5 minutes and the DNA was sheared by vortexing for 15 seconds. The samples were kept at –80°C until use.

Nuclear matrix fractionation

For the nuclear matrix fractionation all the steps were done at 4°C except when otherwise indicated as previously described (42). Briefly, cells that had or had not been previously UV-irradiated were washed in cold PBS, then scraped off the plate in 1 mL of PBS and spun at 14000xg for 25 seconds. The cells were resuspended in 37.5 µL RSB buffer and left on ice for 10 minutes. The cells were then homogenized with a dounce and spun for 10 minutes at 750xg at 4°C. The resulting supernatant is the cytoplasmic fraction. The pellet was washed twice by adding 50 µL of RSB buffer and spinning at 750xg for 10 minutes. The pellet was then incubated with digestion buffer + 200 U of DNase I (Boehringer Mannheim) for 50 minutes at 30°C. 12.5 µL of $(NH_4)_2SO_4$ 1 M was added and the samples were mixed by pipetting. They were then spun for 10 minutes at 750xg. The supernatant is fraction 2 (soluble nuclear and chromatin-associated proteins). The pellet was resuspended in 50 µL of digestion buffer + 2 M NaCl, then spun for 10

minutes at 750xg. The supernatant is fraction 3 (proteins weakly associated with the nuclear matrix). The pellet was resuspended in 47 μL of 1X digestion buffer + 5 μg of RNase A and 2U of RNase T, left for 1 hour at room temperature and then spun down for 10 minutes at 750xg at 4°C. The supernatant is fraction 4 (proteins strongly associated with the RNA part of the nuclear matrix) and the pellet is fraction 5 (proteins strongly associated with the nuclear matrix). The different fractions were put in 1X Laemmli sample buffer and then frozen at –80°C until they were to be used in a PAGE.

Protein analysis by gel electrophoresis and western blotting

SDS-PAGE

Sodium dodecyl-sulfate polyacrylamide gel electrophoresis, or SDS-PAGE, were performed as described by Laemmli in 1970. The resolving gel was composed of 10-15% acrylamide:bisacrylamide (29:1 ratio), depending on the size of the proteins to resolve. The samples, already in loading buffer, as well as the protein standard (broad range standard, New England Biolabs #7708S) were loaded on the gel and electrophoresed at 100-150 V for 1-2 hours, until the running dye had reached the bottom of the gel. The protein gels were subsequently stained with Coomassie Blue or the proteins were transferred to a nitrocellulose membrane to use in a western blot as described below.

Coomassie Staining

After completion of electrophoresis, gels were placed into a Coomassie staining solution, rocking gently at room temperature for 15 minutes. The gel was then washed with successive changes of destaining solution, usually overnight with pieces of Kimwipe paper to absorb the dye. The gel was then dried on Whatman 3MM paper at 80°C for 1 hour.

Transfer of Proteins to Nitrocellulose

Proteins were transferred from the gel to Optitran nitrocellulose membranes (Schleicher & Schuell #10439396). Pre-chilled transfer buffer was used. The transfer was performed at 4°C at 50V for 1 hour.

Western Blotting

Freshly transferred nitrocellulose membranes were saturated with a blocking solution overnight at 4°C. The membrane was then incubated with the primary antibody (in TBS-T + 1% non-fat milk) recognizing the desired protein for at least 1 hour at room temperature with agitation. The membrane was washed 3 times with TBS-T + 1% non-fat milk, then incubated with a specific secondary antibody (in TBS-T + 1% non-fat milk), coupled to HRP for 1 hour at room temperature. After the second incubation, the membrane was washed 3 times with TBS-T, then incubated with a 1:1 ratio of the two solutions of the chemiluminescence reagent from NEN Life Science Products for 2 minutes. The membrane was placed sealed into a plastic bag and exposed to KODAK X-Omat blue XB-1 film (NEN Life Science).

Antibodies used for Western blotting

ING1 proteins were labeled with a cocktail of 4 mouse monoclonal antibodies (CAb1-4, (12)) or a rabbit polyclonal anti-ING1 antibody. p53 was labeled with the mouse DO-1 and pAB240 antibodies. PCNA was labeled with a rabbit polyclonal antibody (Santa Cruz FL-261). The PML mouse monoclonal antibody PG-M3 (Santa Cruz Biotechnology, Inc., sc-966) was used to recognize PML. Cyclin D1 was labeled with a rabbit polyclonal antibody (Santa Cruz, H-295). The secondary antibodies used for western blotting were a goat anti-rabbit or a goat anti-mouse antibody coupled to horseradish peroxidase (HRP) (Jackson).

Manipulation and amplification of DNA

Agarose gels

1% agarose gels were made by adding 1 g of agarose powder (Gibco BRL) to 100 mL of 1X TAE (Tris, acetic acid, EDTA) buffer, and boiling gently in a microwave until all the agarose was dissolved. Ethidium bromide (Gibco BRL) was added to the liquid gel (0.10% (W/V)) and then, the solution was poured into agarose gel moulds and allowed to cool at room temperature for approximately 30 minutes. The gels were run in 1X TAE buffer at 100 V until desired separation was achieved. Bands were visualized directly using an ultraviolet light source. A 6X DNA loading buffer was added to the DNA samples to allow proper loading and visualization.

Agarose Gel Purification of DNA

Restriction endonuclease fragments of DNA separated on agarose gel were excised using a clean scalpel. DNA fragments were then extracted from the agarose gel using a QIAquick gel extraction kit (QIAGEN, #28704).

Restriction endonuclease digestions

The DNA that was to be digested was mixed with 25 μg of RNase A, the appropriate concentration of restriction endonuclease buffer as recommended by the supplier, 1 to 5 units of enzyme and H_2O to complete the volume. Restriction digests were performed in a 37°C air incubator unless otherwise specified for 1 to 3 hours.

T4 DNA Ligase Reactions

Molar ratios of 1:1 and 3:1 insert:vector were used for ligation of DNA. Purified DNA inserts (previously digested or not) were mixed with the vector DNA in a minimum volume. The 10X ligase reaction buffer was then added to a final concentration of 1X and 1 mM ATP as well as 1 unit of T4 DNA ligase (USB #27-

0870-04) was added. The reaction was allowed to proceed for 16-24 hours at 16°C. The reaction was then diluted and used for transformation.

Preparation of Competent Bacterial Cells

To prepare heat shock-competent cells, a single colony from a freshly grown plate of DH5α was transferred into 100 mL of LB broth medium and incubated for 3 hours at 37°C until the $O.D._{600}$ reached 0.5 - 0.8. The cells were then transferred into ice-cold 50 mL polypropylene Falcon tubes and incubated on ice for 10 minutes. The cells were spun down at 4000x rpm for 10 minutes and the pellets were resuspended in 10 mL of ice-cold 0.1 M $CaCl_2$ and kept on ice. The cells were once again spun down at 4000x rpm for 10 minutes and the pellets were resuspended in 1.5 mL of ice-cold $CaCl_2$, aliquoted in 1.5 mL Eppendorf tubes, snap frozen in liquid nitrogen and kept at –80°C for long term storage.

Transformation of Bacterial Cells

100 μL of competent DH5 alpha bacteria were placed into prechilled 15 mL Falcon tubes and mixed with 10 ng of plasmid DNA. The cells were allowed to sit on ice for 30 minutes. The mixture was then incubated for 90 seconds at 42°C and immediately put back on ice for 2 minutes. Following the heat shock, 1 mL of LB medium without antibiotic was added and the bacteria were allowed to recover at 37°C for 1 hour with shaking at 250 rpm. 100 μL of bacteria were then plated on LB agar plates containing the appropriate antibiotic (either ampicillin at 100 ug/mL or kanamycin at 30 ug/mL). The plates were incubated overnight at 37°C in an incubator.

Small Scale Preparation of Plasmid DNA (miniprep)

To prepare small amounts of plasmid DNA, individual colonies were picked from the LB agar plates and allowed to grow in 2 mL of LB containing the appropriate antibiotic (either ampicillin at 100 μg/mL or kanamycin at 30 μg/mL) overnight at 37°C with vigorous shaking. The next day, a miniprep was performed

on the culture as recommended by the supplier (QIAprep Spin Miniprep Kit, QIAGEN, #27106). The resulting plasmid DNA was digested and run on a gel (as previously described) to verify its size.

Large Scale Preparation of Plasmid DNA

For large scale preparation of plasmid DNA (~1 mg), QIAGEN Plasmid Maxi Kits (QIAGEN, #12163) were used. The starting volume of culture was usually between 100 to 200 mL. The protocol supplied by the manufacturer was followed. The DNA was resuspended in 500 µL of milliQ filtered distilled water.

Storage of Bacterial Cells

Master stocks of the host strains, or the host strains containing plasmid, were kept in 50% (V/V) glycerol at –80°C in cryotubes. For propagation of bacterial cells, a small sample of the frozen stock was put into antibiotic containing media and incubated overnight at 37°C with vigorous shaking.

Cloning of different ING1 constructs

PCR reactions

Many different PCR reactions were performed. In all cases, from 10 to 100 ng of DNA was mixed with 10 pmol of each primer and 0.2 mM dNTP. The polymerases used were Advantage cDNA polymerase from Clontech (for the RACE-PCR reactions, #8417-1) and the Taq DNA polymerase (Amersham Pharmacia #27-0799) and Pfu polymerase (Stratagene #600135-81) for the other PCR reactions. The polymerases and their respective buffers were added as suggested by the manufacturer. Usually, 25 to 35 PCR cycles were carried out at 94°C for 45 seconds, 55° for 30 seconds and 72° for 1 to 4 minutes. Site directed mutagenesis PCR reactions were carried out at 94°C for 45 seconds, 42° for 30 seconds and 72° for 1 to 4 minutes, to allow the mutated primers to anneal to the template. Touchdown PCR was performed for all the RACE-PCR reactions (5 cycles at 94°C for 30 seconds, 72° for 3-6 minutes; 5 cycles at 94°C for 30

seconds and 70°C for 3-6 minutes and; 25 cycles at 94°C for 20 seconds and 68° for 3-6 minutes).

Primers used to generate the different ING1 constructs

The cloning of the NTS (nucleolar targeting sequence) of ING1 and the NLS (nuclear localization signal) of ING1 in pEGFP-N in frame with the GFP was done by PCR. Primers N1 (CGCAGGAATTCATGGACAAGCCCAACAGCAAG) and N2 (GTCCAAGGGCCCACGGTTCTCGTTGTTGC) were used to prepare the NTS construct. Primers N3 (CGCAGGAATTCATGACACCCAAGGAGAAGAA) and N4 (GTCCAAGGGCCCCGCCTTGGCCTTGGAGCG) were used to prepare the NLS construct and primers N1 and N4 were used to prepare the construct containing both the NTS and the NLS. The PCR products were gel-purified as previously described. The resulting fragments of DNA were digested with both EcoRI and ApaI and cloned into the pEGFP-N1 vector cloned in frame with GFP. The constructs were then transfected into cells, which were visualized by immunofluorescence microscopy as previously described.

Site-directed mutagenesis and deletion constructs

Primers RR2 (CGATCACGCGTCCTGTCTGCTCCAACCTTG) and RF2 (CTCACACGCGTTCCCCTGCCGACCTCCCC) were used in a PCR reaction to clone the ΔN1N4 construct.

Primers mut3r (GTTATTGTTATTTGATCGCTTGCTGTTGGGCTTGTC) and mut3f (AACAACGAGAACCG) were used to create the mut3p and mut3G ING1-NTS mutated constructs.

Primers mut4f (AACAATAACAATCGCTCCAAGGCCAAG) and mut4r (GCAGGTCTTGGCCTTCTTCTCC) were used to create the mut4p and mut4G ING1-NLS mutated constructs.

Primers mut5f (AAGAAGAAGAAGCGCTCCAAGGCC) and mut5r (GGAGGTCTTGGCATTGTTATTGTTGGGTGT) were used to create the mut5p and mut5G ING1-NLS mutated constructs. All of the resulting PCR products were

gel-purified and circularized by ligation as previously described. These constructs were amplified in competent bacteria, transfected into mammalian cells, and encoded products were then visualized by immunofluorescence microscopy as previously described.

Isolation of new ING1 isoforms

Purification of polyA+ mRNA

Frozen mouse and human tissues were ground to a fine powder in liquid nitrogen (to avoid contamination by RNases) and then sonicated in Trizol (Gibco BRL, 20 mL of Trizol/g of tissue). 2 mL of chloroform was added per 20 mL of Trizol. The samples were shaken for 15 seconds, transferred to RNase-free 14 mL Falcon tubes and then spun for 20 minutes at 10 000 rpm at 4°C. The aqueous phase was transferred to RNase-free 14 mL tubes and an equal volume of isopropanol (BDH #B10224) was added. The samples were left to incubate at 4°C for 2 hours and then spun at 10 000 rpm for 20 minutes at 4°C. The pellet was washed with 75% ethanol and spun again at 10 000 rpm for 10 minutes at 4°C. The supernatant was then removed and the pellet, which contains total RNA, was air-dried and disolved in 100 µL of DEPC (Sigma D-5520) treated H_2O. Poly A+ mRNA was isolated from the total RNA by using the QIAGEN mRNA puification kit as recommended by the supplier (QIAGEN #72041).

Preparation of gels for RNA

1.4g of agarose was dissolved in 77 mL of DEPC-H_2O and 10 mL of 10X MOPS buffer by heating it in a microwave. When cooled down to 60°C, 18 mL of formaldehyde (BDH #ACS357) was added and the gel was poured in a fume hood. To prepare the samples, 4-5 µg of polyA+ mRNA in DEPC-H_2O (total volume of 5,5 µL) was placed in an RNase-free eppendorf and 1.0 µL of 10X MOPS, 10.0 µL of deionized formamide (BDH #B90133) and 3.5 µL of formaldehyde were added in that order. The samples were heat denatured for 15 minutes at 65°C, cooled on ice for 5 minutes and 2 µL of RNA loading buffer was added. The samples were

loaded on the gel which was run overnight at room temperature in 1x MOPS buffer at 15V. The RNA molecular weight standard used was supplied by Gibco (#15620-016).

The part of the gel containing the molecular weight standard was cut off and stained with ethidium bromide (4 μL of the stock solution in 200 mL of H_2O, Gibco BRL) for 15 minutes at room temperature with gentle shaking, then destained with H_2O for 15 minutes at room temperature and further destained with fresh H_2O for several hours. The gel was then photographed under UV-illumination. The rest of the gel containing the RNA samples was soaked in DEPC-treated H_2O 3X for 5 minutes each with gentle shaking at room temperature and then put in 20X DEPC-treated SSPE with gentle shaking for 20 minutes. RNA gels were then transferred to nitrocellulose membranes with 20X DEPC-SSPE, by northern blotting, overnight at room temperature. When the transfer was done, the RNA was UV-crosslinked to the membrane with a UV-Stratalinker 1800 (Stratagene) at the setting "auto-crosslink". All the DEPC-solutions were treated in the same way: 1 mL of DEPC was added to 1 L of solution, which was then shaken several times to assure even exposure to DEPC. The solution was left overnight in a fumehood and then autoclaved the next day. Only RNase-free pipets were used to transfer DEPC-treated solutions.

Preparation of probes for northern blots

The DNA constructs containing the sequence to be used as a probe were linearized with appropriate enzymes. A sample of the digestions was run on a gel to verify digestion efficiency. The rest of the digestions (95 μL) were incubated with 1 μL of proteinase K (20 mg/mL) at 37°C for 30 minutes to eliminate the proteins. The solutions were then extracted 3 times with a phenol-chloroform procedure as follows: to each sample, 50 μL of Ultra-pure Phenol (Gibco BRL #15513-039) and 50 μL of chloroform (BDH #ACS210) were added. The samples were spun for 3 minutes at 13 000 rpm and the aqueous phase was kept. After the third extraction, the samples were precipitated as follows: 10 μL of DEPC-treated

3M NaOAc pH 5.2 and 250 µL of 100% ethanol were added. The precipitation was allowed to proceed at –80°C for at least 30 minutes and the samples were then spun down for 20 minutes at 4°C and 14 000 rpm. The resulting pellet was washed with 70% ethanol, spun again for 5 minutes and air-dried. It was resuspended in 12 µL of DEPC-H_2O. To prepare and label the probes, 1 µg of the precipitated linearized template was mixed on ice with 2 µL of the DIG RNA labeling mix, 2 µL of the 10X transcription buffer supplied by the kit (DIG labeling kit, Boehringer Mannheim #1004760), 1.5 µL of the appropriate RNA polymerase (T3 or T7), 1 µL RNA guard and H_2O to reach a final volume of 20 µL. Reactions were incubated for 2 hours at 37°C. The reaction was stopped by adding 2 µL of 0.2M EDTA pH 8.0 and the mixture was precipitated as previously described. The labeling efficiency was measure as recommended by the supplier.

Northern blots with the DIG-easy-hyb system

Northern blots using the DIG-easy-hyb system (Boehringer Mannheim) were performed on the RNA membranes as follows. The membranes were put in a roller tube with 20 mL of DIG-easy-hyb for 1 hour for prehybridization at 65°C. 1 µg of the labeled probe was boiled and added to 10 mL of DIG-easy-hyb hybridization solution, which was poured on the membrane. The hybridization was allowed to proceed overnight at 65°C. The next day, the membrane was washed 2 times with 2X SSC, 0.1% SDS at 65°C and 2 times with 0.5XSSC, 0.1% SDS at 65°C. The membrane was then incubated in washing buffer for 1 minute at room temperature. In a clean dish, blocking solution was added to the membrane for 30-60 minutes with shaking at room temperature. The anti-DIG antibody (Boehringer Mannheim #1 098 519(1)) was diluted 1:10 000 in blocking solution and added to the membrane for 30 minutes with gentle shaking. The membrane was then washed 2X in washing buffer and equilibrated in detection buffer for 2 minutes at room temperature. The substrate (CSPD, Boehringer Mannheim #1 654 012(1)) was diluted 1:100 in detection buffer and added to the membrane which was then

sealed in a plastic bag. An autoradiogram was performed on the membrane with Kodak X-Omat AR film (NEN Life Science #165 1454).

Preparation of the cDNA sets with the Marathon cDNA amplification kit (Clontech #K1802-1)

As described in Clontech's procedures handbook, 1 μg of the polyA+ mRNA was mixed with 1.0 μL of the cDNA synthesis primer and H_2O to a total volume of 5.0 μL, then incubated at 70°C for 2 minutes and cooled on ice for 2 minutes. 2 μL of 5X first strand buffer, 1 μL dNTP mix (10mM), 1 μL sterile H_2O and 1 μL AMV reverse transcriptase (20 U/μL) were added to each reaction and then incubated at 42°C for 1 hour. The tubes were placed on ice to stop the reaction. 48.4 μL sterile H2O, 16 μL 5X second strand buffer, 1.6 μL dNTP mix and 4 μL 20X second strand enzyme cocktail were added and the reaction was incubated at 16°C for 90 minutes. 2 μL of T4 DNA polymerase was then added and incubated at 16°C for 45 minutes. 4 μL of EDTA/glycogen mix was added to stop the reaction. A phenol/chloroform extraction was performed on the sample, which was then precipitated with ethanol, air-dried and resuspended in 10 μL as recommended by the supplier. The sample was then run on an agarose gel to verify the procedure. 5 μL of the double-stranded cDNA was added to 2 μL of the Marathon cDNA adaptor (10 μM), 2 μL 5X DNA ligation buffer and 1 μL of the T4 DNA ligase (400 U/μL) which was then incubated for 4 hours at room temperature. The set was then heated to 70°C for 5 minutes and then diluted in tricine-EDTA for the RACE-PCR reactions. All the solutions used to prepare the cDNA sets were supplier with the kit.

RACE-PCR

For the 5' RACE reactions, the first primers used were H2 (CATAGGAGACCTGGTTGCACAGACAGT) and AP1 (CCATCCTAATACGACTCACTATAGGGC) which was supplied with the kit.

Subsequent nested 5' RACE-PCR reactions were performed with the H3 and H4 primers (CTCCACCATCTGACTCAC) and (TCAGGATCTCGGAAACGC). For 3' RACE, the primers used were H1 (ACTGTCTGTGCAACCAGGTCTCCTATG) and AP1 (which is supplied with the kit). The RACE reactions were performed as previously described in the section PCR reactions and in the Marathon cDNA amplification kit handbook by Clontech (#K1802-1).

Cloning of the RACE products

The RACE products were ligated into the pGEM-T vector by A/T cloning. The resulting ligation products were then transformed into competent bacteria grown on plates, single colonies were amplified and minipreps were performed on the cultures as described previously. The minipreps were digested with appropriate enzymes, run on gels and examined to see which ones contained inserts of the expected size. Southern blots using ING1 specific probes prepared with the DIG labeling and detection kit (Boehringer Mannheim) were also performed as recommended by the supplier in order to verify which constructs contained ING1 sequences.

Once the new isoforms were identified, the 3' and the 5' regions of each isoform were subcloned into pBS II (Stratagene). The 5' and the 3' regions overlapped and both contained a common restriction site (Bsa I) making it easy to recreate the full-length isoform, which was then ligated into the Sma I site of pBS II. The isoforms were also subcloned into the mammalian expression vector pCIneo. The ING1b isoform was cloned into the Xba I and Xho I sites, the ING1c isoform was cloned into the Nhe I and Acc I sites and the ING1e, f and g isoforms were cloned into the Xba I and Acc I sites of the pCIneo vector.

Sequencing

All the constructs generated including the mouse isoforms and the human ING1b mutation and deletion constructs were sequenced with appropriate primers. The DNA primers used were the M13 reverse sequencing primer (ACGGGATAACAATTTCACACAGCA), the M13 universal sequencing primer (CGCCAGGGTTTTCCCAGTCACGAC) and the pCI T7 sequencing primer (TAATACGACTCACTATAGG). The PCR reactions were performed in our laboratory with the Big Dye sequencing kit (ABI prism #4303150) as recommended by the supplier and then were precipitated and sent to the DNA sequencing facility of the University of Calgary.

CHAPTER 3:
RESULTS

PART 1:

ING1 is involved in the UV-induced DNA-damage response of cells

To address the first hypothesis of this research project, which was that ING1 proteins are involved in the post-UV response of cells and consequently behave differently when cells are induced to undergo DNA repair, we decided to treat normal diploid cells with different doses of UV light and observe the pattern of ING1 localization in the cell as well as its interaction with several other proteins. However, before this was done, the amino acid sequence of ING1 was searched for relevant protein motifs, which could specify an interaction with proteins involved in DNA repair. The unique region of ING1 was found to possess a PIP box (PCNA interacting protein box) which is known to allow interaction with PCNA. Several proteins have been shown to possess a PIP box including p21, Fen-1, MCMT and XPG. The PIP box present in the ING1b isoform is compared to PIP boxes previously identified in other proteins in figure 4. Because of the presence of this PIP box in the ING1b isoform and the fact that PCNA is known to play a role in DNA repair, the subcellular localization of the ING1 proteins and PCNA were compared. As well, because ING1 had been reported to physically interact with the tumor suppressor p53, we also examined and compared the subcellular localization of ING1 and p53.

ING1 colocalizes with PCNA after UV-irradiation

Digital deconvolution confocal microscopy experiments in untreated normal diploid fibroblasts show ING1 and PCNA to be nuclear but do not reveal any significant degree of colocalization of these proteins (Fig.5A-D). Control experiments show that these two proteins colocalize to a similar degree as any two non-interacting proteins, including CBP and HDAC1. When the cells are irradiated with low amounts of ultraviolet light, which elicits a DNA damage-response, the degree of colocalization of ING1 and PCNA as visualized by digital deconvolution microscopy dramatically increases (Fig.5E-H). The degree of colocalization of the two proteins can be shown to start increasing as soon as 10 minutes after cells are irradiated and this colocalization increases to a maximum at 120 minutes after UV irradiation (Fig.6). This can be shown in quiescent cells as well as in cells in S

phase (figure 6) and cells in log phase (data not shown). ING1 and p53, on the other hand, can not be shown to colocalize under the same conditions (Fig.5 I-P) or under any other condition examined to date in these cells.

ING1 is targeted to the nucleolus when overexpressed and after UV irradiation

To continue the study of the subcellular localization of the ING1 proteins after UV-irradiation, normal human diploid cells were irradiated with higher doses of UV and a time-course was performed. Visualization of endogenous ING1 using a cocktail of monoclonal antibodies (12) against the common region of ING1 reveals a uniform, slightly punctate staining of the nucleoplasm with no staining of the nucleolus in unirradiated cells (Fig.7A-B-C). This is observed in normal diploid fibroblasts and in the vast majority of other cell types examined, including primary human astrocytes, established murine fibroblasts, most human glioblastoma and breast cancer cells, 293 cells and SK-N-SH cells (data not shown). However, when normal diploid fibroblasts were irradiated with relatively high doses of UV light ($60J/m^2$), which causes DNA damage and leads to apoptosis in most cells (71), ING1 translocated to the nucleolus and was found in this organelle as early as 12 hours and up to 48 hours after UV irradiation (Fig.7G-H-I). The localization of the ING1 proteins to the nucleolus can also be observed in cells overexpressing the ING1b isoform (Fig.7D-E-F). The nucleolus is known to be a specialized region of the nucleus where transcription and processing of rRNA as well as ribosomal assembly occurs (reviewed in (38, 89, 96)). As well, several regions of specific chromosomes, which contain clusters of the tandemly repeated ribosomal genes, localize to the nucleolus (70, 80).

The targeting of ING1 to the nucleolus did not occur before 12 hours after UV irradiation of cells, indicating that further DNA damage response events are necessary to allow this translocation. Other proteins, such as p53, which has been reported to interact with ING1b (32), and PCNA which binds ING1b after cells are

irradiated with low doses of UV light, did not translocate with ING1b to the nucleolus under the same conditions (data not shown).

$p33^{ING1b}$ contains a functional NTS

Because the ING1 proteins are capable of translocating to the nucleolus under conditions of DNA-damage caused by UV-irradiation, these proteins were examined to see if they contain a potential nucleolar targeting sequence (NTS) as defined previously (49). Examination of the amino acid sequence of ING1 revealed the presence of a complete NTS as shown in figure 8A where it is compared to the sequences found in other cellular and viral proteins that are targeted to the nucleolus. In order to determine if this sequence is responsible for targeting ING1 to the nucleolus, a construct of 156 bp (amino acids 142 to 194 of the protein) consisting of the putative NTS as well as the NLS (nuclear localization signal) found in ING1 was cloned into pEGFP-N2 in frame with the cDNA encoding green fluorescent protein (Fig.8B). An ATG codon was added 5' of the 156bp sequence to allow proper translation of the fusion protein. This fusion protein localizes almost exclusively in the nucleolus (data not shown). Several other fusion proteins of ING1 were next constructed (shown in figure 8B) to further define the regions of this protein required for nucleolar targeting. Only the proteins containing the amino acids 142 to 194 localized to the nucleolus.

To better characterize the NTS in ING1b, several additional fusion proteins were constructed (Fig.9A and B), some of which contain mutations in the NTS. The constructs were transfected into different cell types and then fixed and visualized 24 hours later by immunofluorescence microscopy. Since previous reports have indicated that some nucleolar proteins do not contain an NTS or contain an NTS as defined by Henderson *et al* (49), but depend on other sequences for nucleolar targeting (97), (52), constructs of ING1b mutated in other key residues were made. As shown in figures 9A and B, the amino acids 142 to 194 are sufficient to target ING1b-GFP to the nucleolus. More precisely, amino acids 142 to 159 (construct N1N2) alone can target GFP to the nucleolus, defining

a sequence sufficient for the targeting effect. Surprisingly, amino acids 174 to 194 (construct N3N4), which were believed to contain a unique NLS (nuclear localization signal), can also target GFP to the nucleolus. This result is similar to the finding that a putative NLS (one of 3 found in the nucleolar protein Rpp38) is an efficient nucleolar targeting sequence (52).

To determine more precisely the exact amino acids required for nucleolar targeting, a number of mutated clones of ING1b were next generated. Mutational analysis of ING1b shows that the targeting of this protein to the nucleolus requires a bipartite signal, which contains the amino acids RRQR within the NTS and the amino acids KKKK within the NLS (Fig.9A and B). Mutation of these 8 amino acids (mut3-4p) completely abrogates the translocation of ING1b to the nucleolus. Mutation of other residues does not inhibit the nucleolar targeting of ING1b (Fig.9A and data not shown). As well, mutation of the amino acids RRQR or KKKK separately (mut3p and mut4p in Fig.9A) does not prevent nucleolar localization of the full length protein. Mutation of RRQR in a portion of the protein that does not contain KKKK (mut3G) and vice versa (mut4G) does, however, block the nucleolar targeting of these portions of ING1b, although they are still localized to the nucleus. Interestingly, the amino acids KEKK (which form the other half of the bipartite NLS with amino acids KKKK) are not responsible for nucleolar targeting (mut5G2 in Fig.9A). Taken together, these results indicate that this protein contains 2 regions of 4 amino acids that function as a nucleolar targeting signal. Each one is individually capable of localizing ING1b and heterologous fusion proteins to the nucleolus. It is important to note that the nucleolar targeting sequence is present in the common region of the ING1 isoforms, which suggests that all the ING1 isoforms should have the capacity of translocating to the nucleolus under certain conditions. More studies will be necessary to address this question. The mutational analysis of the ING1 NTS was done in the ING1b isoform because at the time of the study, it was the only ING1 isoform cloned.

ING1 is not retained in the nucleoplasm by a limiting factor that binds a consensus NTS

Since no detectable endogenous ING1 is present in the nucleolus of untreated cells (Fig.7), there must be a mechanism to retain these proteins in the nucleoplasm. When overexpressed, ING1 localizes to the nucleolus, consistent with high levels of ING1 titrating out a factor responsible for maintaining ING1 in the nucleoplasm. To address this question, cells were transfected with a construct encoding the viral protein Tat, which contains an NTS very similar to one of the NTS elements present in ING1 (Fig.8A). When Tat is overexpressed, it localizes mainly to the nucleolus but endogenous ING1 remains in the nucleoplasm (Fig.10A-D). This indicates that ING1 is not retained in the nucleoplasm by a limiting factor that is titratable by Tat. If it were, the limiting factor would also bind the NTS present on Tat and would not be present in amounts large enough to keep all the ING1 in the nucleoplasm. As well, when ING1 and Tat are cotransfected into cells, both proteins are highly enriched in the nucleolus, to the same degree as when only one of these proteins is transfected into cells (Fig.10E-H). This implies that these proteins do not compete for the binding of a limiting factor in the nucleolus to remain in this organelle. In addition, inhibition of phosphorylation or dephosphorylation by staurosporine and okadaic acid, respectively, do not cause a relocalization of endogenous ING1 to the nucleolus (data not shown).

RNA pol I is not inhibited under conditions of DNA damage that induce translocation of ING1 to the nucleolus

We next wished to examine the potential function of ING1 nucleolar localization. Since the nucleolus is the site of rRNA transcription by RNA polymerase I (RNA pol I), we asked whether the higher concentrations of ING1 found in some cells might influence transcription by RNA pol I compared to transcription by RNA polymerases II and III. Normal diploid fibroblasts were therefore subjected to UV irradiation, left to recover for 48 hours and then incubated with 5-fluorouridine (5-FU) for 30 minutes. Cells were then labeled with

both polyclonal antibodies against ING1 proteins and monoclonal antibodies against BrdU as described previously (11). 5-FU is a uridine analogue that is incorporated into nascent RNA transcribed by RNA polymerases I, II and III (12, 41, 122). The antibodies against BrdU also recognize 5-FU, which allows visualization of transcriptional activity by immunofluorescence microscopy. As expected, in cells treated with UV, ING1 localized to the nucleolus (Fig.11G), whereas in untreated cells, ING1 was detected only in the nucleoplasm and was not concentrated in the nucleolus (Fig.11C). As shown by the DNA-specific DAPI stain, the nuclei of cells irradiated with UV (Fig.11E) are larger than those of the untreated cells (Fig.11A), and show a DNA staining pattern that is consistent with the finding that UV irradiation, at the dose used, induces apoptosis in these cells. Transcription was detected throughout the nucleus of all untreated cells, with higher amounts of transcription being visualized in the nucleolus (Fig.11B). However, in cells irradiated with UV, transcription occurred only in the nucleolus (Fig.11F).

We next wished to confirm the identity of the RNA polymerase responsible for the transcription observed in the cells after UV irradiation by an independent method. We therefore treated cells, which had or had not been previously UV-irradiated, with different inhibitors of RNA polymerases and then allowed them to incorporate 5-FU as described above. The cells were then labeled and visualized by immunofluorescence microscopy. As shown in Fig.12B and 12E, DRB (5,6-dichloro-β-D-ribofuranosylbenzimidazole), which inhibits RNA polymerase II (68), (107), does not eliminate the transcription seen in the nucleolus either in the absence or in the presence of UV irradiation, but does appreciably inhibit transcription in the nucleoplasm. However, actinomycin D (Fig.12C and 12F), which inhibits all three RNA polymerases (103), does inhibit nucleolar transcription following UV irradiation. The drug α-amanitin, which inhibits RNA polymerases II and III (57), (118), also inhibited transcription in the nucleoplasm but not in the nucleolus, similar to DRB (data not shown). Taken together, these results indicate that RNA polymerases II and III are efficiently inhibited after cells are UV-irradiated,

as previously reported by many groups. In contrast, RNA polymerase I is not inhibited and continues to transcribe RNA under conditions of DNA damage caused by UV-irradiation, during the same time period that the candidate tumor suppressor ING1 translocates to the nucleolus.

Figure 4: ING1b possesses a PIP box motif

ING1b, but not other ING1 splicing isoforms, contains a PIP (PCNA interacting protein) box motif in its amino-terminal region. This motif is also found in several other proteins including the Fen-1 endo-exonuclease, the DNA-repair protein XPG and the cell cycle regulatory protein p21, all of which have been shown to interact with PCNA through this motif. The h represents a hydrophobic residue, a indicates aromatic residues and X can be any residue. The conserved residues are indicated in bold.

Figure 4: ING1b possesses a PIP box motif

$p33^{ING1b}$	G E **Q** L H **L** V N **Y** V E D
Fen1	S T **Q** G R **L** D D **F** F K V
XPG	Q T **Q** L R **I** D S **F** F R L
$p21^{WAF}$	R R **Q** T S **M** T D **F** Y H S

Consensus PIP box: **Q X X h X X a a**

Figure 5: ING1 and PCNA colocalize after UV-induced DNA damage

Hs68 normal diploid fibroblasts were irradiated (E-H and M-P) or not (A-D and I-L) with ultraviolet light and then allowed to recover for two hours, after which they were fixed and stained for DNA (A,E,I,M) and ING1 (B,F,J,N), PCNA (C,G) and p53 (K,O) proteins. Colocalization can be seen between the ING1 proteins and PCNA following UV irradiation (H) but not in untreated cells (D). Colocalization of ING1 proteins and p53 can not be seen under conditions examined to date (L,P, data not shown). The scale bar represents 10 μm.

Figure 5: ING1 and PCNA colocalize after UV-induced DNA damage

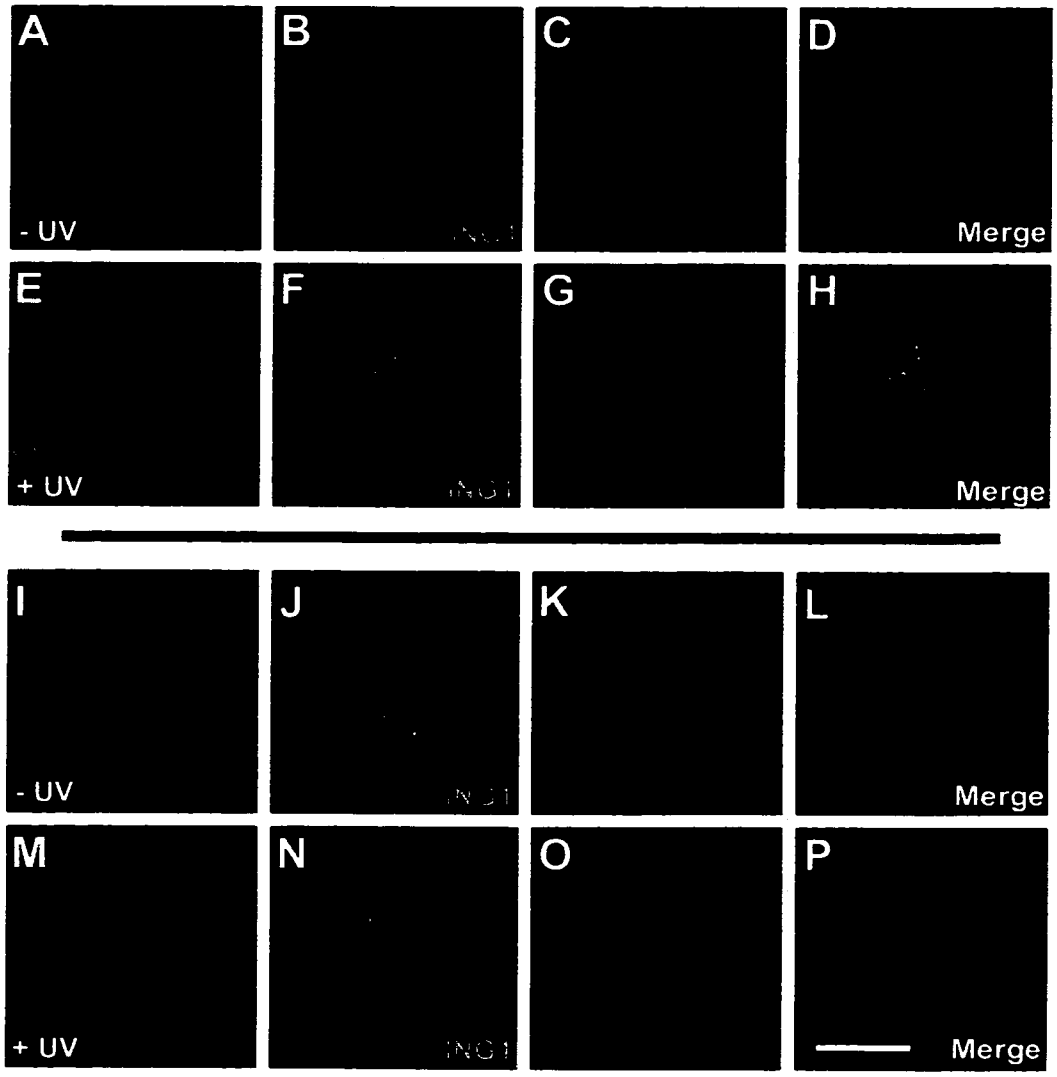

Figure 6: ING1 and PCNA colocalize for several hours after UV-induced DNA damage

ING1 and PCNA can be shown to colocalize for several hours after cells are induced by UV light, as shown by immunofluorescence microscopy. Here, the degree of colocalization between the two proteins examined has been measured in 5 cells for each time point. The triangles represent the percentage of colocalization of ING1 and PCNA and the squares represent the percentage of colocalization of ING1 and p53. In quiescent cells (G_o), the degree of colocalization of ING1 and PCNA passes from 17.4 % to a peak of 28.4 % at 120 minutes and then starts slowly going down again. The degree of colocalization of ING1 and p53 does not significantly vary during this time period. In cells in S phase, the degree of colocalization of ING1 and PCNA passes from 11.9 % to a peak of 28.0 % at 120 minutes and then starts going down. Again, the degree of colocalization of ING1 and p53 does not significantly vary during this time period, in this phase of the cell cycle.

Figure 6: ING1 and PCNA colocalize for several hours after UV-induced DNA damage

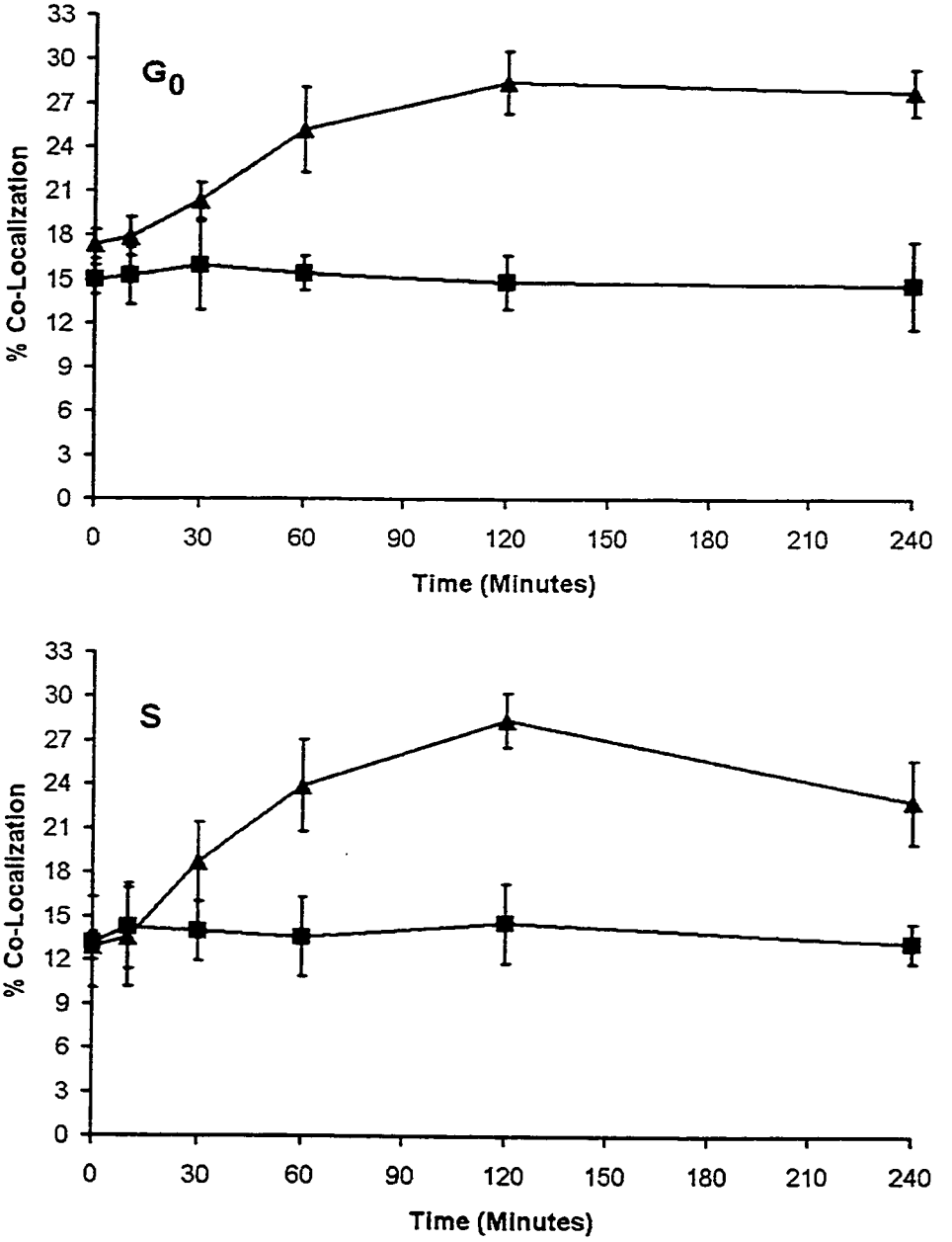

Figure 7: ING1 proteins are nucleolar when overexpressed and after UV-induced DNA-damage

Hs68 fibroblasts were fixed and stained for ING1 (B,E,H) and DNA (A,D,G). Endogenous ING1 (B) is found in the nucleus but not in the nucleolus (which is shown in the differential interference contrast (DIC) images C,F and I). However, when these proteins are overexpressed, they localize mainly to the nucleolus and can also be seen in the nucleoplasm (E). Endogenous ING1 proteins translocate to, and localize within the nucleolus 48 hours after UV-induced DNA damage as shown in panel H. The scale bar represents 5 μm.

Figure 7: ING1 proteins are nucleolar when overexpressed and after UV-induced DNA-damage

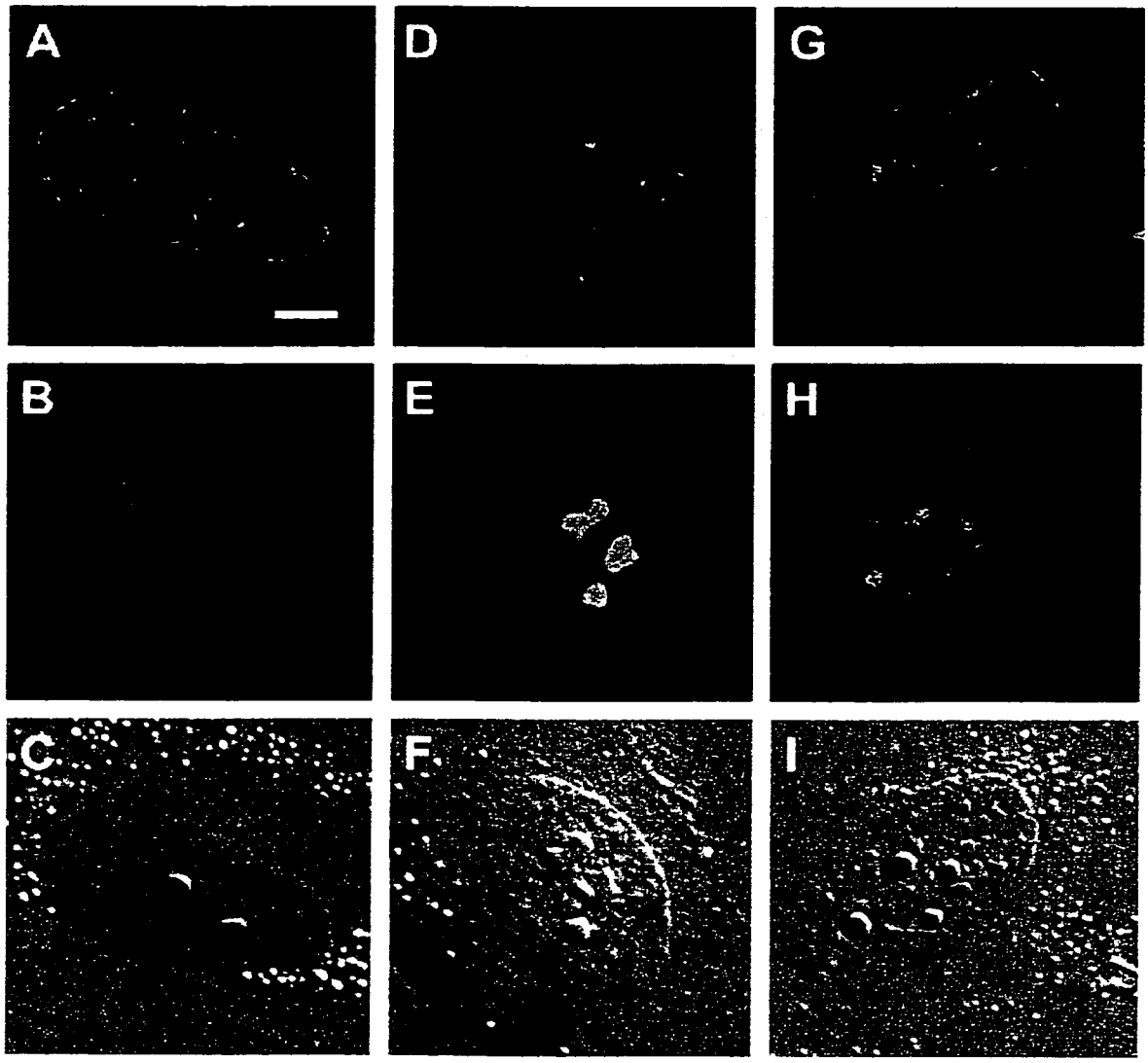

Figure 8: ING1 proteins contain a nucleolar targeting sequence

Examination of the amino acid sequence of $p33^{ING1b}$ reveals the presence of a complete nucleolar targeting sequence (NTS) (49) in the second half of the protein. Several known cellular and viral proteins, which can be found in the nucleolus at least under certain conditions, contain this targeting sequence (A). Cells were transfected with ING1 deletion constructs and examined for subcellular distribution by indirect immunofluorescence. As indicated in panel B, only the ING1 constructs containing the amino acids 142 to 194 localized to the nucleolus.

Figure 8: ING1 proteins contain a nucleolar targeting sequence

A

human ING1	^{142}DKPNSKRSRRQRNNENR^{153}
mouse ING1	^{142}DKPNNKRSRRQRNNENR^{158}
HTLV-1 Rex protein	^{1}MPKTRRRPRRSQRKRPPTP^{19}
HIV-1 Rev protein	^{35}RQARRNRRRRWRERQR^{50}
HIV-1 Tat protein	^{48}GRKKRRQRRRAP^{57}
FGF3	^{236}QPRQRRQKKQSPG^{248}
Rpp29	^{65}KRKEKKKKAKGLSARQRRELR^{85}
PTHrP	^{87}GKKKKGKPGKRREQEKKKRRT^{107}
NOLP	^{320}KEKIQAIIDSCRRQFPEYQERAR^{342}
S7	^{96}AQRRILPKPTRK^{107}
DEDD	^{164}KRPARGRATLGSQRKRRKSV^{183}

Consensus sequence: **RRQR**

B

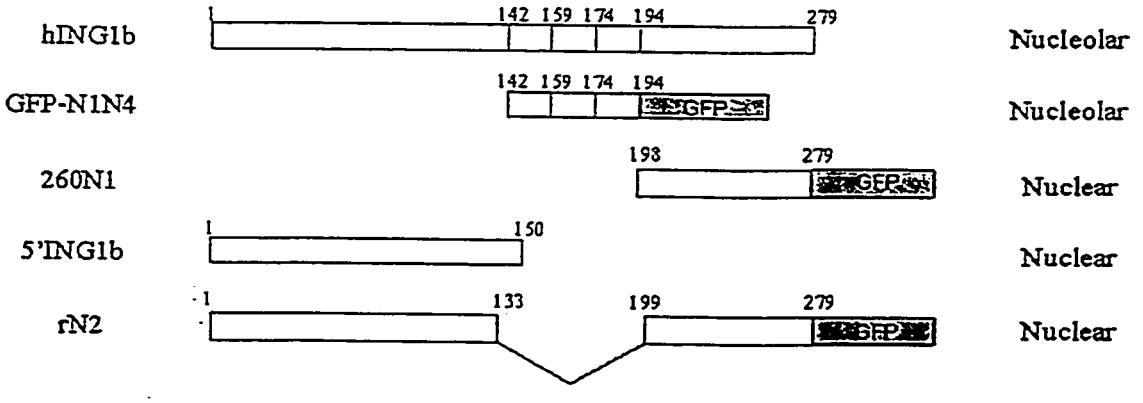

Figure 9: Two distinct regions of 4 amino acids each are responsible for the nucleolar targeting of ING1

(A) Mutated versions of $p33^{ING1b}$ were generated and transfected into Hs68 fibroblasts. Their subnuclear localization was studied. The most interesting are shown in panels B-M. Cells were stained for DNA (B,E,H,K) and ING1 proteins (C,F,I,L). Mutational analysis of $p33^{ING1b}$ shows that the targeting of this protein to the nucleolus (which is shown in the differential interference contrast (DIC) images D,G,J,M) uses a bipartite signal which contains both the amino acids RRQR within the NTS (original nucleolar targeting sequence) and the amino acids KKKK within the consensus NLS (nuclear localization signal). Mutation of these 8 amino acids (mut3-4p) completely abrogates the translocation of $p33^{ING1b}$ to the nucleolus (K) whereas mutation of each individually (mut3p or mut4p), or of other local residues does not inhibit the nucleolar targeting of $p33^{ING1b}$. The scale bar represents 5 μm.

Figure 9: Two distinct regions of 4 amino acids each are responsible for the nucleolar targeting of ING1

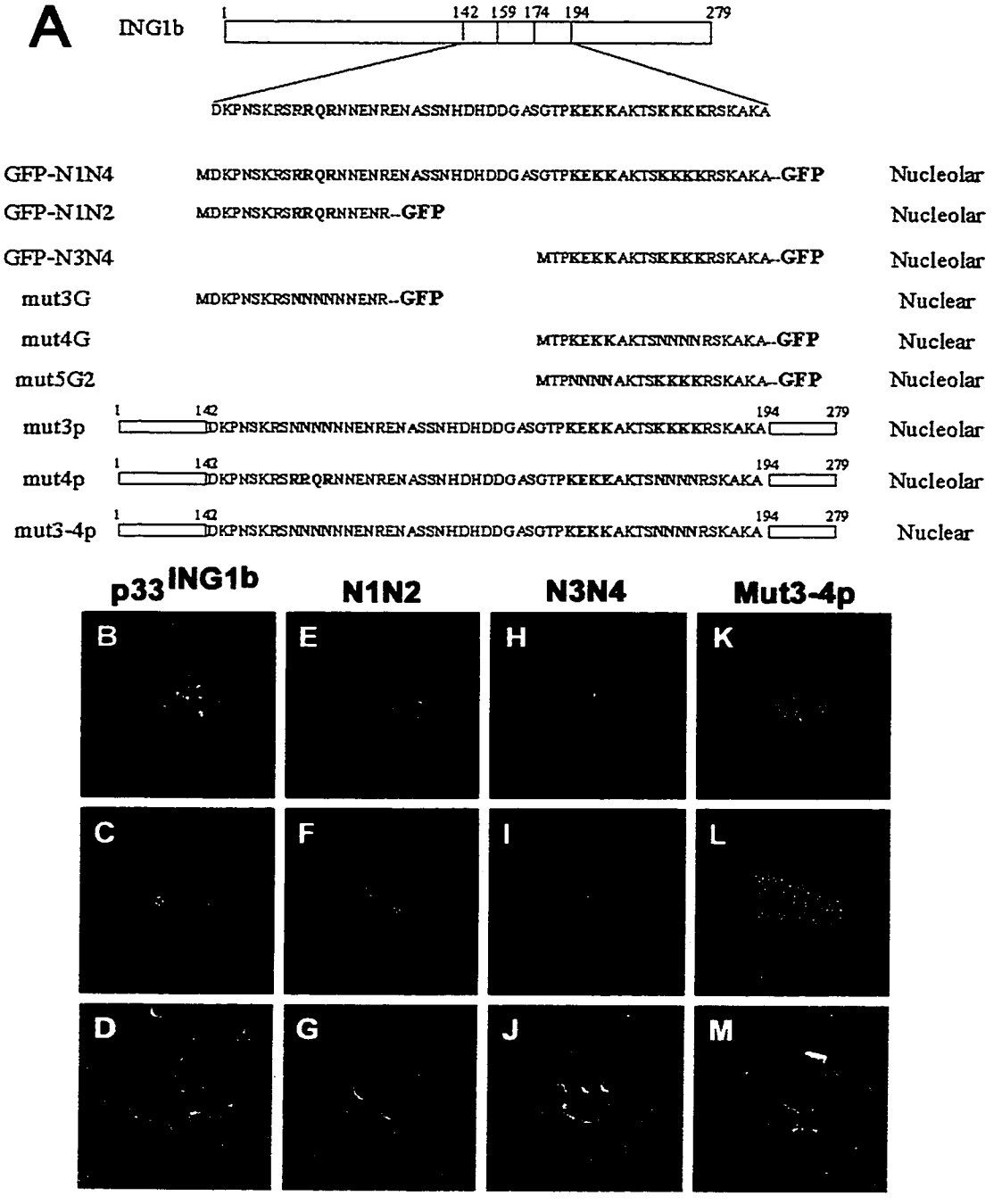

Figure 10: ING1 is not retained in the nucleoplasm by a limiting factor

Hs68 fibroblasts were transfected with Tat (A,B,C,D) or with Tat and GFP-ING1b (E,F,G,H). Cells were stained for DNA (A,E), Tat (B,F) and ING1 (C,G). When overexpressed, Tat localizes to the nucleolus (shown by DIC in D) but does not cause relocation of ING1 to the nucleolus (C). Overexpression of both Tat and ING1 does not decrease the amounts of either protein in the nucleoli, which are visualized by differential interference contrast microscopy (panel H). The scale bar represents 5 μm.

Figure 10: ING1 is not retained in the nucleoplasm by a limiting factor

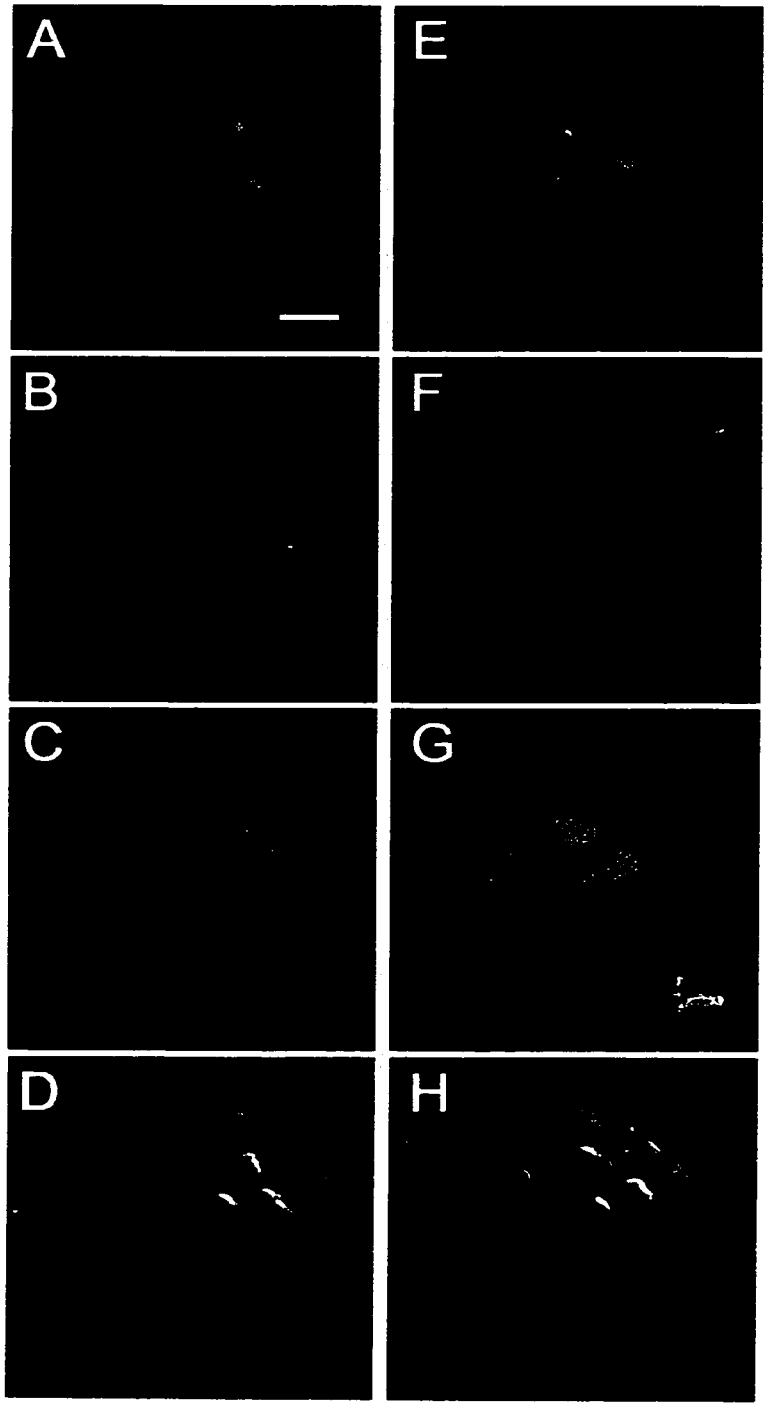

Figure 11: When ING1 is present in the nucleolus, RNA transcription is inhibited in the nucleoplasm but not in the nucleolus

Hs68 fibroblasts were subjected to UV irradiation, allowed to recover for 48 hours and then incubated for 30 minutes with 5-FU. Cells were then labeled with both polyclonal antibodies against ING1 (C,G) and monoclonal antibodies against BrdU which also recognize 5-FU (B,F). In cells treated with UV (E-H), ING1 localized to the nucleolus (G) whereas in untreated cells (A-D), ING1 was detected only in the nucleoplasm (C). Transcription was detected throughout the nucleus of all untreated cells with higher amounts of transcription found in nucleolus (B). However, in cells treated with UV irradiation, transcription was found uniquely in the nucleolus (F). The scale bar represents 5 μm.

Figure 11: When ING1 is present in the nucleolus, RNA transcription is inhibited in the nucleoplasm but not in the nucleolus

A B

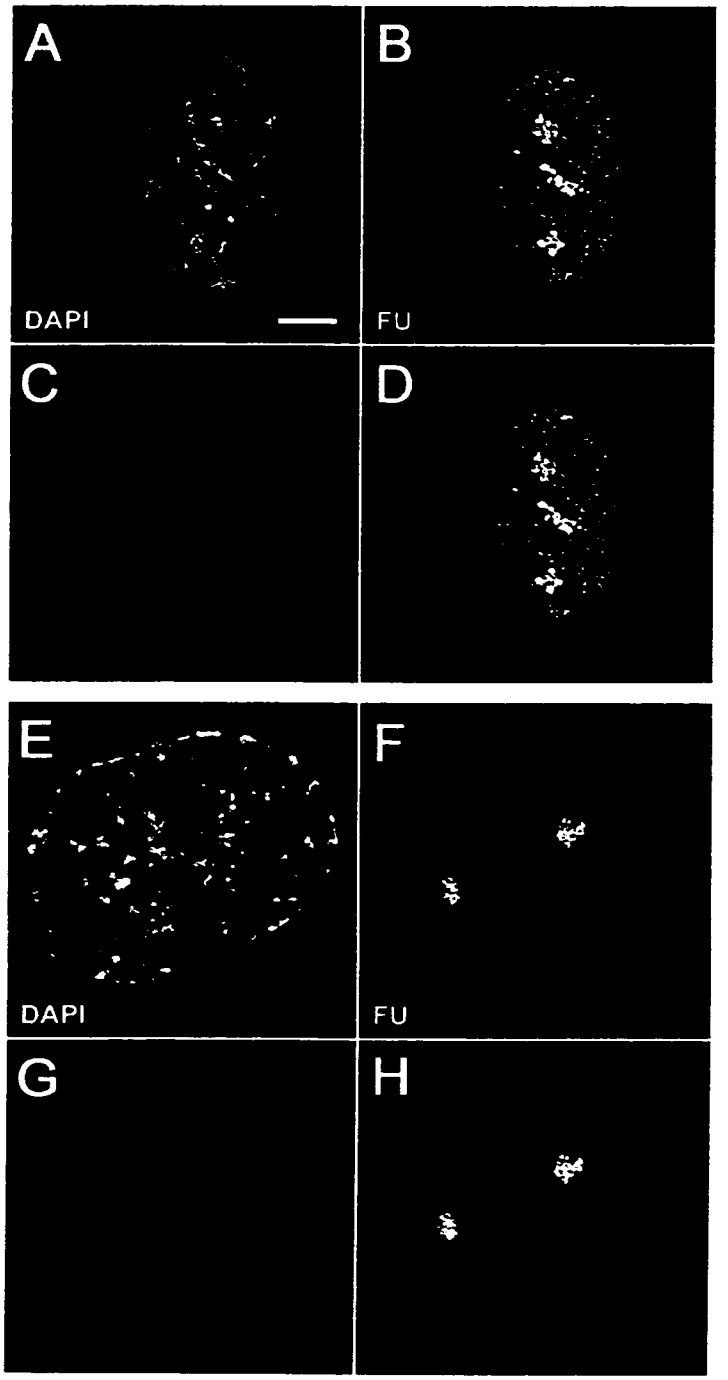

Figure 12: RNA pol I is not significantly inhibited under conditions of DNA damage that induce translocation of ING1 to the nucleolus

Cells which had (D-F) or had not (A-C) been previously UV-irradiated were treated with different inhibitors of RNA polymerases (B,C,E,F) or left untreated (A,D) and then allowed to incorporate 5-fluorouridine (5-FU). DRB does not block the transcription seen in nucleoli with or without UV irradiation (B,E) but does inhibit transcription in the nucleoplasm. However, actinomycin D (C,F) does inhibit nucleolar transcription in both untreated and UV irradiated cells. The scale bar represents 5 μm.

Figure 12: RNA pol I is not inhibited under conditions of DNA damage that induce translocation of $p33^{ING1b}$ to the nucleolus

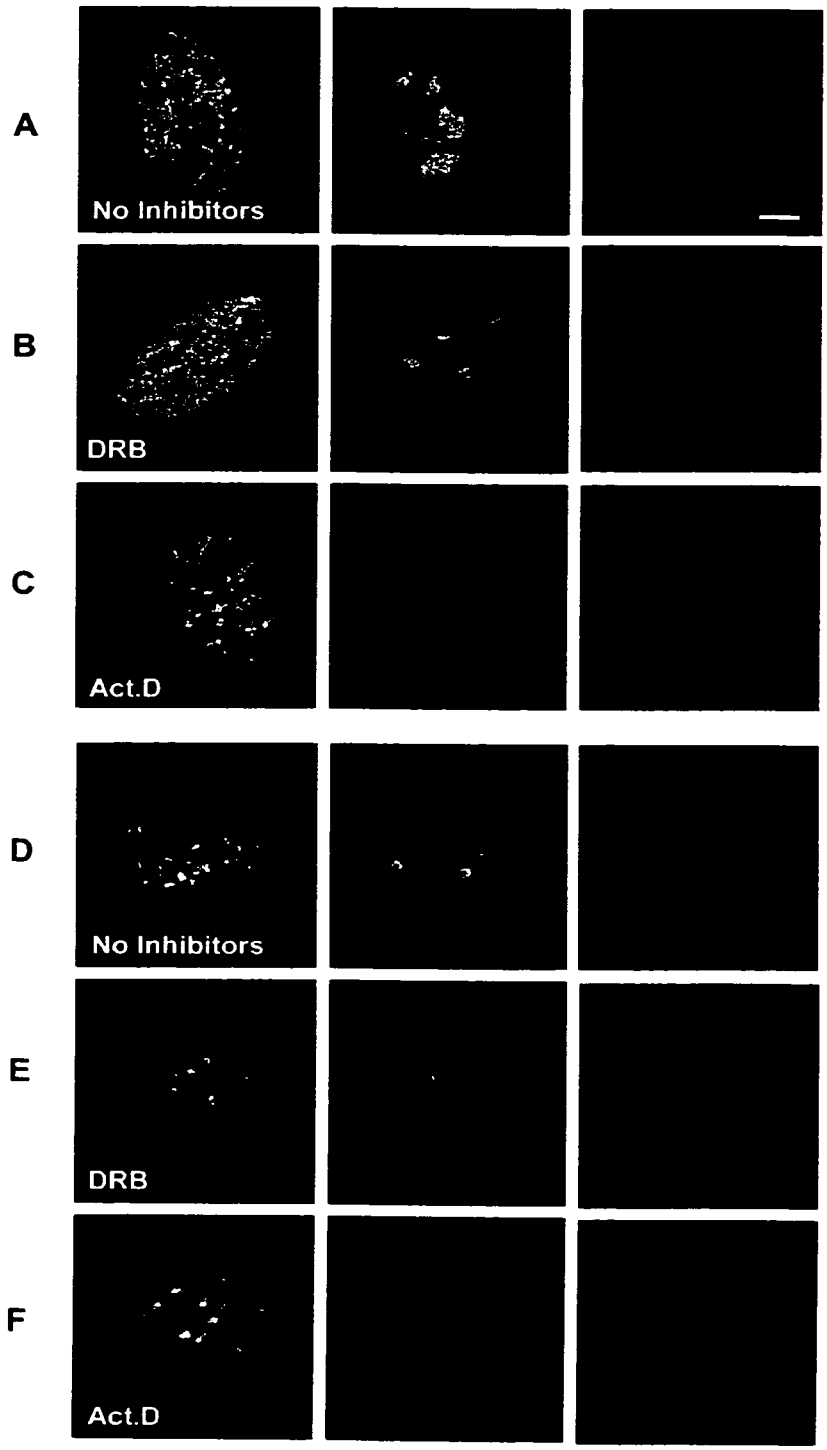

PART 2:

The nuclear matrix, mitosis and chromatin remodeling

ING1 proteins are tightly associated with the nuclear matrix

It is known that ING1 proteins localize to the nucleus in normal untreated cells (as shown in chapter 3, part I). To better characterize the subnuclear localization of the ING1 proteins in normal cells and to address the second hypothesis of the research project which was that ING1 proteins can bind the nuclear matrix because they are known to be very insoluble, a nuclear fractionation protocol (42) was performed on normal human diploid fibroblasts. This fractionation separates the protein into 5 subcellular groups (illustrated in figure 13):

1-cytoplasmic,

2-soluble nuclear and associated with DNA (87.4% of total nuclear proteins)

3-weakly associated with the nuclear matrix (4.4% of total nuclear proteins)

4-strongly associated with the RNA part of the nuclear matrix (3.3% of total nuclear protein)

5-strongly associated with the protein components of the matrix and the components of the matrix itself (4.9% of total nuclear protein)

In all the experiments in this section of my thesis work, these five fractions were loaded in different lanes of a gel to reflect the amount of protein of each fraction extracted from the same number of cells.

It is possible to show by western blot of extracts of log phase cells that ING1a and ING1b are mostly found in the fifth fraction (Fig.14A), which contains the proteins strongly associated with the nuclear matrix. PML, which is an integral component of the PML bodies and is known to be part of the nuclear matrix (10), is also found in fraction 5 (Fig.14B). p53 can be shown to be present in all the fractions though its amounts are greater in fractions 5 and 2 (Fig.14C). Cyclin D1 is found in the cytoplasmic fraction (fraction 1) as well as in the DNA-associated fraction (fraction 2) and associated with the proteinaceous part of the nuclear matrix (fraction 5) (Fig.14D). This is consistent with reports that indicate that cyclin D1 is cytoplasmic during S phase and soluble in the nucleus during the G1 phase

of the cell cycle (6). However, a subpopulation of cyclin D1 (approximately 20%) has also been shown to be present in an insoluble form in the nucleus, tightly bound to the nuclear matrix, with maximal levels during middle to late G1 phase (98). PCNA is found almost uniquely in fraction 1 (Fig.14E) as has been previously reported (50) and can only be detected in fraction 2 with very long exposures.

Cell cycle experiments suggest that the subnuclear localization of the ING1 proteins seen above probably depends on the phase of the cell cycle and whether the cells are responding to different forms of DNA damage. When cells are synchronized by serum starvation and then allowed to reach S phase, ING1b can be found primarily in fraction 5 but is also seen in fraction 2, with little difference in distribution seen between UV-irradiated and non-irradiated cells (Fig.15A). However, ING1a is not detected in fraction 5 but is present in much larger amounts than at other times in the cell cycle in fraction 2 (soluble nuclear proteins or proteins associated with DNA) with no significant difference between irradiated and non-irradiated cells (Fig.15A). Significant amounts of ING1a are also seen in the cytoplasmic fraction. PCNA can be shown to be more cytoplasmic than nuclear during S phase (though this may be due to contamination of the cytoplasmic fraction by the nucleus during the fractionation protocol) but seems to translocate to the nucleus in greater amounts when cells are irradiated with UV-inducing DNA damage (Fig.15B), consistent with PCNA's role in DNA repair (110). The same extracts used to study the ING1 and PCNA proteins were run on a gel which was stained with Coomassie (Fig.15C) to verify that the fractionation had been successful (by ensuring that the proportions of cells in all the fractions were adequate and similar in UV-irradiated and untreated cells). In contrast to other phases of the cell cycle, in quiescent cells, both ING1a and ING1b seem to be downregulated by UV-irradiation (Fig.16A) and additional, prominent ING1 antibody-reactive bands of approximately 40 and 60 kDa increase markedly in intensity. These may represent unique isoforms of ING1 or modified versions of ING1a or ING1b. Very little ING1b is present, both in UV-treated and untreated cells, whereas much more substantial amounts of ING1a can be seen in these

cells. PCNA can be detected almost uniquely in the cytoplasm of quiescent cells (Fig.16B). Another gel with protein from the same extracts was stained with Coomassie Blue to verify the similarity of fractionation in the absence and presence of UV irradiation (Fig.16C).

The ING1 proteins are retained in the nucleus late during mitosis

Immunofluorescence microscopy of SK-N-SH cells shows ING1 proteins to be nuclear but not cytoplasmic or nucleolar throughout interphase (Fig.17A). During mitosis, these proteins can be shown to remain in the nucleus in prophase (Fig.17B) but they start to leave the nucleus in pro-metaphase (Fig.17C), which is when the nuclear envelope breaks down (29). During metaphase (Fig.17D) and anaphase (Fig.17E) ING1 proteins seem uniformly distributed throughout the cell. They reenter the nuclei of the daughter cells in telophase (Fig.17F), at the same time as the nuclear envelope starts to reform around the chromosomes (37, 82).

When compared to other proteins, ING1 seems to stay associated longer with nuclear structures prior to nuclear membrane dissolution. Furthermore, p53 and ING1 do not leave and reenter the nucleus during the same phases of mitosis. p53 has already started to leave the nucleus in prophase while ING1 proteins are still only detected in the nucleus (Fig.18E). In addition, ING1 reenters the nucleus before p53 as the nuclear envelope reforms. For example, as shown in figure19, p53 has not completely reentered within the nucleus in telophase whereas ING1 proteins are only found in the nucleus at this time (Fig.19E). ING1 proteins spend more time associated with nuclear structures during mitosis than p53 does.

The ING1 proteins reenter the nucleus when acetylation of histones increases after mitosis

When SK-N-SH cells in log phase are fixed and stained, it is possible to show that ING1 proteins become associated with nuclear structures at the same time as acetylation of histones increases, during telophase (Fig.20). Not all nuclear proteins have reentered the nucleus at this time but one study

demonstrates that acetylation of histones increases when HATs reenter within the nucleus (62).

In parallel to this observation, it is also possible to show that in prometaphase, when some ING1 has already left the nuclear structures, the ING1 still present in the nuclear space segregates to regions devoid of condensed chromosomes (Fig.20). This is also observed with HATs, which are shown to avoid regions of condensed chromosomes during this phase of mitosis (62).

Overexpression of ING1a and ING1b modifies histone acetylation *in vivo*

When ING1b expression constructs were microinjected into the nuclei of Hs68 cells, it was observed that 24 hours after the plasmids entered the cells, the levels of acetylation of histones H3 and H4 significantly increased (Fig.21L and H). This increase was estimated to be 2.7 and 2.8 fold for histones H3 and H4 respectively using ERGOvista software v4.4. The acetylation status of these histones was detected by antibodies that recognize specific acetylated lysine residues, which are the last residues to be acetylated by histone acetyltransferases. These specific residues are thus a good indicator of hyperacetylation of their respective histones and regulation of the acetylation status of these lysine residues is believed to contribute significantly to regulation of chromatin conformation. Overexpression of ING1b clearly increases the amount of hyperacetylated histones H3 and H4. It does not, however, modify the levels of acetylation of histone H2b (data not shown), which indicates that the effect is histone-specific.

In contrast, overexpression of ING1a causes a noticeable and reproducible decrease of histones H3 and H4 acetylation, which can be estimated to be between 35 and 55% by ERGOvista software v4.4 (data not shown and Fig.21D). Similarly to ING1b, ING1a does not modify the acetylation pattern of histone H2b. Microinjection of empty vector does not modify the acetylation pattern of any of the histones, which indicates that it is not the microinjection and overexpression

procedures themselves that are responsible for the changes (Fig.21P). The relative intensities of the changes are compared for several injected cells in figure 22.

ING1b contains part of a bromodomain motif

Bromodomains are highly conserved sequences (46) that allow recognition of specific acetylated lysines on other proteins, and are found in many proteins involved in chromatin remodeling (25, 54). Since we found that ING1 isoforms could affect histone acetylation, we next asked whether ING1 might contain such a domain. The study of the amino acid sequence of ING1 reveals that the ING1b isoform contains a significant part of a bromodomain motif. This motif is very long (more than 100 amino acids) and specifies a four-helix bundle with a left-handed twist (25). ING1b possesses approximately 40 amino acids of a bromodomain with a high degree of conservation of the key residues. The bromodomain found in ING1 is compared to other proteins in figure 23.

Figure 13: Cellular fractionation protocol to obtain the nuclear matrix

This fractionation protocol separates cellular proteins into 5 fractions as previously described (42). Fraction 1 contains the cytoplasmic proteins and is obtained by hypotonic lysis. Fraction 2 contains all soluble nuclear proteins and proteins associated with DNA. Fraction 3 represents proteins weakly attached to the nuclear matrix. These proteins are washed off the matrix by a 2M NaCl treatment. Fraction 4 contains proteins associated with the RNA part of the nuclear matrix (these proteins are washed off the matrix by an RNase A and T treatment). Fraction 5 contains proteins strongly associated with the nuclear matrix and the proteins that are part of the matrix itself.

Figure 13: Cellular fractionation protocol to obtain the nuclear matrix

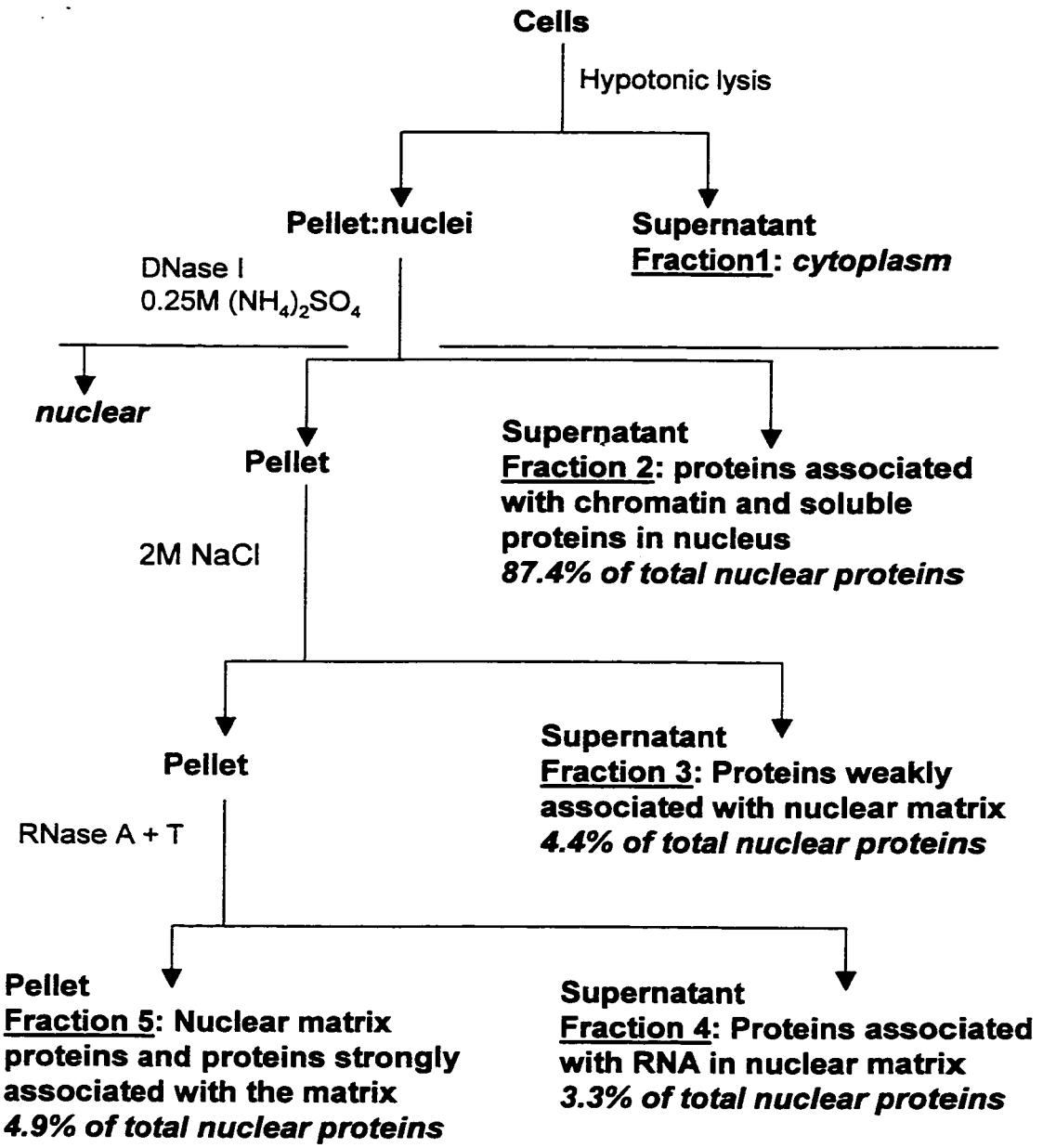

Figure 14: ING1 proteins are tightly associated with the nuclear matrix

Log phase normal diploid fibroblasts were harvested and their protein was separated into 5 different groups following the protocol outlined in figure 13. The different fractions were run on a SDS-PAGE gel and transferred to a nitrocellulose membrane, which was probed with different antibodies. ING1 proteins are mostly found in fraction 5 (strongly associated with the nuclear matrix) but are also present in fractions 2 (soluble and chromatin-associated proteins of the nucleus) and 4 (strongly associated with the RNA part of the matrix) (A). PML is present exclusively in fraction 5 (B). p53 can be shown in all fractions (C). Cyclin D1 is found mostly in fraction 1 (cytoplasmic proteins) but is also present in fractions 2 and 5 (D). PCNA is found in fraction 1 (E).

Figure 14: ING1 proteins are tightly associated with the nuclear matrix

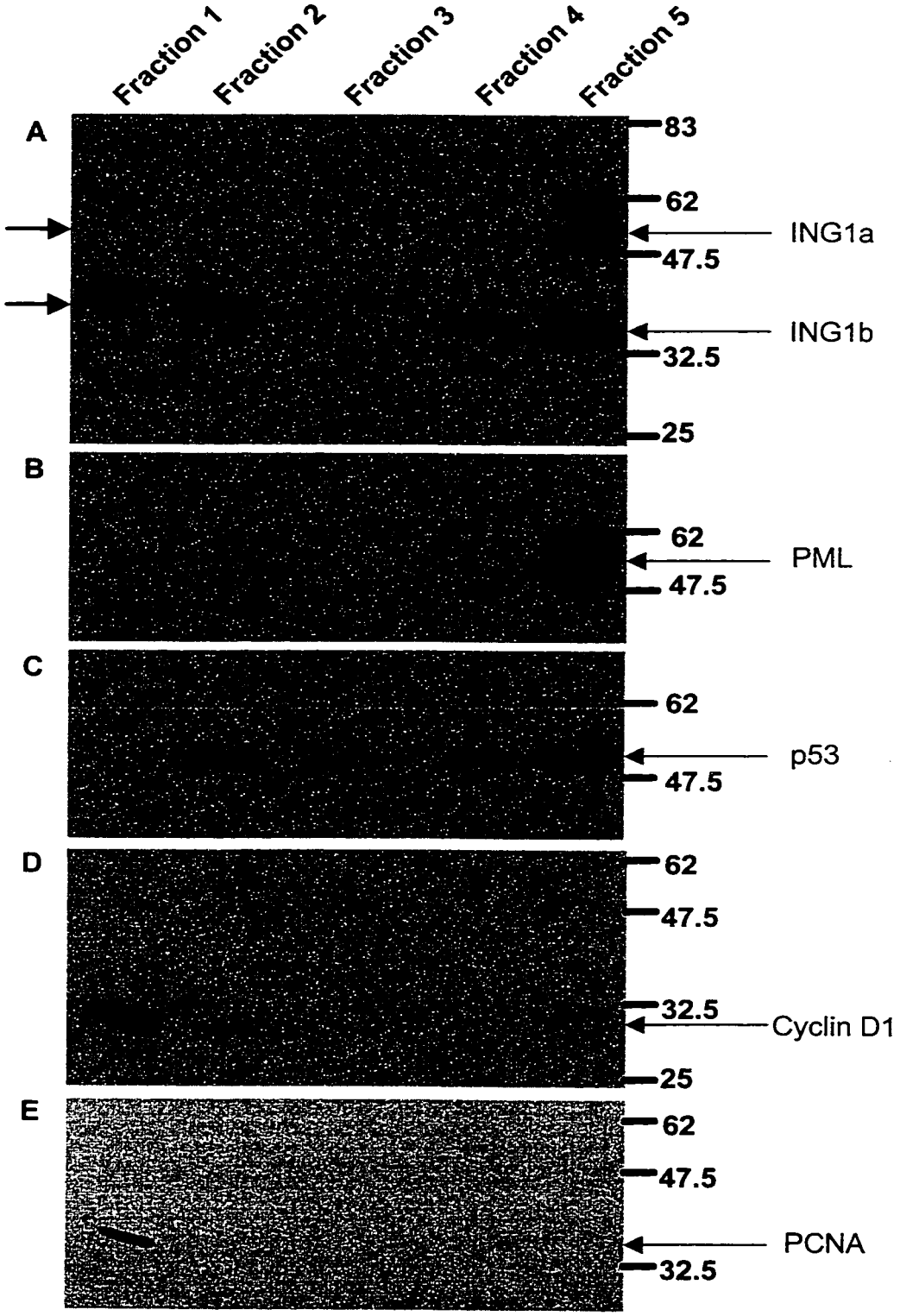

Figure 15: Distribution of the ING1 proteins in S phase

Normal diploid fibroblasts synchronized in S phase and UV irradiated or not, were harvested and their protein was separated into 5 different fractions following the protocol outlined in figure 13. Fractions were run on an SDS-PAGE gel and transferred to a nitrocellulose membrane, which was probed with antibodies against ING1 (A) and PCNA (B). ING1a can be shown to be mostly in fraction 2 in S phase cells whereas ING1b is divided between fractions 2 and 5 (A). Asterisks indicate ING1 antibody-reactive bands that increase in relative proportions upon serum starvation. PCNA is present in fractions 1 and 2. A duplicate gel was stained with Coomassie blue to visualize the results of the fractionation procedure (C).

Figure 15: Distribution of the ING1 proteins in S phase

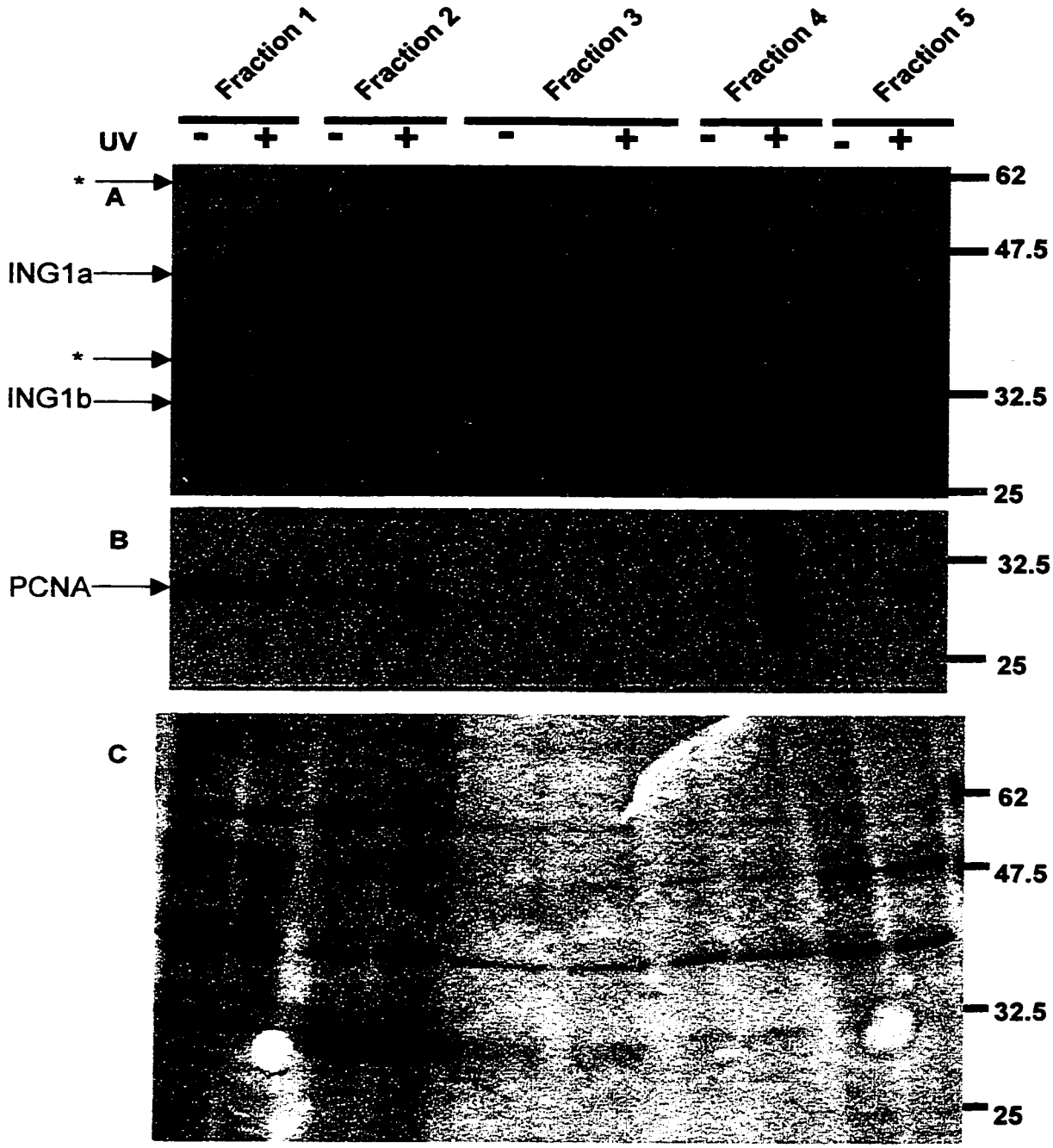

Figure 16: Distribution of the ING1 proteins in quiescent cells

Quiescent normal diploid fibroblasts which were UV irradiated or not, were harvested and their protein was separated into 5 different groups following the protocol outlined in figure 13. The different fractions were run on an SDS-PAGE gel and transferred to a nitrocellulose membrane, which was probed with antibodies against ING1 (A) and PCNA (B). ING1a can be shown to be mostly in fractions 1 and 2 in UV-irradiated cells but is present in fractions 1, 2 and 5 in untreated cells. ING1b is mostly in fraction 5 in untreated cells and its amounts seem to decrease in fraction 5 in UV-irradiated cells (A). Asterisks indicate ING1 antibody-reactive bands that increase in relative proportions upon serum starvation. PCNA is present almost uniquely in fraction 1 (B). Another gel was Coomassie stained to very the fractionation procedure (C).

Figure 16: Distribution of the ING1 proteins in quiescent cells

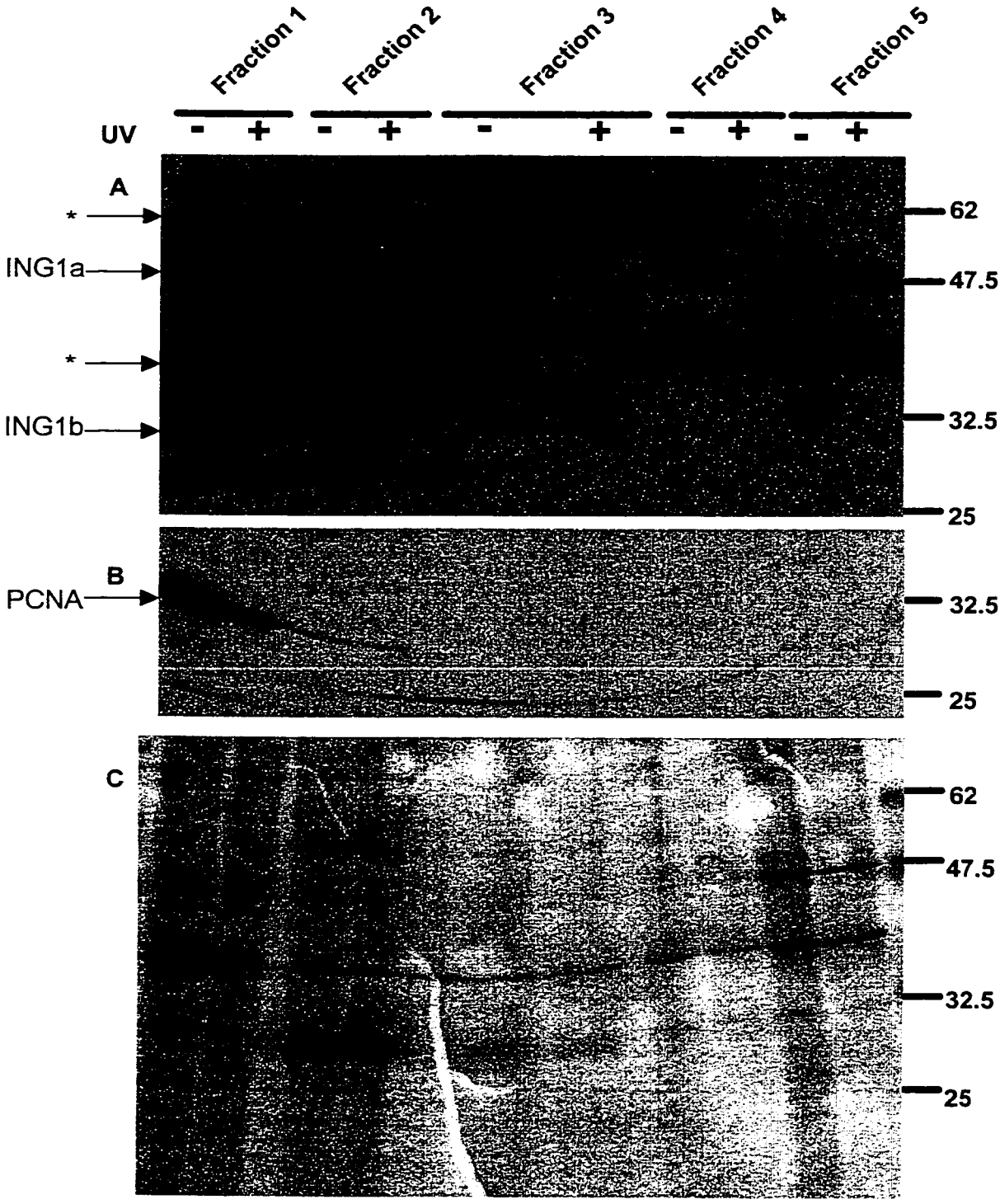

Figure 17: Subcellular localization of ING1 during mitosis

SK-N-SH cells were fixed and stained for ING1 proteins and DNA (DAPI). ING1 proteins are nuclear during interphase (A) and prophase (B) but start dissociating from nuclear structures in pro-metaphase (C) and remain distributed throughout the cell in metaphase (D) and anaphase (E). They reassociate with nuclear structures in telophase (F). The scale bar represents 5 μm.

Figure 17: Subcellular localization of ING1 during mitosis

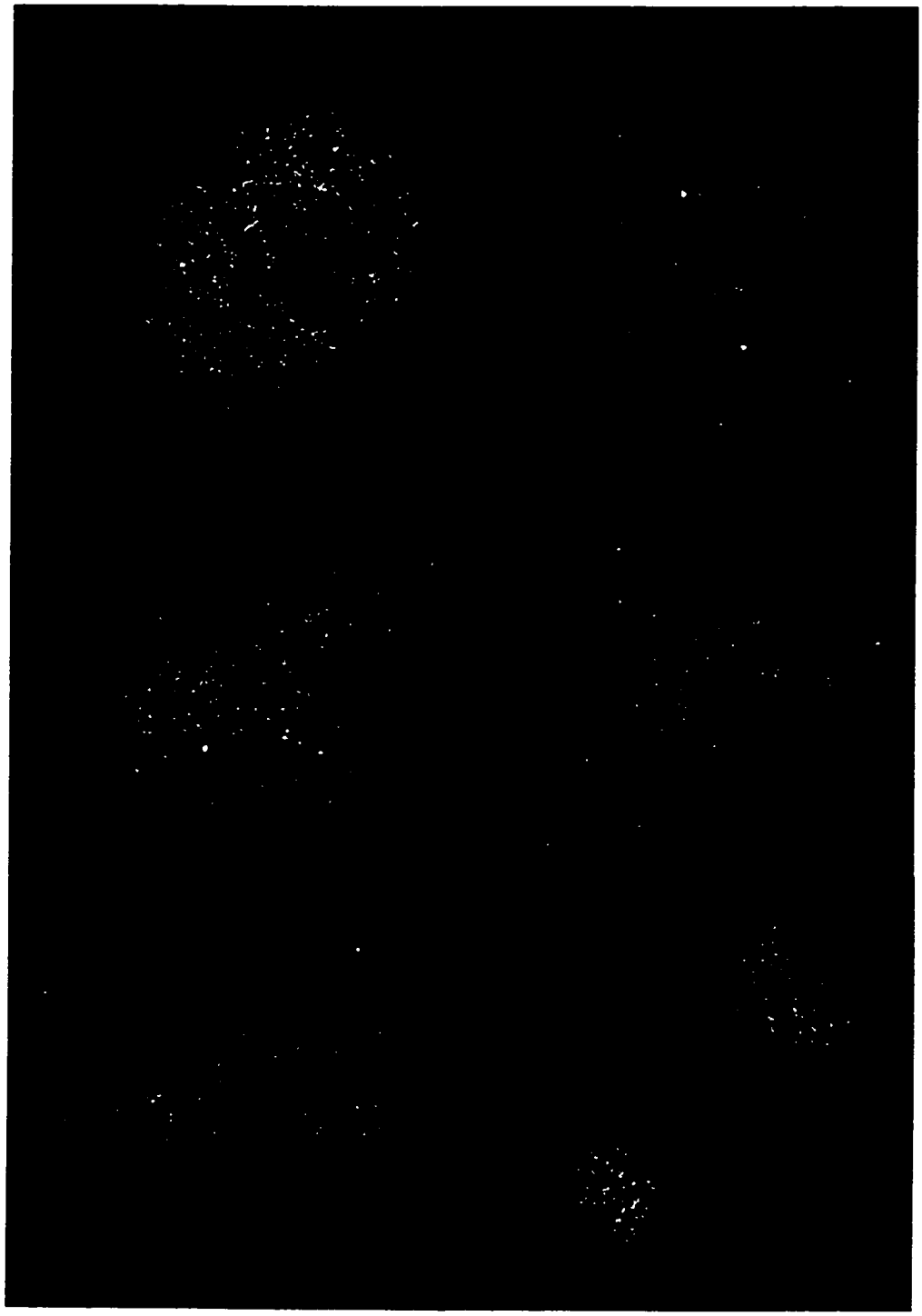

Figure 18: ING1 but not p53 is associated with nuclear structures in prophase

SK-N-SH cells, which are wild type for p53, were fixed and stained for ING1 proteins (green), p53 (red) and DNA (DAPI in blue). In prophase, ING1 is still associated with nuclear structures (C) but p53 is distributed throughout the cell (A). The two proteins do not colocalize during prophase and appear to occupy separate compartments within the cell (E). The scale bar represents 5 μm.

Figure 18: ING1 but not p53 is associated with nuclear structures in prophase

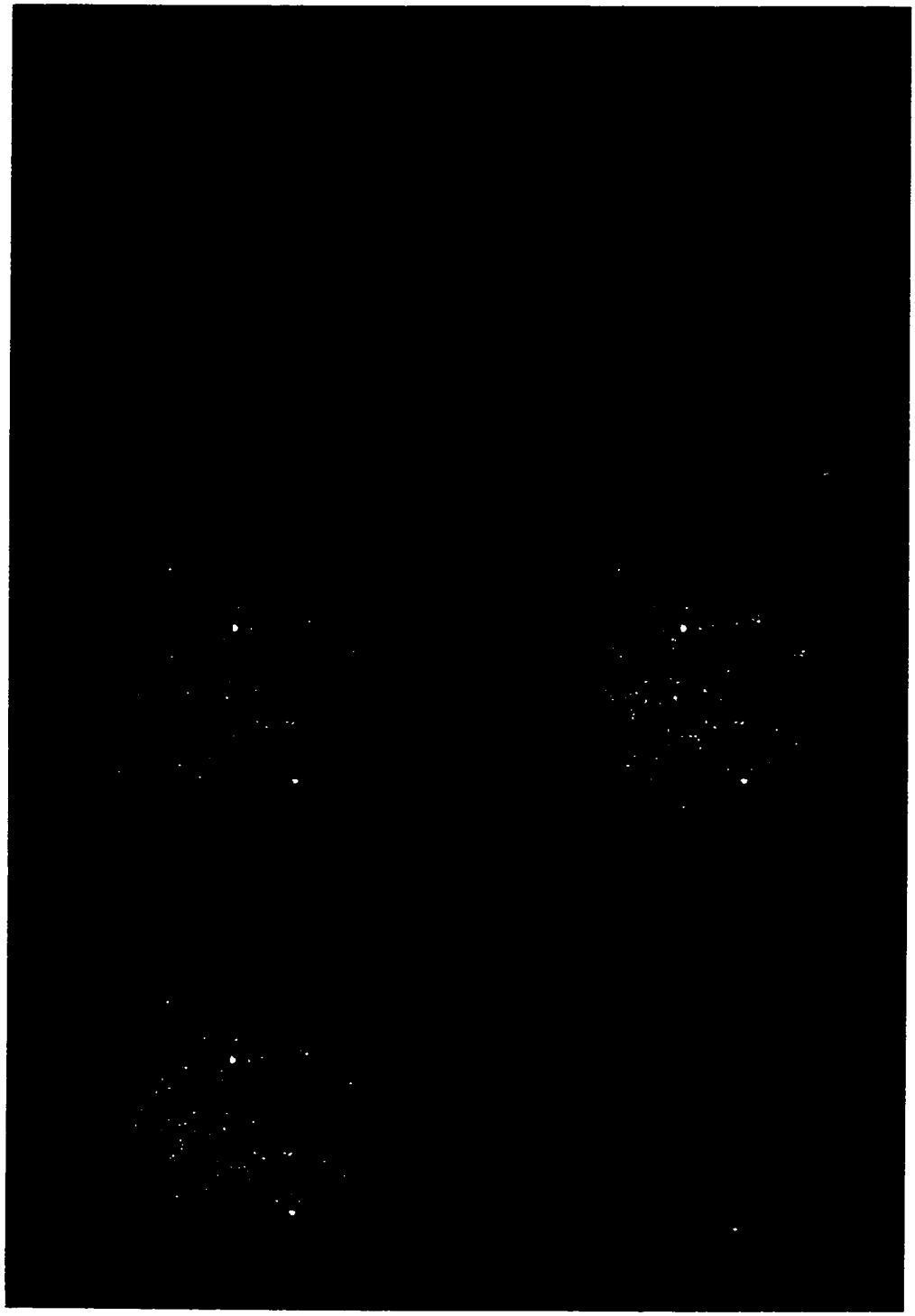

Figure 19: ING1 but not p53 is associated with nuclear structures in telophase

SK-N-SH cells were fixed and stained for ING1 proteins (green), p53 (red) and DNA (DAPI in blue). In telophase, ING1 is already associated with nuclear structures (C) but p53 is distributed throughout the cell, including at the intracellular bridge (A). The two proteins do not colocalize during telophase (E), similar to what is seen at other phases of mitosis. The scale bar represents 5 μm.

Figure 19: ING1 but not p53 is associated with nuclear structures in telophase

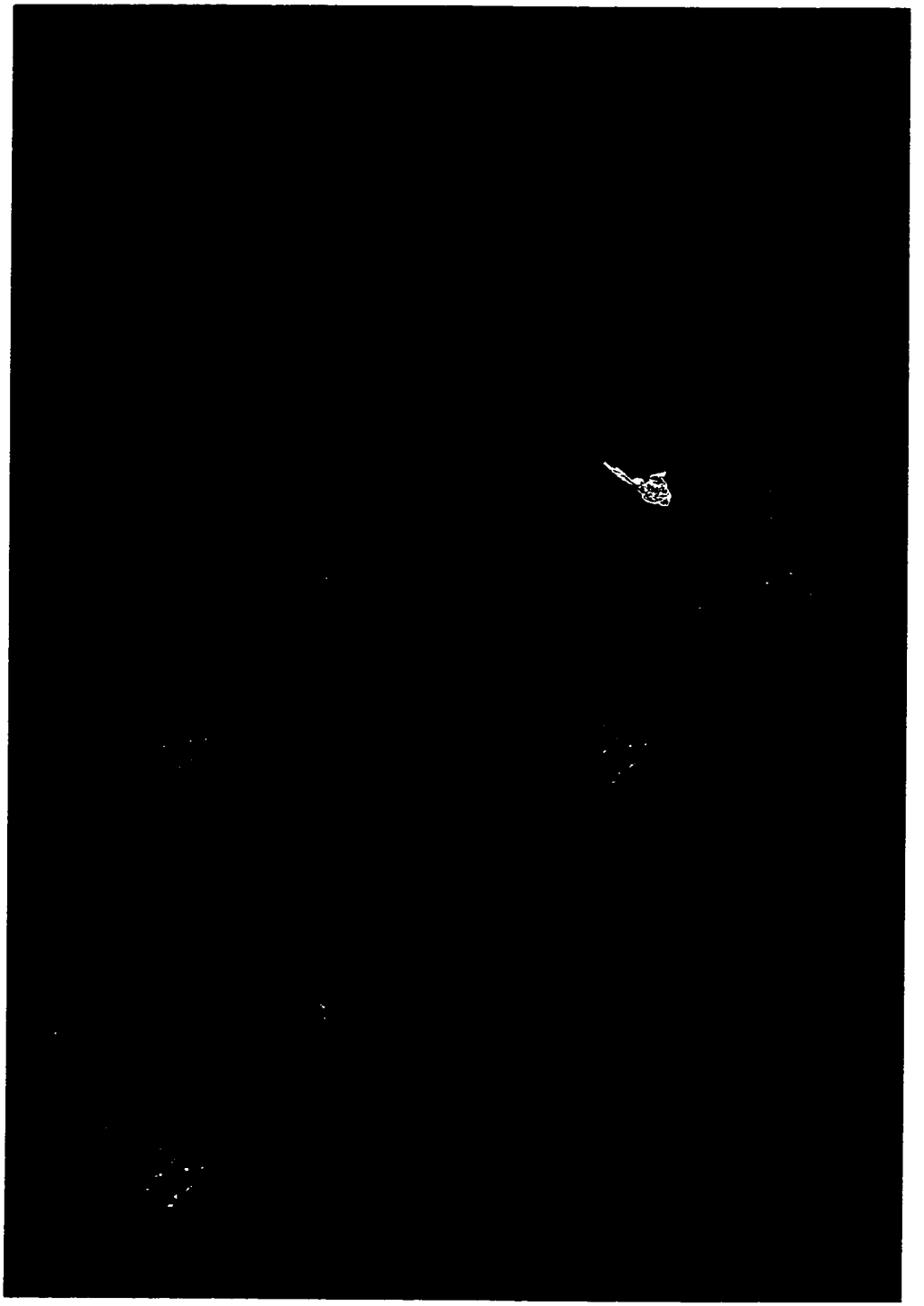

Figure 20: ING1 and acetylation during mitosis

SK-N-SH cells were fixed and stained for ING1 proteins (green), hyperacetylated histone H4 (red) and DNA (DAPI in blue). In pro-metaphase (A-C), ING1 is distributed throughout the cell (B) but seems to avoid regions of condensed chromatin (B compared to A) and histone H4 (C) can be shown to colocalize to a significant degree with DNA (C compared to A). In telophase (D-F), ING1 proteins are already associated with nuclear structures (E). Telophase is the phase of mitosis when acetylation of histones increases (F and (62)). The scale bar represents 5 μm.

Figure 20: ING1 and acetylation during mitosis

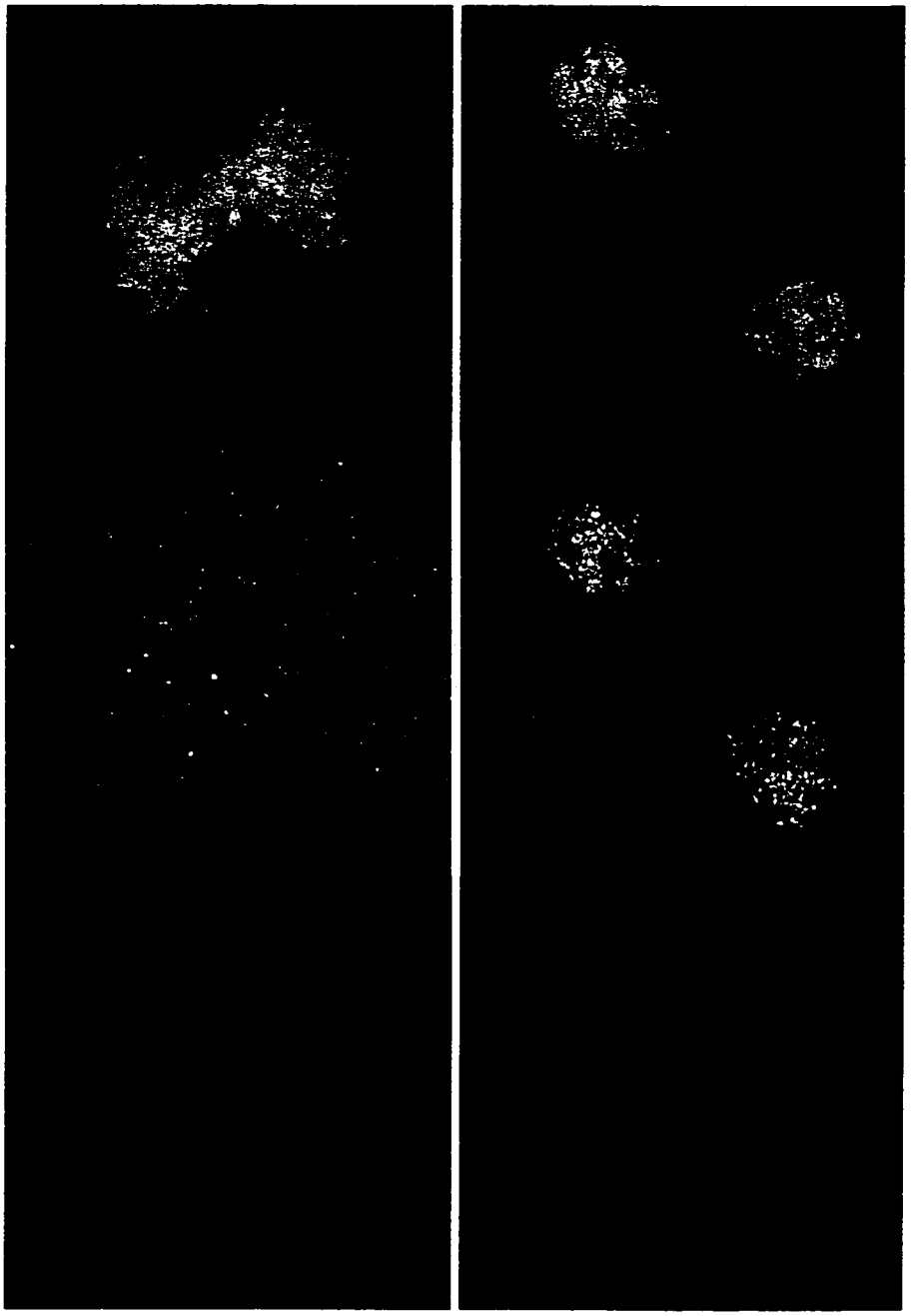

Figure 21: ING1 proteins regulate acetylation of histones *in vivo*

Expression constructs encoding green fluorescent protein (GFP) as well as ING1a, ING1b or pCI empty vector control were microinjected into the nuclei of Hs68 cells which were then allowed to express the protein for 24 hours. They were then fixed and stained for DNA (DAPI), ING1 and hyper-acetylated histones H3 (AcH3) or H4 (AcH4). When ING1a constructs are injected into cells (C), acetylation of histones decreases (D). However, when ING1b constructs are injected into cells (G,K), acetylation of histones increases markedly (H,L). Acetylation of histones does not significantly change when cells are microinjected with empty vector (P). GFP (B,F,J,N) is shown to confirm which cells were microinjected. The large arrows (D,H,L,P) point to cells that were microinjected with the indicated expression constructs. The small arrows (D,H,L,P) point to cells that were not microinjected with expression constructs. The scale bar represents 15 μm.

Figure 21: ING1 proteins regulate acetylation of histones *in vivo*

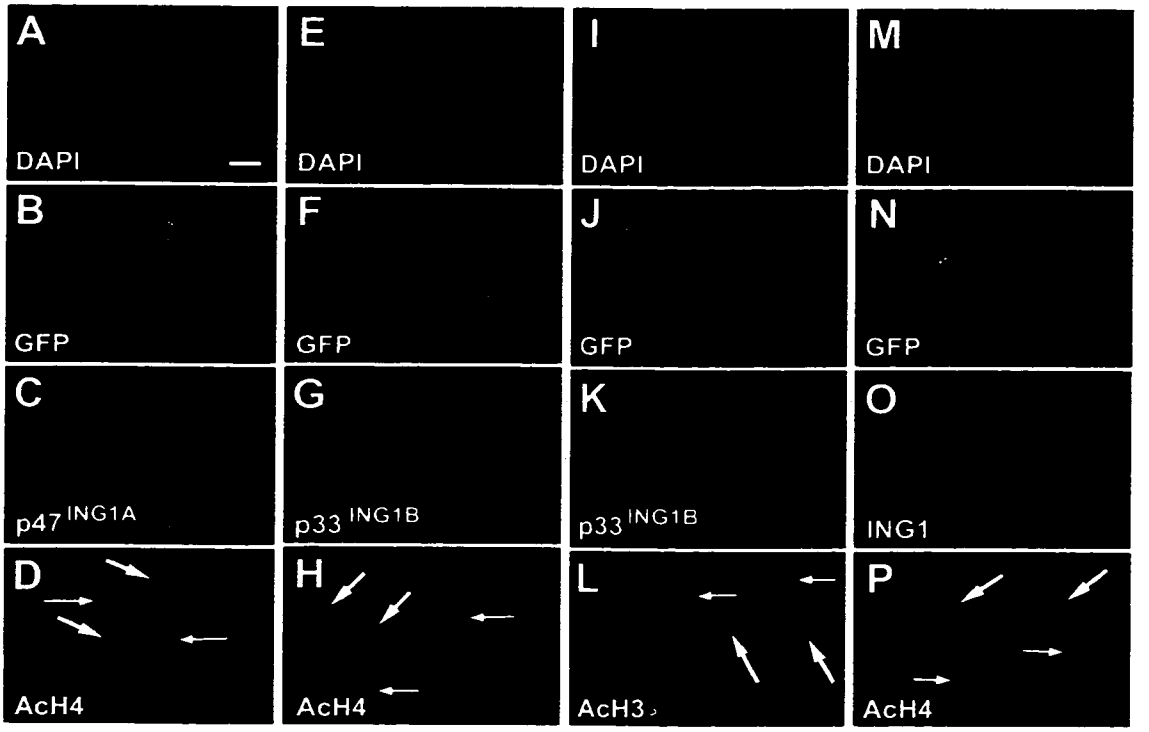

Figure 22: Relative levels of histones H3 and H4 acetylation after microinjection of ING1a and ING1b

The relative intensities of histone acetylation of cells microinjected with either empty vector, ING1a expression construct or ING1b expression construct were compared. The error bars represent the standard deviation between 10 different cells in each case. Acetylation of histones H3 and H4 can be shown to increase by 2.7 and 2.8 -fold (170% and 180% increase respectively) when cells are microinjected with ING1b, and to decrease by 55 and 35%, respectively, when cells are microinjected with ING1a.

Figure 22: Relative levels of histones H3 and H4 acetylation after microinjection of ING1a and ING1b

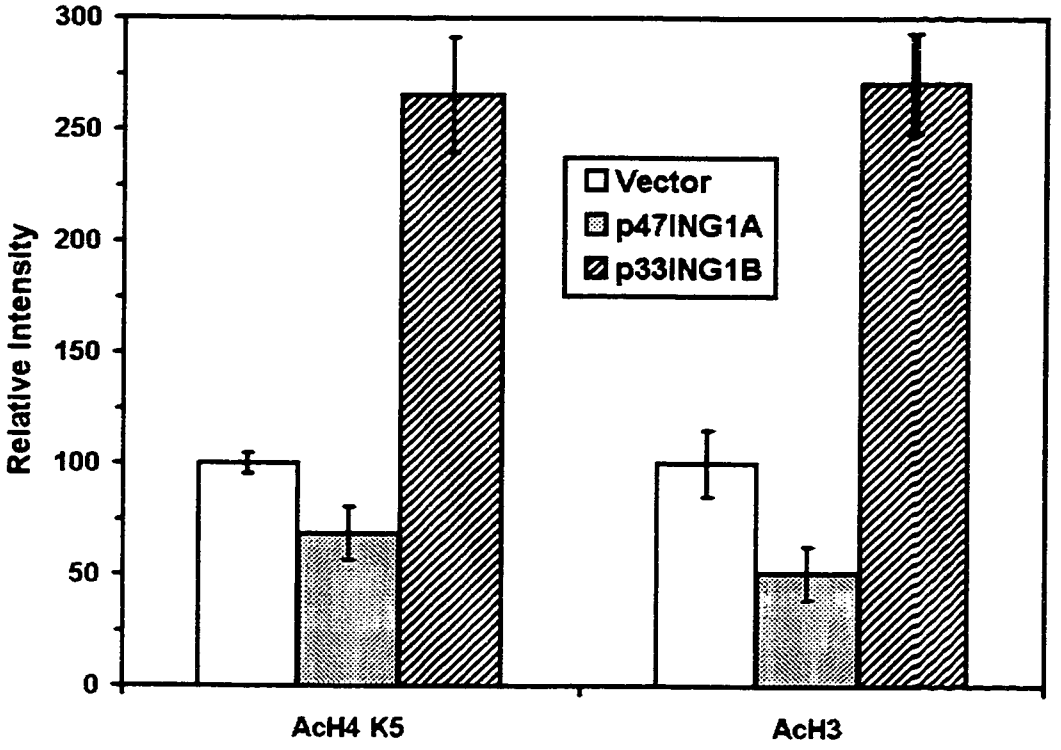

Figure 23: ING1b contains part of a bromodomain motif

The ING1b isoform contains 40 amino acids with similarity to bromodomain motifs. This region is compared to other proteins that contain full bromodomains. The residues in bold are identical in at least 9 of the 10 proteins compared. The GenBank accession numbers of the other proteins are: hsGCN5 U57136, scGCN5 Q03330, hs p300 A54277, hsCBP S39162, hsP/CAF U57317, ttP55 U47321, scBDF1 P3817, hsCCG1 P21675. h represents hydrophobic residues, a and b indicate respectively aromatic and basic residues and X can be any residue.

Figure 23: ING1b contains part of a bromodomain motif

ING1b	NYVE DYLDSIESL**P**F**D**LQRNVS LMR E I DAK**Y**QE I LKE L - **D** E CY
hsGCN5	D**Y**YE V IRF- - - - -**P** I **D**LKTMTER L R SR- -Y **Y**VT R KLF V A**D** L QR
scGCN5	DYYD F IKE- - - - -**PMDL**STME IK LE SN- - K **Y**QKM EDF I Y **D**A R L
hsp300	D**Y**FD I VKS- - - - -**PMDL**ST I KRK LD TG- - Q **Y**QEPWQY V **DD** I W L
hsCBP	D**Y**FD I VKN- - - - -**PMDL**ST I KRK LD TG- - Q **Y**QEPWQY V **DD**VW L
hsP/CAF	G**Y**YEV I RS- - - - -**PMDL**KTMSER LK NR- - Y **Y**VSK K L FM A**D**L Q R
ttP55	D**Y**YDV I TD- - - - -**P** I **D**I K AI EKK LQ NN- - Q **Y**VDK DQF I K**D**V K R
scBDF1-1	F**Y** FNYI KR- - - - -**PMDL**S T I ERK LN VG- -A **Y**E VP EQ I T E **D**F N L
hsCCG1-1	D**Y**YK I I TR- - - - -**PMDL**Q TL RENVR KR- - L **Y**PSR EE FR E HL E L
hsGCC1-2	D**Y**YKV I VN- - - - -**PMDL**E T I RKN IS KH - -K **Y**QSR ES F L D **D**V N L
Consensus sequence:	D**Y**Y**E** hh XXXXXX**P**h**DLS** T h Xb b hXXX XX**K** **Y**Q**E**X EX a h D **D**X X L $\widehat{D}$ $\widehat{Q}$ $\widehat{Q}$ $\widehat{S}$

PART 3:

The cloning and analysis of 5 novel ING1 transcripts isolated from mouse brain

Expression of ING1 isoforms in different mouse tissues

As a first step towards understanding the different biological and biochemical effects seen with different ING1 isoforms and to address the last hypothesis of the research project, I next began to clone additional isoforms of ING1 to get some idea of the total number of ING1 splicing isoforms that are generated. Poly A+ mRNA was isolated from frozen mouse and human tissues to examine the expression patterns of ING1. Many different mouse ING1 transcripts can be shown to exist by northern blot (Fig.24). As many as 9 different mouse ING1 transcripts are recognized by an RNA probe against the common region of the human gene (Fig.24A). The most strongly expressed of these transcripts have sizes of approximately 1.4kb and 2.6kb. However, most of the other bands were very faint. This could mean that they are not as highly expressed as the two other transcripts in the brain or perhaps that they are not as well recognized by the probe which would suggest that some of them may be transcripts from ING1 homologous genes. Considering that three ING1 related genes have recently been discovered and that the common region of these genes is very conserved, it would not be surprising if the probes recognize some of these sequences despite the fact that hybridization was done under high stringency conditions. Alternatively, the high GC content of the probe may preclude a good degree of hybridization specificity. All the transcripts recognized in mouse brain are present in liver (Fig.24A) but to a lesser extent.

Three major mouse transcripts are recognized by a probe against the unique region of the human ING1b isoform (Fig.24B). The most strongly expressed of these transcripts has a molecular size of approximately 1.9 kb which is very close to the actual size of the mouse ING1b transcript published by another group after these results were generated (122). No mouse transcripts were detected when the RNA probe against the unique region of the human ING1a transcript was used (Fig.24C). This is consistent with the fact that by RACE-PCR, neither our group nor Gudkov's group who has reported some ING1 sequences, has identified a mouse ING1a isoform (this is discussed in chapter 4). However, if

the mouse ING1a isoform does exist, it could be expressed exclusively in tissues that have not been examined to date.

Preparation of the cDNA sets

Because the northern blots showed that the mRNA was in good condition, it was then used to prepare cDNA sets with Clontech's Marathon cDNA amplification kit. This kit starts with reverse transcription of the mRNA followed by a second strand synthesis step. The resulting double stranded cDNA is then ligated at both ends to an adaptor. All these steps are performed with the experimental samples as well as with control placenta mRNA supplied with the kit. At the end of the procedure, the experimental double stranded adaptor ligated cDNA samples and the placenta control were run on an agarose gel with another control set supplied with the kit to verify if all the steps were successful and to make sure that the cDNA sets had the right size distribution (Fig.25). Later on, other human libraries were also generated.

Identification of new ING1 isoforms by 5' RACE-PCR

Because the 3' region of the ING1 gene is believed to be present in all the transcripts made from the gene, 5' RACE (rapid amplification of cDNA ends) PCR was performed from a primer in the common region of the gene, to find the sequences of the other isoforms. This primer was designed by Dr. Caren Helbing who previously used it to successfully isolate *Xenopus* homologues of ING1 by RACE-PCR. The resulting DNA amplified from the reaction appeared as a smear of approximately 600bp to 1.5 kb when run on an agarose gel (Fig.26), although some tissues, including human testis and to a lesser extent human brain, showed some very high molecular weight products (over 20kb). It is possible to see some distinct bands in the smears of figure 26. These bands as well as other parts of the smear were purified from the gel, ligated to the pGEM-T PCR cloning vector, and subsequently amplified in competent DH5α bacterial hosts. Minipreps of the plasmids of some of the resulting colonies were digested with restriction enzymes

to release the inserts and Southern blots with probes specific to the common region of the ING1 gene were performed in order to verify if the plasmids contained ING1 specific sequences (Fig.27). Some of the positive plasmids were sequenced and though a considerable number of plasmids had seemingly unrelated sequence, some contained potential new ING1 isoforms (like mING1b and mING1c in figure 27).

The first novel isoform to be cloned was the mouse homologue of human ING1b (Fig.28). Its sequence is very similar to human ING1b with an 88% identity between them. Following this, other primers in the ING1 conserved region were generated to perform nested PCR. Four additional new mouse ING1 transcripts were isolated (Fig.29). Interestingly, three of these transcripts (mING1c,e and f) will generate the same isoform, a protein with a predicted size of 26 kDa. This protein does not possess a 5' unique region, it only has most of the 3' common region of the ING1 proteins. The fourth transcript, mING1g encodes a 31 kDa protein which contains the 3' common region and a small 5' unique region. All together, these five novel transcripts encode three new mouse ING1 protein isoforms that are illustrated in figure 30.

Sequence analysis of the mouse isoforms

The three newly identified mouse ING1 isoforms were examined for different protein motifs by submitting their sequences to different databases. The PHD domain (indicated in *italics* in figure 30) was identified in the common region of the three isoforms. Apart from a few phosphorylation sites, no other protein motif was recognized by any of the databases. However, the nuclear/nucleolar targeting sequence identified in all human ING1 isoforms (part I of chapter 3) is also present in the three mouse ING1 isoforms (in bold in figure 30). As well, the PIP box present in the human ING1b isoform (part I of chapter 3) is also present in the mouse ING1b isoform (underlined in figure 30). It can thus by hypothesized that

the mouse ING1b isoform can translocate to the nucleolus and interact with PCNA as can the human ING1b isoform.

Cloning of the full length mouse ING1 transcripts in a mammalian expression vector

Since the novel ING1 transcripts were isolated by 5' RACE-PCR, they were lacking part of the 3' end common to all ING1 transcripts. The novel ING1 transcripts were thus ligated to the known mouse 3' end. Control 3' RACE-PCR experiments were performed to verify that these transcripts did indeed possess this 3' region. The complete transcripts were cloned into the pCI-neo mammalian expression vector.

Figure 24: Expression of ING1 in different mouse tissues

Poly A+ mRNA was isolated from different mouse tissues and run on a 1.4% agarose gel, which was transferred to a nitrocellulose membrane and probed with different RNA probes: the ING1 common region (A), the unique ING1b region (B) and the unique ING1a region (C). As many as 9 different mouse ING1 transcripts isolated from the brain (b) are recognized by an RNA probe against the common region of the human gene (A). The most strongly expressed of these transcripts have sizes of approximately 1.4kb and 2.6kb. All the transcripts recognized by the common region probe in mouse brain (b) are present in liver (l) but to a lesser extent. Three major transcripts are recognized by a probe against the unique region of the human ING1b isoform, in both brain and liver (B). The most strongly expressed of these transcripts has a size of approximately 1.9kb. No mouse transcripts were detected when the RNA probe against the unique region of the human ING1a transcript was used (C).

Figure 24: Expression of ING1 in different mouse tissues

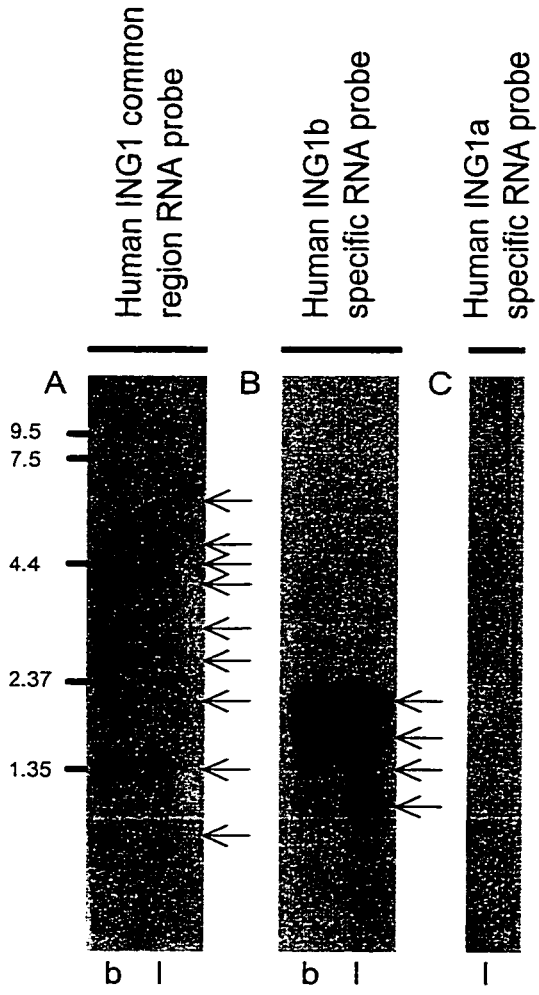

Figure 25: Mouse brain adaptor ligated cDNA set

The mouse brain adaptor ligated cDNA set made with Clontech's Marathon procedure was run on a gel and photographed. The size distribution is in the right range as compared with the placenta cDNA set provided with the kit.

Figure 25: Mouse brain adaptor ligated cDNA set

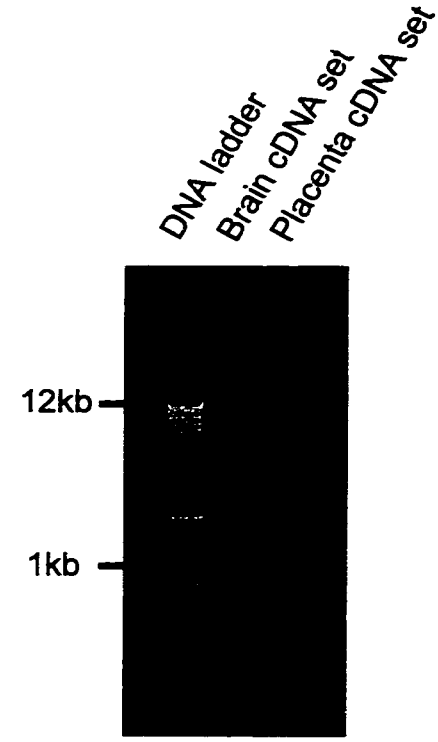

Figure 26: ING1 specific 5' RACE products

5' RACE PCR was performed on the mouse brain, human brain, human testis and human placenta adaptor ligated cDNA sets. These RACE products were then run on a gel and photographed. The majority of products range in size from 600bp to 2kb. However, some products are much larger, up to over 20kb (in human testis more prominently but also in human brain).

Figure 26: ING1 specific 5' RACE products

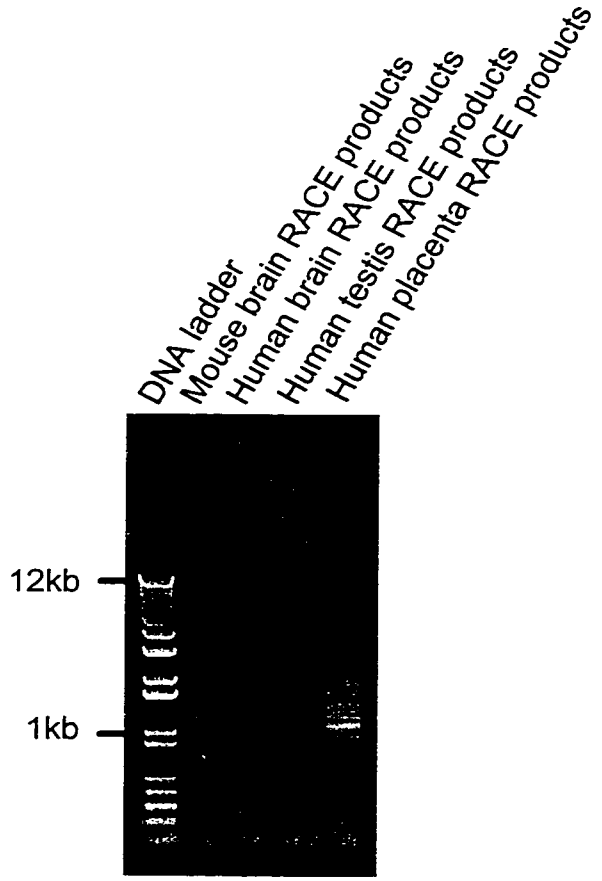

Figure 27: Southern blot of 5' RACE products cloned into pGEM-T and hybridized with an ING1 specific probe

5' RACE-PCR products were purified from the gel and ligated into the PCR cloning vector pGEM-T. Competent DH5α bacteria were transformed with these plasmids and some of the resulting colonies were amplified and minipreps were performed with them. The minipreps were digested with ApaI and then run on a gel that was transferred to a membrane and probed with an ING1 specific probe. Two of the minipreps contained ING1 sequences, mouse ING1b and mouse ING1c.

Figure 27: Southern blot of 5' RACE products cloned into pGEM-T and hybridized with an ING1 specific probe

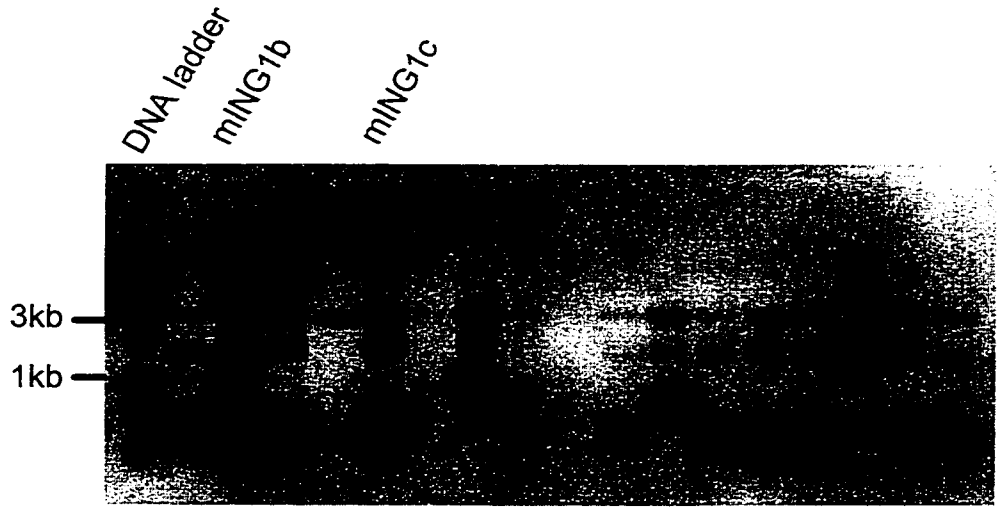

Figure 28: Sequence comparison of human and mouse ING1b

The newly discovered mouse ING1b is compared to its human homologue, $p33^{ING1b}$. This protein is very conserved among species. It is 88% identical between mouse and human. The differing residues are indicated by an asterisk. The nucleolar/nuclear targeting signals and the PHD domain, indicated respectively by bold and italic letters, are completely identical. The PIP box (underlined) is also very conserved between the two species.

Figure 28: Sequence comparison of human and mouse ING1b

mouse MLSPANGEQI HLVNY VEDYLDSIESLPFDLQRNVSLMREIDAKY[44]

human MLSPANGEQLHLVNY VEDYLDSIESLPFDLQRNVSLMREIDAKY[44]

mouse QEILKELDDYYEKFKRETDGTQKRR VLHC IQRALIRSQELGDEK[88]

human QEILKELDECYERFSRETDGAQKRRMLHCVQRALIRSQELPNEK[88]

mouse IQIVSQMVELVENRSRQVDSHVELFEAHQDI SDGTGGSGKAGQD[132]

human IQIVSQMVELVENRTRQVDSHVELFEAQQELGDTAGNSGKViGAD[132]

mouse KSKSE AI TQADKPNNKRS**RRQR**NNENRENASNNHDHDD I TSGT[175]

human RPKGDAVAQSDKPNSKRS**RRQR**NNENRENASSNHDHDDGASGT[175]

mouse P**KEKK**AKTS**KKKK**RSKAKAEREASPADFPIDPNEP*TYCLCNQV*[218]

human P**KEKK**AKTS**KKKK**RSKAKAEREASPADLPIDPNEP*TYCLCNQV*[218]

mouse *SYGEMIGCDNDECPIEWFHFSCVGLNHKPKGKWYCPKCR*GES[260]

human *SYGEMIGCDNDECPIEWFHFSCVGLNHKPKGKWYCPKCR*GEN[260]

mouse EKTMDKALEKSKKERAYNR[279]

human EKTMDKALEKSKKERAYNR[279]

Figure 29: Newly identified mouse ING1 transcripts

Five different mouse ING1 transcripts have been identified to date. All five transcripts have a 5' unique region and share a common 3' exon. ING1b and ING1g both possess an in-frame ATG in their 5' unique region and thus encode different proteins. ING1c, e and f do not possess an in frame ATG in their unique region and thus can probably only specify a protein initiated from an ATG in the common 3' exon. These three different transcripts thus encode one unique protein. Start codons are in bold letters and stop codons are underlined. The 5' end of all the transcripts illustrated here only starts at the last stop codon present before the first start codon of the transcripts due to a lack of space and uncertainty regarding the actual transcriptional initiation site. However, more 5' untranslated sequence is known for all of these isoforms.

Figure 29: Newly identified mouse ING1 transcripts

ING1b tgaacc**ATG**TTGAGTCCTGCCAACGGGGAGCAGATCC
ACCTGGTGAACTATGTGGAGGATTACCTGGACTCAA
TCGAGTCACTGCCTTTCGACCTGCAGAGGAACGTCT
CGCTGATGCGGGAGATCGACGCCAAATACCAAGAG

ING1c taggctgagtggatcgcggccactttccggctgcgaggctatggcggcggtg
gcctccgggaggatgctgcgcttaccttctctgctctggctccccgcgggagcc
tctgatcgcttgtcgcgtttccgag

ING1e tagcccagcggagggtggttcttctcagag

ING1f taatgcctctcgcttctgtctgcagag

ING1g taatag**ATG**GCAAAAAGGTCTCAAGGAAAATCTGATAC
CATTTACTGTTTGAGAAAAATACTCTTGGAGTTTTCT
GAG

mouse ING1 common 3' exon ATCCTGAAGGAGCTGGACGACTACTATGAGAAGTTC
AAACGGGAGACAGCGGCACCCAGAAGCGCCGGGTA
CTGCACTGCATCCAGAGGGCCCTGATCCGCAGCCA
GGAGCTAGGCGATGAGAAGATCCAGATCGTGAGTC
AG**ATG**GTGGAGCTGGTGGAGAACCGCAGCAGACAG
GTGGACAGTCACGTGGAGCTCTTCGAAGCACACCAG
GACATCAGTGACGGCACTGGTGGCAGCGGCAAGGC
GGGCCAGGACAAGTCGAAGAGTGAGGCCATGACAC
AGGCAGATAAGCCGAATAACAAGCGGTCCAGGAGG
CAGCGAAACAATGAGAATCGAGAGAACGCGTCGAAT
AATCACGACCATGATGACATCACCTCAGGAACGCCC
AAGGAGAAGAAAGCAAAAACCTCAAAGAAGAAGAAG
CGCTCCAAGGCCAAAGCAGAGAGGGAAGCGTCTCC
TGCCGACCTTCCCATCGACCCCCAACGAGCCCACGT
ACTGTCTGTGCAACCAGGTCTCCTACGGGGAGATGA
TCGGCTGTCGACAACGACGAATGCCCCATCGAGTG
GTTCCACTTCTCCTGCGTGGGGCTCAACCATAAACC
AAAGGGCAAGTGGTACTGCCCCAAGTGCCGTGGGG
AGAGCGAGAAGACCATGGACAAAGCCCTGGAGAAG
TCCAAGAAAGAGAGGGCTTACAACAGGTAGTGA

Figure 30: Mouse ING1 isoforms

Three different mouse ING1 proteins have been identified to date, mING1b, mING1c and mING1g. These three different isoforms, which are illustrated in this figure, are encoded by five different transcripts. The three isoforms share a common 3' region. Both mING1b and mING1g possess a unique 5' region. However, mING1c is initiated by an internal ATG in the common exon of the gene and thus does not contain a unique 5' region different from the 2 other isoforms. The PHD domain is indicated in italics and the bold regions highlight the nucleolar targeting sequence (NTS) and nuclear localization signal (NLS). The underlined residues indicate the PIP box previously identified in human ING1b.

Figure 30: Mouse ING1 isoforms

mING1b MLSPANGEQI HLVNYVEDYLDSIESLPFDLQRNVSLMREIDAKY
mING1g MAKRSQGKSDTIYCLRKILLEF

mING1b QEILKELDDYYEKFKRETDGTQKRR VLHC IQRALIRSQELGDEK
mING1g SEILKELDDYYEKFKRETDGTQKRR VLHC IQRALIRSQELGDEK

mING1b IQIVSQMVELVENRSRQVDSHVELFEAHQDI SDGTGGSGKAGQ
mING1g IQIVSQMVELVENRSRQVDSHVELFEAHQDI SDGTGGSGKAGQ
mING1c MVELVENRSRQVDSHVELFEAHQDI SDGTGGSGKAGQ

mING1b DKSKSE AI TQADKPNNKRS**RRQR**NNENRENASNNHDHDD I T
mING1g DKSKSE AI TQADKPNNKRS**RRQR**NNENRENASNNHDHDD I T
mING1c DKSKSE AI TQADKPNNKRS**RRQR**NNENRENASNNHDHDD I T

mING1b SGTP**KEKK**AKTS**KKKK**RSKAKAEREASPADFPIDPNEP*TYCLC*
mING1g SGTP**KEKK**AKTS**KKKK**RSKAKAEREASPADFPIDPNEP*TYCLC*
mING1c SGTP**KEKK**AKTS**KKKK**RSKAKAEREASPADFPIDPNEP*TYCLC*

mING1b *NQVSYGEMIGCDNDECPIEWFHFSCVGLNHKPKGKWYCPKCR*
mING1g *NQVSYGEMIGCDNDECPIEWFHFSCVGLNHKPKGKWYCPKCR*
mING1c *NQVSYGEMIGCDNDECPIEWFHFSCVGLNHKPKGKWYCPKCR*

mING1b GESEKTMDKALEKSKKERAYNR
mING1g GESEKTMDKALEKSKKERAYNR
mING1c GESEKTMDKALEKSKKERAYNR

CHAPTER 4:
DISCUSSION

The PCNA-ING1b/p21 molecular switch hypothesis in response to low doses of UV

The ING1 proteins have been shown to be involved in the post-UV response of cells. When cells are irradiated with low doses of DNA-damaging ultraviolet light, ING1 and PCNA are induced to colocalize. However, it is not known if the colocalization of ING1 and PCNA requires DNA to be damaged or whether other post-UV responses of the cells allow the colocalization. To address this question, it would be interesting to study whether the colocalization still occurs when cells are stressed with other agents. It should also be mentioned that the antibodies used recognize all known ING1 isoforms. However, other experiments using different techniques indicate that it is indeed ING1b that is interacting with PCNA, as is suggested by the presence of the PIP box in the unique region of ING1b. ING1b, but not ING1a, can be co-immunoprecipitated with PCNA in cells that were UV-irradiated (manuscript in preparation).

In addition, under the same conditions, no colocalization can be seen between ING1 and p53, which has been reported to bind ING1b. However, preliminary experiments suggest that p53 binds ING1a rather than ING1b as was first reported. Since the cell type used (Hs68 normal diploid fibroblasts) expresses a higher amount of ING1b than ING1a, it can be proposed that no significant amount of colocalization of ING1 and p53 is detected in these cells because there is not enough ING1a present.

Interestingly, it can be shown that overexpression of p21 can out-compete ING1b for the binding of PCNA (manuscript in preparation). Similar results have also been reported between Fen-1 and p21 (115). Fen-1 binds PCNA to participate in DNA replication but when the DNA is damaged, p21 levels increase, possibly through p53 regulation (120), and p21 can cause the dissociation of Fen-1 and PCNA (17, 115). It has been proposed that this dissociation allows DNA repair, instead of DNA replication, to proceed. p21 has been shown to have a 5 times higher affinity for PCNA than Fen-1 does but is usually present in the cell in very low amounts. The ratio of p21 and Fen-1 therefore seems to act as a

molecular switch in the decision to allow DNA replication or repair to proceed. Overexpression of ING1b has been shown to cause an up-regulation of the expression of p21 (32, 113). ING1b interacts with PCNA almost immediately after DNA is damaged. A model can be proposed in which both p21 and ING1b could outcompete Fen-1 for the binding of PCNA. As well, they could be competing each other at that moment for the binding of PCNA, or alternatively, they could both bind simultaneously on different PCNA molecules of the PCNA homotrimer (Fig.31). However, it can be hypothesized that ING1 binds PCNA before the levels of p21 have started increasing after UV-irradiation since this increase presumably requires the involvement of the transcription and translation machinery. It will be important to determine what role ING1 and p21 are playing in the post-UV response of cells, when these proteins are bound on PCNA. ING1b constructs mutated in the PIP box will help in addressing these questions. The PIP box mutants of ING1b will also be very useful to verify if ING1 is indeed enhancing DNA repair or whether it has a completely different function when it is bound to PCNA.

Nucleolar translocation of ING1 in response to high doses of UV

It can be shown that overexpression of $p33^{ING1b}$ causes this protein to be highly enriched in the nucleolus and that endogenous ING1 also translocates to the nucleolus in response to treatments that cause DNA damage. It can thus be concluded that ING1b interacts with PCNA immediately after cells are irradiated with low doses of UV light and that it translocates to the nucleolus in response to higher doses of irradiation. The nucleolar translocation of $p33^{ING1b}$ is possible because this protein possesses two regions of 4 amino acids each (shown in Fig.32), which act as nucleolar targeting sequences and which are also capable of targeting heterologous fusion proteins to the nucleolus. It is interesting to note that the targeting sequence responsible for the translocation of $p33^{ING1b}$ to the nucleolus is located in a region common to all splicing isoforms of the ING1 gene. This implies that the other two known human isoforms of the ING1 gene, $p47^{ING1a}$

and $p24^{ING1c}$, also possess the nucleolar targeting sequence and should be able to localize to the nucleolus under some circumstances. Further studies using isoform-specific reagents will be necessary to address this question. However, given the opposing functions of $p33^{ING1b}$ and $p47^{ING1a}$ in regulating histone acetylation and gene expression (113), and the role of murine $p33^{ING1b}$ and $p24^{ING1c}$ in regulating p53 activity (32), it will be interesting to examine temporal aspects of this translocation to the nucleolus and functions of the isoforms in the nucleolus, if all isoforms are indeed capable of nucleolar localization.

It is also interesting to note that two of the other known ING1 family members (ING2 and ING1L) both have an identical NTS (all 8 residues are conserved) when compared to the ING1 NTS. This underlies the importance of this targeting signal. These two proteins could thus be able to translocate to the nucleolus like ING1b. It will be important to consider all the ING1 isoforms and family members since some of these proteins might regulate some of the others, during different cellular events, including in response to DNA-damage and during the nucleolar translocation.

It is presently unknown why endogenous $p33^{ING1b}$ does not localize to the nucleolus under normal cell growth conditions or what regulates its translocation to the nucleolus after DNA damage. The nucleolar targeting sequence may possibly be masked in the native protein and become exposed during the post-UV response of cells by conformational changes of the protein itself. Competition experiments using the viral protein Tat indicate that the NTS that is common to Tat and ING1 is not bound by a common limiting factor that retains the protein in the nucleoplasm. It is possible, however, that a protein that binds a region near the NTS could serve such a role. In that case, ING1 and Tat would use different limiting factors to stay in the nucleoplasm. Additionally, inhibition of phosphorylation and dephosphorylation by staurosporine and okadaic acid do not cause endogenous ING1 to become nucleolar nor do they prevent ING1 from entering the nucleolus in response to UV irradiation (data not shown). Staurosporine inhibits PKC and

CDKs 1 through 9 (41), (53). Okadaic acid is a potent inhibitor of type 1 (PP1) and type 2A (PP2A) protein phosphatases (23), which represent a large proportion of the known protein phosphatases. Phosphorylation, as a post-translational modification of ING1, can not be ruled out in the regulation of subnuclear localization of this protein but if it did occur, it must require the activity of other kinases or phosphatases. Alternatively, other post-translational modifications of the protein such as acetylation may be responsible for its subnuclear targeting.

Whatever mechanism regulates the targeting of ING1 to the nucleolus, it is not immediately responsive to DNA damage. Furthermore, this translocation does not appear to occur simultaneously in all cells examined, which indicates that this change in subcellular localization of ING1 is regulated by additional cell-specific events that may be related to position within the cell cycle or to cell-cell interactions.

It is not presently known why ING1 proteins translocate to the nucleolus in response to high doses of UV irradiation. ING1 could play an active role in this organelle during apoptosis or might be trying to prevent apoptosis. As well, it could be sequestered in this organelle similarly to Mdm2 by ARF (117). To address the question of the role of ING1 in the nucleolus when cells are responding to UV-irradiation, it will be possible to use the ING1 constructs that are mutated in the nucleolar targeting sequence. This should allow to see whether the survival of the cells increases or decreases when the ING1 proteins can no longer translocate to the nucleolus.

A role for RNA pol I during the post-UV response of cells?

Several groups have previously demonstrated that UV-irradiation of cells inhibits RNA pol II (26), leads to p53 induction (68) and eventually causes apoptosis (71). In this study, we show that 5-fluorouridine, instead of the more commonly-used bromouridine, is a better reagent to visualize newly synthesized transcripts, especially within the nucleolus. With this technique, we have shown

that under conditions that cause DNA damage, RNA polymerases II and III are strongly inhibited, perhaps allowing DNA damage to be repaired by PCNA-mediated complex reorganization, but that RNA polymerase I is still active in the nucleolus. This inhibition of all RNA polymerases except RNA pol I occurs during the same time period that the candidate tumor suppressor ING1 is present in the nucleolus, after UV-irradiation. The inhibition of nucleoplasmic, but not nucleolar transcription is in agreement with studies demonstrating that rDNA in the nucleolus does not undergo transcription-coupled repair after cells are UV-irradiated (19), nor does it undergo repair of cyclobutane pyrimidine dimers after UV (4). The lack of repair of the ribosomal DNA after UV-induced DNA damage could be rationalized by the fact that many copies of the ribosomal genes exist and it may be more important to continue synthesizing rRNA than to repair a few copies of these genes. If these cells are undergoing apoptosis however, it may be possible that this polymerase is involved in programmed cell death in some way. It is interesting to note that the inhibition of RNA polymerases II and III but not RNA pol I does happen when ING1 is in the nucleolus but does not require the presence of ING1 in this organelle. All cells show the inhibition of RNA pol II and III 48 hours after were irradiated but ING1 was present in the nucleolus of only a subset of these cells. Further studies will be necessary to address this question and to determine whether ING1 is somehow associated with the function of RNA pol I in nucleolus of irradiated cells.

Defining a new functional class of proteins

Several other studies have shown that proteins that are non-nucleolar under normal cell growth conditions translocate to the nucleolus under conditions of DNA damage and apoptosis. The protein DEDD is cytoplasmic but translocates to the nucleolus when CD95 is stimulated in 293T cells. DEDD is thought to be involved in the CD95 apoptotic pathway as an effector molecule (104).

Additionally, the tumor suppressor ARF has been shown to localize to the nucleolus and can drag mdm2 in this subnuclear organelle in response to the activation of Myc or when mouse fibroblasts become senescent (117). Mdm2 is known to bind the tumor suppressor p53 and causes it to be exported to the cytoplasm where it is degraded by proteosomes (30). When mdm2 is sequestered in the nucleolus by ARF, p53 is activated in the nucleoplasm and can, among other things, increase the expression of p21 and thus inhibit cell proliferation (117). One group has shown that many tumor-associated mutations of ARF occur in exon 2 of the protein, which contains the nucleolar targeting sequence (123). Several of these mutations disturb the nucleolar localization of ARF and this diminishes the p53 stabilization effect (123). Like ARF, ING1 might also be targeted to the nucleolus during senescence. This possibility should be examined.

As well, the parathyroid hormone-related peptide (PTHrP) has been shown to be a secreted protein also found in the cytoplasm of normal murine cells, but can be present in the nucleolus of a subpopulation of these cells (49). PTHrP can enhance the survival of chondrocytes undergoing apoptosis, but only when the nucleolar targeting sequence (NTS) of the protein is intact and the protein is found in the nucleolus (1, 49).

These three proteins, together with ING1, may specify a new functional class of proteins that are involved in cell cycle control and/or apoptotic events and that translocate to the nucleolus during these events. Moreover, this also underlines the involvement of the nucleolus during these cellular events which were not previously associated with this organelle and the importance of re-examining the roles of this organelle in the cell.

ING1 proteins can be tightly bound to the nuclear matrix

Nuclear fractionation experiments have demonstrated that both ING1a and ING1b are tightly associated with the nuclear matrix in untreated normal cells. However, this association is not permanent and seems to be a very dynamic process. The ING1 proteins can become associated with DNA or become soluble

in the nucleus during certain steps of the cell cycle. It has also been shown that ING1b and PCNA do not localize in large amounts in the same fraction, even after UV-irradiation. It should be noted that proteins from one fraction can interact with proteins from another fraction and that the protein from different fractions do not necessarily localize in different compartments of the nucleus. And as shown in chapter 3, ING1b and PCNA do interact after UV-irradiation. This fractionation procedure demonstrates the affinity of the ING1 proteins for the nuclear scaffold and the insolubility of these proteins.

It has been suggested that damaged DNA can be brought to the nuclear matrix were it is repaired. Perhaps ING1b can recruit PCNA to matrix-bound DNA repair complexes after cells are irradiated with UV but the interaction between PCNA and ING1b might not be strong enough to withstand a 2M NaCl treatment (which is used to obtain fractions 4 and 5). Further studies will be necessary to define the role and the importance of the tight association of the ING1 to the nuclear matrix.

A role for ING1 proteins in chromatin remodeling

The ING1 proteins can also be shown to stay bound to nuclear structures late during mitosis and to reassociate with the daughter cells nuclei early after their formation, when compared to p53. This long association corroborates the tight binding of the ING1 proteins to the nuclear matrix. ING1 proteins have also been found to reenter the nucleus when acetylation of histones increases. Additionally, two of the ING1 isoforms have been shown to be involved in chromatin remodeling by causing changes in the acetylation pattern of histones when these isoforms are overexpressed. ING1a causes a slight but significant decrease of acetylation of both histones H3 and H4. ING1b greatly increases the acetylation of those two same histones. Both isoforms do not modify histone H2b. This is consistent with findings that ING1 proteins can be co-immunoprecipitated with histone acetyltransferase activity and that they interact with some proteins involved in chromatin remodeling including CBP and TRRAP (113). This is also in agreement

with an observation made by D. Reinberg's group who found that an ING1 isoform was in a complex containing a histone deacetylase (unpublished data), which could potentially explain why ING1a can decrease the acetylation of histones H3 and H4. An alternative interpretation of the increase in histone acetylation by the ING1b isoform and the decrease in histone acetylation by the ING1a isoform could be that ING1b recruits HATs and that ING1a can bind ING1b and inhibit it from interacting with these HATs. This possibility should be examined.

The fact that ING1b contains a significant part of a bromodomain (illustrated in Fig.32) suggests that it might be interacting with other proteins involved in chromatin remodeling through this region. Several of the proteins involved in chromatin remodeling have been shown to be acetylated on specific lysines, which could be recognized by bromodomain motifs. Alternatively, ING1b might be interacting with histones through its bromodomain. Constructs of ING1b mutated in key residues of the bromodomain might help to address these questions.

The fact that ING1 can modify the acetylation pattern of histones is similar to other reports that demonstrate that tumor suppressors and proteins involved in growth regulation interact with HATs and HDACs. Rb interacts with HDACs to regulate cell cycle progression and repress the transcription of specific promoters (72). As well, p53 is known to interact with HATs including CBP, p300 and P/CAF but this might be only to acetylate p53 itself and not to modify histones (44, 95). p53 has also very recently been reported to interact with HDAC1, 2 and 3 which can down-regulate its gene transactivation function (56). BRCA1 interacts with CBP and BRCA2 can be shown to possess intrinsic HAT activity (101). p21 has also been reported to interact with two HATs, CBP and p300, and to stimulate their transactivation function (102). Interestingly, ING1 has been suggested to cooperate with p53 in the regulation of the expression of p21 (32). Overexpression of ING1b increases the levels of p21 in the cell. And when ING1b levels increase, histone acetylation also increases. But in parallel, increases of the amount of ING1 protein also leads to an upregulation of the expression of p21 which in turn will

stimulate the transactivation function of p300 and CBP with which ING1 can interact. It can thus be hypothesized that ING1 can stimulate DNA repair by two mechanisms: ING1b probably recruits HATs including CBP to DNA and possibly to the PCNA repair complex and ING1b can upregulate the expression of p21 which in turn activates the transactivation function of CBP and p300. The HAT and the transactivation activities of both CBP and p300 have been shown to be distinct and mediated by different part of the proteins (102). Other experiments are necessary to address these questions comprehensively.

It is also interesting to note that the growth inhibitory effect of ING1 has been shown to be repressed in the presence of the SV40 large T antigen oncoprotein (33). This is similar to the inactivation of the tumor suppressors p53 and Rb by large T antigen (67). Large T antigen, as well as other viral proteins including E1A, are thought to bind the exact same sequence in the pocket domain of Rb as HDAC 1,2 and 3 (64). Rb co-immunoprecipitates with these HDACs but not when the viral proteins are present. Preliminary experiments indicate that the same might be true for ING1. In cells that express the viral proteins, ING1b does not seem to be able to increase the acetylation of histones H3 and H4 when it is overexpressed. More experiments will be needed to verify this observation.

Multiple transcripts of the ING1 gene

Five different mouse ING1 transcripts have been identified by performing 5' RACE-PCR on adaptor ligated sets of cDNA generated from brain mRNA. These 5 different transcripts have the potential to encode at least 3 different ING1 isoforms which all possess a 3' common region. mING1c, e and f transcripts can only generate one protein, by internal initiation of the 3' exon. This protein has a predicted size of 26 kDa. mING1b, which specifies a protein of 33 kDa, encodes the mouse homologue of human ING1b and contains the full 3' exon and a unique 5' exon. mING1g encodes a predicted 31 kDa protein that also contains the full 3' exon and a unique 5' exon.

Another group reported similar findings during the time these results were generated (122). They isolated three different transcripts from mouse spleen and mouse brain tissues. The three transcripts have the same 3' region and are suggested to encode 2 different proteins. Transcripts 1a and 1c generate the 26 kDa protein that lacks the 5' region of the common exon. Transcript 1c is identical to our mING1c whereas transcript 1a has only been found by their group. Transcript 1b is identical to our mING1b. This group has generated data that suggest that all three isoforms have their own separate promoter.

The ING1 gene seems thus to be able to generate many different isoforms. All together, 3 different mouse isoforms and 5 different human isoforms (two of which are homologous to the mouse isoforms) have been identified. However, many other transcripts and proteins, including very large specimens, have been seen on northern blots, in 5' RACE-PCR reactions as well as in westerns blots using polyclonal anti-ING1 antibodies against protein from many different tissues, which suggests that there might be many other ING1 isoforms not yet isolated.

Interestingly, the ING1 gene seems to generate multiple transcripts to produce one unique isoform. This is illustrated in mouse where four different transcripts have been found to produce the same 26 kDa protein. This isoform is believed to cooperate with p53 in cell growth control and to be necessary for transcriptional activation of p53-responsive genes (122). If this is true, the expression of this isoform might need very tight and unique regulation, which could explain the necessity for multiple transcripts to generate one protein. Additionally, if these transcripts are under the control of different promoters and perhaps different transcription factors, there might be a mechanism in place to allow one transcript to compensate for potential down-regulation of another of the transcripts. This might allow an assurance that the expression pattern of this protein can not be easily changed by any mutation or change of expression of other proteins. Many human cancers have been shown to have a decreased expression of the ING1b isoform. It will be interesting to determine whether the 26 kDa isoform is involved

in tumorigenic processes and to study the role of the multiple transcripts encoding the same protein.

Conclusions and perspectives: can ING1 still be considered a tumor suppressor?

The ING1 proteins have been shown to be involved in many different cellular processes. In untreated healthy cells, the ING1 proteins are associated with the nuclear matrix and seem to regulate some aspects of chromatin remodeling by being able to modify the acetylation state of histones and by interacting with histone acetyltranferases and localizing in similar compartments as them during mitosis. When cells are UV-irradiated and undergo DNA repair, ING1b interacts with PCNA, possibly to allow DNA repair and can also translocate to the nucleolus. The translocation to the nucleolus could be necessary to sequester ING1 from other events happening in the nucleoplasm, ING1 could be sequestering another protein in the nucleolus (like Arf sequesters Mdm2 in the nucleolus) or ING1 could play an active role in this organelle.

However, these three different functions of ING1 might not be independent one from another. When ING1b binds PCNA after UV-damage, it could be recruiting histone acetyltransferases to the damaged DNA to allow DNA repair to proceed with more ease. As well, when ING1 translocates to the nucleolus, it might recruit HATs or HDACs to this organelle or could possibly interact with the nucleolar HATs and HDACs. Domains of ING1 involved in one of these processes could also mediate other interactions. All these possibilities should be studied in light of the fact that many ING1 isoforms seem to exist and might even be regulating each other.

The ING1 proteins were initially proposed to be tumor suppressors because of their role in growth inhibition and apoptosis as well as their modified expression in many types of cancer. The more recent findings about the function of the ING1 proteins reveal that they are also involved in many other cellular processes.

However, the newly discovered functions of ING1 still seem to allow these proteins to be considered tumor suppressors. Their role in chromatin remodeling is consistent with very recent findings that most of the well-accepted tumor suppressors themselves interact with proteins involved in chromatin remodeling or even possess intrinsic histone acetyltransferase activity. As well, the potential role of ING1 in DNA repair through the binding of PCNA is also consistent with a tumor suppressive function. ING1 could help induce a cell cycle arrest after cells are irradiated and then enhance DNA repair through its interaction with PCNA. Although little is known about the functional role of ING1 in the nucleolus, by analogy with ARF, this localization could also serve a tumor suppressor role. Consequently, the data presented in this thesis provides additional evidence that ING1 fulfills biological roles consistent with its functioning as a tumor suppressor. It is however important to consider that the ING1 gene can generate many different isoforms and some of these proteins might not be tumor suppressors per se and might even inhibit other ING1 isoforms.

The ING1 proteins seem involved in many very different cellular processes, including apoptosis, chromatin remodeling, DNA repair and nucleolar function under some conditions. Their study is thus all the more important because they might allow researchers to link these different events and better understand the cell as a whole entity.

Figure 31: The PCNA-p21/ING1b molecular switch hypothesis

Under normal cellular conditions, p21 and ING1b levels are low and PCNA binds to Fen-1 to allow DNA replication to proceed. However, when cells are irradiated by UV light, levels p21 increase and p21 (as well as possibly ING1b) can outcompete Fen-1 for binding to PCNA. This inhibits DNA replication and potentially allows DNA repair to proceed. Three molecules of Fen-1 have been shown to bind one PCNA homotrimer (17). The same thing is true for p21 and thus possibly for ING1.

Figure 31: The PCNA-p21/ING1b molecular switch hypothesis

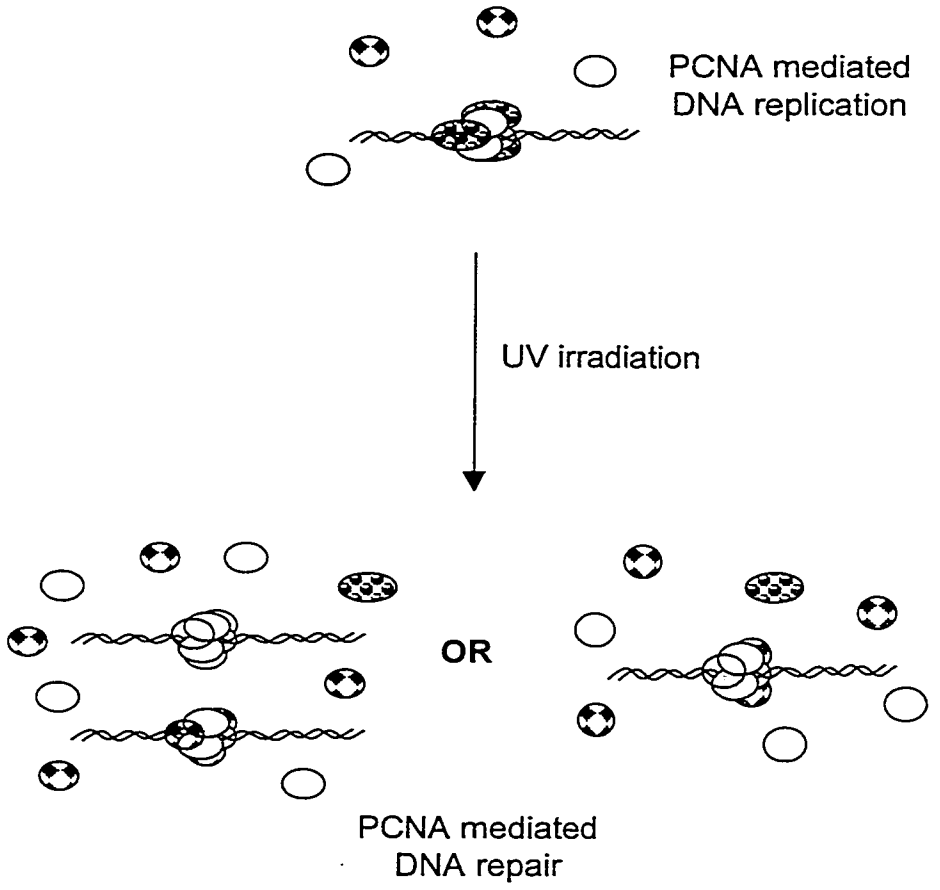

Legend:

PCNA homotrimer

Fen-1 endonuclease

ING1b

p21

Figure 32: The known functional motifs of ING1 isoforms

The functional motifs of three of the ING1 isoforms are compared here. All known ING1 isoforms contain the PHD domain and the nuclear-nucleolar localization sequences (N) which are present in the common region of the proteins. The ING1b isoform also possesses, in its unique region, a PIP box motif, which allows interaction with PCNA (P), as well as part of a bromodomain (indicated by the striped box). The PIP box and the bromodomain motif overlap slightly. The sequences of the PIP box and the nuclear-nucleolar localization sequences are shown.

Figure 32: The known functional motifs of ING1 isoforms

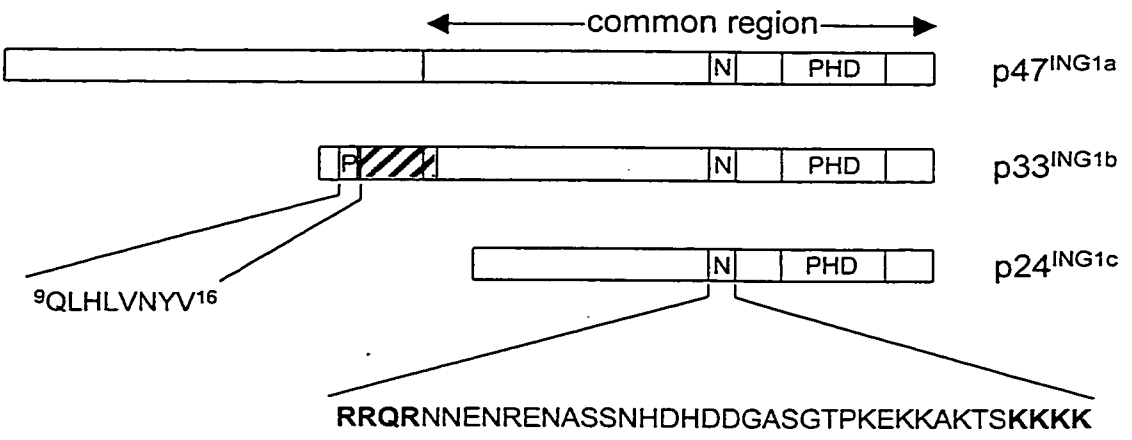

CHAPTER 5:
BIBLIOGRAPHY

1. **Aarts, M. M., A. Rix, J. Guo, R. Bringhurst, and J. E. Henderson.** 1999. The nucleolar targeting signal (NTS) of parathyroid hormone related protein mediates endocytosis and nucleolar translocation. J. Bone Miner. Res. **14:**1493-1503.
2. **Aasland, R., T. J. Gibson, and A. F. Stewart.** 1995. The PHD finger: implication for chromatin-mediated transcriptional regulation. Trends Biochem. Sci. **20:**56-59.
3. **Allard, S., R. T. Utley, J. Savard, A. Clarke, P. Grant, C. J. Brandl, L. Pillus, J. L. Workman, and J. Cote.** 1999. NuA4, an essential transcription adaptor/histone H4 acetyltransferase complex containing Esa1p and the ATM-related cofactor Tra1p. EMBO J. **18:**5108-5119.
4. **Balajee, A. S., A. May, and V. A. Bohr.** 1999. DNA repair of pyrimidine dimers and 6-4 photoproducts in the ribosomal DNA. Nucleic Acids Res. **27:**2511-2520.
5. **Balasubramaniam, U., and N. L. Oleinick.** 1995. Preferential cross-linking of matrix-attachment region (MAR) containing DNA fragments to the isolated nuclear matrix by ionizing radiation. Biochemistry **34:**12790-12802.
6. **Baldin, V., J. Lukas, M. J. Marcote, M. Pagano, and G. Draetta.** 1993. Cyclin D1 is a nuclear protein required for cell cycle progression in G1. Genes Dev. **7:**812-821.
7. **Berezney, R., and D. S. Coffey.** 1974. Identification of a nuclear protein matrix. Biochem. Biophys. Res. Commun. **60:**1410-1417.
8. **Berezney, R., and D. S. Coffey.** 1975. Nuclear protein matrix: association with newly synthesized DNA. Science **189:**291-292.
9. **Berezney, R., and X. Wei.** 1998. The new paradigm: integrating genomic function and nuclear architecture. J. Cell. Biochem. Supp. **30/31:**238-242.
10. **Boddy, M. N., E. Duprez, K. L. Borden, and P. S. Freemont.** 1997. Surface residue mutations of the PML RING finger domain alter the

formation of nuclear matrix-associated PML bodies. J. Cell. Sci. **Pt18:**2197-2205.

11. **Boisvert, F.-M., M. J. Hendzel, and D. P. Bazett-Jones.** 2000. Promyelocytic leukemia (PML) nuclear bodies are protein structures that do not accumulate RNA. J. Cell Biol. **148:**283-292.
12. **Boland, D., V. Olineck, P. Bonnefin, D. Vieyra, E. Parr, and K. Riabowol.** 2000. A panel of CAb antibodies recognize endogenous and ectopically expressed ING1 protein. Hybridoma, in press **19.**
13. **Bond, J. A., F. S. Wyllie, and D. Wynford-Thomas.** 1994. Escape from senescence in human diploid fibroblasts induced directly by mutant p53. Oncogene **9:**1885-1889.
14. **Brehm, A., and T. Kouzarides.** 1999. Retinoblastoma protein meets chromatin. Trends Biochem. Sci. **24:**142-145.
15. **Brehm, A., E. A. Miska, D. J. McCance, J. L. Reid, A. J. Bannister, and T. Kouzarides.** 1998. Retinoblastoma protein recruits histone deacetylase to repress transcription. Nature **391:**597-601.
16. **Carter, K. C., D. Bowman, W. Carrington, K. Fogarty, J. A. McNeil, F. S. Fay, and J. B. Lawrence.** 1993. A three-dimensional view of precursor messenger RNA metabolism within the mammalian nucleus. Science **259:**1330-1335.
17. **Chen, U., S. Chen, P. Saha, and A. Dutta.** 1996. p21Cip1/Waf1 disrupts the recruitment of human Fen1 by proliferating-cell nuclear antigen into the DNA replication complex. Proc. Natl. Acad. Sci. USA **93:**11597-11602.
18. **Chiu, S. M., L. Y. Xue, L. R. Friedman, and N. L. Oleinick.** 1995. Differential dependence on chromatin structure for copper and iron induction of DNA double-strand breaks. Biochemistry **34:**2653-2661.
19. **Christians, F. C., and P. C. Hanawalt.** 1993. Lack of transcription-coupled repair in mammalian ribosomal RNA genes. Biochem. **32:**10512-10518.

20. **Clarke, A. S., J. E. Lowell, S. J. Jacobson, and L. Pillus.** 1999. Esa1 is an essential histone acetyltransferase required for cell cycle progression. Mol. Cell. Biol. **19:**2515-2526.

21. **Cook, P. R., and I. A. Brazell.** 1976. Conformational constraints in nuclear DNA. J. Cell. Sci. **22:**287-302.

22. **Davie, J. R.** 1997. Nuclear matrix, dynamic histone acetylation and transcriptionally active chromatin. Mol. Biol. Rep. **24:**197-207.

23. **Dawson, J. F., and C. F. Holmes.** 1999. Molecular mechanisms underlying inhibition of protein phosphatases by marine toxins. Front. Biosci. **4:**D646-658.

24. **Devilee, P., and C. J. Cornelisse.** 1994. Somatic genetic changes in human breast cancer. Biochim. Biophys. Acta **1198:**113-130.

25. **Dhalluin, C., J. E. Carlson, L. Zeng, C. He, A. K. Aggarwal, and M.-M. Zhou.** 1999. Structure and ligand of a histone acetyltransferase bromodomain. Nature **399:**491-496.

26. **Donahue, B. A., S. Yin, J. S. Taylor, D. Reines, and P. C. Hanawalt.** 1994. Transcript cleavage by RNA polymerase II arrested by a cyclobutane pyrimidine dimer in the DNA template. Proc. Natl. Acad. Sci. USA **91:**8502-8506.

27. **Dworetzky, S. I., K. L. Wright, E. G. Fey, S. Penman, J. B. Lian, J. L. Stein, and G. S. Stein.** 1992. Sequence-specific DNA-binding proteins are components of a nuclear matrix-attachment site. Proc. Natl. Acad. Sci. USA **89:**4178-4182.

28. **Emiliani, S., W. Fischle, C. Van Lint, Y. Al-Abed, and E. Verdin.** 1998. Characterization of a human RPD3 ortholog, HDAC3. Proc. Natl. Acad. Sci. USA **95:**2795-2800.

29. **Fields, A. P., and L. J. Thompson.** 1995. The regulation of mitotic nuclear envelope breakdown: a role for multiple lamin kinases. Prog. Cell Cycle Res. **1:**271-286.

30. **Freedman, D. A., and A. J. Levine.** 1998. Nuclear export is required for degradation of endogenous p53 by mdm2 and human papillomavirus E6. Mol. Cell. Biol. **18:**7288-7293.

31. **Garkavtsev, I., D. Demetrick, and K. Riabowol.** 1997. Cellular localization and chromosome mapping of a novel candidate tumor suppressor gene (ING1). Cytogenet. Cell Genet. **76:**176-178.

32. **Garkavtsev, I., I. A. Grigorian, V. S. Ossovskaya, M. V. Chernov, P. M. Chumakov, and A. V. Gudkov.** 1998. The candidate tumour suppressor $p33^{ING1}$ cooperates with p53 in cell growth control. Nature **391:**295-298.

33. **Garkavtsev, I., A. Karazov, A. Gudkov, and K. Riabowol.** 1996. Suppression of the novel growth inhibitor $p33^{ING1}$ promotes neoplastic transformation. Nature Genet. **14:**415-420.

34. **Garkavtsev, I., and K. Riabowol.** 1997. Extension of the replicative life span of human diploid fibroblasts by inhibition of the p33ING1 candidate tumor suppressor. Mol. Cell. Biol. **17:**2014-2019.

35. **Garrard, W. T.** 1990. , p. 163-175. *In* F. Eckstein, and D. M. J. Lilley (ed.), Nucleic Acids and Molecular Biology. Springer-Verlag, Berlin.

36. **Gary, R., D. L. Ludwig, H. L. Cornelius, M. A. MacInnes, and M. S. Park.** 1997. The DNA repair endonuclease XPG binds to proliferating cell nuclear antigen (PCNA) and shares sequence elements with the PCNA-binding regions of FEN-1 and cyclin-dependant kinase inhibitor p21. J. Biol. Chem. **272:**24522-24529.

37. **Gerace, L., and B. Burke.** 1988. Functional organization of the nuclear envelope. Annu. Rev. Cell Biol. **4:**335-374.

38. **Gerbi, S. A.** 1997. The nucleolus: then and now. Chromosoma **105:**385-387.

39. **Glazer, R. I., and K. D. Hartman.** 1983. In vitro translation of messenger RNA following exposure of human colon carcinoma cells in culture to 5-fluorouracil and 5-fluorouridine. Mol. Pharmacol. **23:**540-546.

40. **Grant, P. A., D. Schieltz, M. G. Pray-Grant, J. R. Yates III, and J. L. Workman.** 1998. The ATM-related cofactor Tra1 is a component of the purified SAGA complex. Mol. Cell. **2:**863-867.

41. **Gray, N., L. Detivaud, C. Doerig, and L. Meijer.** 1999. ATP-site directed inhibitors of cyclin dependent kinases. Curr. Med. Chem. **6:**859-875.

42. **Grondin, B., F. Cote, M. Bazinet, M. Vincent, and M. Aubry.** 1997. Direct interaction of the KRAB/Cys2-His2 zinc finger protein ZNF74 with a hyperphosphorylated form of the RNA polymerase II largest subunit. J. Biol. Chem. **272:**27877-27885.

43. **Grunstein, M.** 1997. Histone acetylation in chromatin structure and transcription. Nature **389:**349-352.

44. **Gu, W., and R. G. Roeder.** 1997. Activation of p53 sequence-specific DNA binding by acetylation of the p53 C-terminal domain. Cell **90:**595-606.

45. **Gu, W., X.-L. Shi, and R. G. Roeder.** 1997. Synergistic activation of transcription by CBP and p53. Nature **387:**819-822.

46. **Haynes, S. R., C. Dollard, F. Winston, S. Beck, J. Trowsdale, and I. B. Dawid.** 1992. The bromodomain: a conserved sequence found in human, Drosophila and yeast proteins. Nucleic Acids Res. **20:**2603.

47. **He, D., J. A. Nickerson, and S. Penman.** 1990. Core filaments of the nuclear matrix. J. Cell Biol. **110:**569-580.

48. **Helbing, C. C., C. Veillette, K. Riabowol, R. N. Johnston, and K. Garkavtsev.** 1997. A novel candidate tumor suppressor, ING1, is involved in the regulation of apoptosis. Cancer Res. **57:**1255-1258.

49. **Henderson, J. E., N. Amizuka, H. Warshawshy, D. Biasotto, B. M. K. Lanske, D. Goltzman, and A. C. Karaplis.** 1995. Nucleolar localization of parathyroid hormone-related peptide enhances survival of chondrocytes under conditions that promote apoptotic cell death. Mol. Cell. Biol. **15:**4064-4075.

50. **Iyengar, B.** 1994. Expression of proliferating cell nuclear antigen (PCNA): proliferative phase functions and malignant transformation of melanocytes. Melanoma Res **4:**293-295.

51. **Jager, D., E. Stockert, M. Scanlan, A. O. Gure, E. Jager, A. Knuth, L. J. Old, and Y.-T. Chen.** 1999. Cancer-testis antigens and ING1 tumor suppressor gene product are breast cancer antigens: characterization of tissue-specific ING1 transcripts and a homologue gene. Cancer Res. **59:**6197-6204.

52. **Jarrous, N., J. S. Wolenski, D. Wesolowski, C. Lee, and S. Altman.** 1999. Localization in the nucleolus and coiled bodies of protein subunits of the ribonucleoprotein ribonuclease P. J. Cell Biol. **146:**559-571.

53. **Jarvis, W. D., and S. Grant.** 1999. Protein kinase C targeting in antineoplastic treatment strategies. Invest. New Drugs **17:**227-240.

54. **Jeanmougin, F., J. M. Wurtz, B. L. Douarin, P. Chambon, and R. Losson.** 1997. The bromodomain revisited. Trends Biochem. Sci. **22:**151-153.

55. **Jonsson, Z. O., and U. Hubscher.** 1997. Proliferating cell nuclear antigen: more than a clamp for DNA polymerases. BioEssays **19:**967-975.

56. **Juan, L. J., W. J. Shia, M. H. Chen, W. M. Yang, E. Seto, Y. S. Lin, and C. W. Wu.** 2000. Histone deacetylases specifically down-regulate p53-dependent gene activation. J. Biol. Chem. **Apr 20**.

57. **Kedinger, C., M. Gniazdowski, J. L. Mandel, F. Gissinger, and P. Chambon.** 1970. Alpha-amanitine: a specific inhibitor of one of two DNA-dependent RNA polymerase activities from calf thymus. Biochem. Biophys. Res. Commun. **38:**165-171.

58. **Kelman, Z.** 1997. PCNA: structure, functions and interactions. Oncogene **14:**629-640.

59. **Kerangueven, F., T. Noguchi, F. Coulier, F. Allione, V. Wargniez, J. Simony-Lafontaine, M. Longy, J. Jacquemier, H. Sobol, F. Eisinger, and d. Birnbaum.** 1997. Genome-wide search for loss of heterozygosity shows

extensive genetic diversity of human breast carcinomas. Cancer Res. **57:**5469-5474.

60. **Koehler, D., and P. C. Hanawalt.** 1996. Recruitment of damaged DNA to the nuclear matrix in hamster cells following ultraviolet irradiation. Nucleic Acids Res. **24:**2877-2884.

61. **Kouzarides, T.** 2000. Acetylation: a regulatory modification to rival phosphorylation? EMBO J. **19:**1176-1179.

62. **Kruhlak, M. J., M. J. Hendzel, W. Fischle, N. Bertos, X. J. Yang, E. Verdin, and D. P. Bazett-Jones.** 2000. Regulation of acetylation in mitosis through loss of histone acetyltransferases and deacetylases from chromatin. Journal Biol. Chem., submitted .

63. **Kuo, M.-H., and C. D. Allis.** 1998. Roles of histones acetylases and deacetylases in gene regulation. BioEssays **20:**615-626.

64. **Lai, A., J. M. Lee, W.-M. Yang, J. A. DeCaprio, W. G. Kaelin, E. Seto, and P. E. Branton.** 1999. RBP1 recruits both histone deacetylase-dependent and -independent repression activities to retinoblastoma family proteins. Mol. Cell. Biol. **19:**6632-6641.

65. **Lawrence, J. B., R. H. Singer, and L. M. Marselle.** 1989. Highly localized tracks of specific transcripts within interphase nuclei visualized by in situ hybridization. Cell **57:**493-502.

66. **Levin, D. S., W. Bai, N. Yao, M. O'Donnell, and A. E. Tomkinson.** 1997. An interaction between DNA ligase I and proliferating cell nuclear antigen: implications for Okazaki fragment synthesis and joining. Proc. Natl. Acad. Sci. USA **94:**12863-12868.

67. **Linzer, D. I. H., and A. J. Levine.** 1979. Characterization of a 54K dalton cellular SV40 tumor antigen present in SV40-transformed cells and uninfected embryonal carcinoma cells. Cell **17:**43-52.

68. **Ljungman, M., F. Zhang, F. Chen, A. J. Rainbow, and B. C. McKay.** 1999. Inhibition of RNA polymerase II as a trigger for the p53 response. Oncogene **18:**583-592.

69. **Loewith, R., M. Meijer, S. P. Lees-Miller, K. Riabowol, and D. Young.** 2000. A family of yeast proteins related to the candidate human tumor suppressor p33ING1 associated with histone acetyl transferase *in vivo*. Mol. Cell Biol. **20:**3807-3816.

70. **Long, E. O., and I. B. Dawid.** 1980. Repeated genes in eukaryotes. Annu. Rev. Biochem. **49:**727-764.

71. **Lu, X., and D. P. Lane.** 1993. Differential induction of transcriptionally active p53 following UV or ionizing radiation: defects in chromosome instability syndrome? Cell **75:**765-778.

72. **Luo, R. X., A. A. Postigo, and D. C. Dean.** 1998. Rb interacts with histone deacetylase to repress transcription. Cell **92:**463-473.

73. **Ma, D., D. Lawless, and K. Riabowol.** 1999. Suppression of the novel growth inhibitor p33ING1 promotes neoplastic transformation. Nature Genetics **23:**373.

74. **Maestro, R., S. Paccinin, C. Doglioni, D. Gasparotto, T. Vukosavljevic, S. Sulfaro, L. Barzan, and M. Boiocchi.** 1996. Chromosome 13q deletion mapping in head and neck squamous cell carcinomas: identification of two distinct regions of preferential loss. Cancer Res. **56:**1146-1150.

75. **Magnaghi-Jaulin, L., R. Groisman, I. Naguibneva, P. Robin, S. Lorain, J. P. Le Villain, F. Troalen, D. Trouche, and A. Harel-Bellan.** 1998. Retinoblastoma protein represses transcription by recruiting a histone deacetylase. Nature **391:**601-605.

76. **Martelli, A. M., R. Bortul, R. Bareggi, V. Grill, P. Narducci, and M. Zweyer.** 1999. Biochemical and morphological changes in the nuclear matrix prepared from apoptotic HL-60 cells: effect of different stabilizing procedures. J. Cell. Biochem. **74:**99-110.

77. **Martelli, A. M., R. Bortul, F. O. Fackelmayer, P. L. Tazzari, R. Bareggi, P. Narducci, and M. Zweyer.** 1999. Biochemical and morphological characterization of the nuclear matrix from apoptotic HL-60 cells. J. Cell. Biochem. **72:**35-46.

78. **McMahon, S. B., H. A. Van Buskirk, K. A. Dugan, T. D. Copeland, and M. D. Cole.** 1998. The novel ATM-related protein TRRAP is an essential cofactor for the c-Myc and E2F oncoproteins. Cell **94:**363-374.

79. **McMahon, S. B., M. A. Wood, and M. C. Cole.** 2000. The essential cofactor TRRAP recruits the histone acetyltransferase hGCN5 to c-myc. Mol. Cell. Biol. **20:**556-562.

80. **Miller, O. L.** 1981. The nucleolus, chromosomes and visualization of genetic activity. J. Cell. Biol. **91:**15s-27s.

81. **Motomura, K., I. Nishisho, S. Takai, H. Tateishi, N. Okazaki, M. Yamamoto, T. Miki, T. Honji, and T. Mori.** 1988. Loss of alleles at loci on chromosome 13 in human primary gastric cancers. Genomics **2:**180-184.

82. **Nigg, E. A.** 1992. Assembly and cell cycle dynamics of the nuclear lamina. Semin. Cell Biol. **3:**245-253.

83. **Ohmori, M., M. Nagai, T. Tasaka, H. P. Koeffler, K. Riabowol, and J. Takahara.** 1999. Decreased expression of p33ING1 mRNA in lymphoid malignancies. Am. J. Hematol. **62:**118-119.

84. **Oki, E., Y. Maehara, E. Tokunaga, Y. Kakegi, and K. Sugimachi.** 1999. Reduced expression of p33ING1 and the relationship with p53 expression in human gastric cancer. Cancer Lett. **:**157-162.

85. **Oleinick, N. L., U. Balasubramaniam, and L. Y. Xue.** 1994. Induction of DNA damage in gamma-irradiated nuclei stripped of nuclear protein classes: differential modulation of double-strand break and DNA-protein crosslink formation. Int. J. Radiat. Biol. **66:**11-21.

86. **Paranjape, S. M., R. T. Kamakaka, and J. T. Kadonaga.** 1994. Role of chromatin structure in the regulation of transcription by RNA polymerase II. Annu. Rev.Biochem. **63:**265-297.

87. **Park, M. S., J. A. Knauf, S. H. Pendergrass, C. H. Coulon, G. F. Strniste, B. L. Marrone, and M. A. MacInnes.** 1996. Ultraviolet-induced movement of the human DNA repair protein, *Xeroderma pigmentosum* type G, in the nucleus. Proc. Natl. Acad. Sci. USA **93:**8368-8373.

88. **Pazin, M. J., and J. T. Kaonaga.** 1997. What's up and down with histone deacetylation and transcription? Cell **89:**325-328.

89. **Pederson, T.** 1998. The plurifunctional nucleolus. Nucleic Acids Res. **26:**3871-3876.

90. **Pederson, T.** 1998. Thinking about a nuclear matrix. J. Mol. Biol. **277:**147-159.

91. **Reynolds, N., E. Warbrick, P. A. Fantes, and S. A. MacNeill.** 2000. Essential interaction between the fission yeast DNA polymerase delta subunit Cdc27 and Pcn1 (PCNA) mediated through a C-terminal p21Cip1-like PCNA binding motif. EMBO J. **19:**1108-1118.

92. **Riabowol, K. T., G. Draetta, L. Brizuella, D. Vendre, and D. Beach.** 1989. The cdc2 kinase is a nuclear protein that is essential for mitosis in mammalian cells. Cell **57:**393-401.

93. **Sager, R.** 1989. Tumor suppressor genes: the puzzle and the promise. Science **246:**1406-1412.

94. **Saito, A., T. Furukawa, S. Fukushige, S. Koyama, M. Hoshi, Y. Hayashi, and A. Horii.** 2000. p24/ING1-ALT1 and p47/ING1-ALT2, distinct alternative transcripts of p33/ING1. J. Hum. Genet. **45:**177-181.

95. **Sakaguchi, K., J. E. Herrera, S. Saito, T. Miki, M. Bustin, A. Vassilev, C. W. Anderson, and E. Appella.** 1998. DNA damage activates p53 through a phosphorylation-acetylation cascade. Genes Dev. **12:**2831-2841.

96. **Scheer, U., and R. Hock.** 1999. Structure and function of the nucleolus. Curr. Opin. Cell Biol. **11:**385-390.

97. **Schmidt-Zachmann, M. S., and E. A. Nigg.** 1993. Protein localization to the nucleolus: a search for targeting domains in nucleolin. J. Cell Sci. **105:**799-806.

98. **Scovassi, A. I., L. A. Stivala, L. Rossi, L. Bianchi, and E. Prosperi.** 1997. Nuclear association of cyclin D1 in human fibroblasts: tight binding to nuclear structures and modulation by protein kinase inhibitors. Exp. Cell Res. **237:**127-134.

99. **Shimada, Y., A. Saito, M. Suzuki, E. Takahashi, and M. Horie.** 1998. Cloning of a novel gene (ING1L) homologous to ING1, a candidate tumor suppressor. Cytogenet. Cell Genet. **83:**232-235.

100. **Shinoura, N., Y. Muramatsu, M. Nishimura, Y. Yoshida, A. Saito, T. Yokoyama, T. Furukawa, A. Horii, M. Hashimoto, A. Asai, T. Kirino, and H. Hamada.** 1999. Adenovirus-mediated transfer of $p33^{ING1}$ with p53 drastically augments apoptosis in gliomas. Cancer Res. **59:**5521-5528.

101. **Siddique, H., J.-P. Zou, V. N. Rao, and E. S. P. Reddy.** 1998. The BRCA2 is a histone acetyltransferase. Oncogene **16:**2283-2285.

102. **Snowden, A. W., L. A. Anderson, G. A. Webster, and N. D. Perkins.** 2000. A novel transcriptional repression domain mediates p21WAF1/CIP1 induction of p300 transactivation. Mol. Cell Bio. **20:**2676-2686.

103. **Sobell, H. M.** 1985. Actinomycin and DNA transcription. Proc. Natl. Acad. Sci. USA **82:**5328-5331.

104. **Stegh, A., O. Schickling, A. Ehret, C. Scaffidi, C. Peterhansel, T. G. Hofmann, I. Grummt, P. H. Krammer, and M. Peter.** 1998. DEDD, a novel death effector domain-containing protein, targeted to the nucleolus. EMBO J. **17:**5974-5986.

105. **Stein, G. S., A. J. van Wijnen, J. L. Stein, J. B. Lian, S. M. Pockwinse, and S. McNeil.** 1998. Linkages of nuclear architecture to biological and pathological control of gene expression. J. Cell. Biochem. Suppl. **30/31:**220-231.

106. **Taunton, J., C. A. Hassig, and S. L. Schreiber.** 1996. A mammalian histone deacetylase related to the yeast transcriptional regulator Rpd3p. Science **272:**408-411.

107. **te Poele, R. H., A. L. Okorokov, and S. P. Joel.** 1999. RNA synthesis block by 5,6-dichloro-1-β-D-ribofuranosylbenzimidazole (DRB) triggers p53-dependent apoptosis in human colon carcinoma cells. Oncogene **18:**5765-5772.

108. **Tokunaga, E., Y. Maehara, E. Oki, K. Kitamura, Y. Kakeji, S. Ohno, and K. Sugimachi.** 2000. Diminished expression of ING1 mRNA and the correlation with p53 expression in breast cancers. Cancer Lett. **152:**15-22.

109. **Toyama, T., H. Iwase, P. Watson, H. Muzik, E. Saettler, A. Magliocco, L. DiFrancesco, P. Forsyth, I. Garkavtsev, S. Kobayashi, and K. Riabowol.** 1999. Suppression of ING1 expression in sporadic breast cancer. Oncogene **18:**5187-5193.

110. **Tsurimoto, T.** 1998. PCNA, a multifunctional ring on DNA. Biochim. Biophys. Acta **1443:**23-39.

111. **van Wijnen, A. J., J. P. Bidwell, E. G. Fey, S. Penman, J. B. Lian, J. L. Stein, and G. S. Stein.** 1993. Nuclear matrix association of multiple sequence-specific DNA binding activities related to SP-1, ATF, CCAAT, C/EBP, OCT-1 and AP-1. Biochem. **32:**3324-3339.

112. **Vassilev, A., J. Yamauchi, T. Kotani, C. Prives, M. L. Avantaggianti, J. Qin, and Y. Nakatani.** 1998. The 400kDa subunit of the PCAF histone acetylase complex belongs to the ATM superfamily. Mol. Cell. **2:**869-875.

113. **Vieyra, D., R. Loewith, M. Scott, P. Bonnefin, F.-M. Boisvert, M. Meijer, D. Lawless, D. P. Bazett-Jones, S. McMahon, M. D. Cole, D. Young, and K. Riabowol.** 2000. ING1 proteins regulate histone acetylation and gene expression, submitted. .

114. **Warbrick, E.** 1998. PCNA binding through a conserved motif. BioEssays **20:**195-199.

115. **Warbrick, E., D. P. Lane, D. M. Glover, and L. S. Cox.** 1997. Homologous regions of FEN-1 and p21Cip1 compete for binding to the same site on PCNA: a potential mechanism to co-ordinate DNA replication and repair. Oncogene **14:**2313-2321.

116. **Warbrick, E., D. P. Lane, D. M. Glover, and L. S. Cox.** 1995. A small peptide inhibitor of DNA replication defines the site of interaction between the cyclin-dependent kinase inhibitor p21Waf1 and proliferating cell nuclear antigen. Curr. Biol. **5:**275-282.

117. **Weber, J. D., L. J. Taylor, M. F. Roussel, C. J. Sherr, and D. Bar-Sagi.** 1999. Nucleolar Arf sequesters mdm2 and activates p53. Nature Cell Biol. **1:**20-26.

118. **Weinmann, R., and R. G. Roeder.** 1974. Role of DNA-dependent RNA polymerase 3 in the transcription of the tRNA and 5S RNA genes. Proc. Natl. Acad. Sci. USA **71:**1790-1794.

119. **Wilkinson, D. S., and H. C. Pitot.** 1973. Inhibition of ribosomal ribonucleic acid maturation in Novikoff hepatoma cells by 5-fluorouracil and 5-fluorouridine. J. Biol. Chem. **248:**63-68.

120. **Xu, J., and G. F. Morris.** 1999. p53-mediated regulation of proliferating cell nuclear antigen expression in cells exposed to ionizing radiation. Mol.Cell. Biol. **19:**12-20.

121. **Zeng, C., A. J. van Wijnen, J. L. Stein, S. Meyers, W. Sun, L. Shopland, J. B. Lawrence, S. Penman, J. B. Lian, G. S. Stein, and S. W. Hiebert.** 1997. Identification of a nuclear matrix targeting in the leukemia and bone-related AML/CBFα transcription factors. Proc. Natl. Acad. Sci. USA **94:**6764-6751.

122. **Zeremski, M., J. E. Hill, S. S. S. Kwek, I. A. Grigorian, K. V. Gurova, I. V. Garkavtsev, L. Diatchenko, E. V. Koonin, and A. V. Gudkov.** 1999. Structure and regulation of the mouse ING1 gene. J. Biol. Chem. **274:**32172-32181.

123. **Zhang, Y., and Y. Xiong.** 1999. Mutations in human ARF exon 2 disrupts its nucleolar localization and impairs its ability to block nuclear export of mdm2 and p53. Mol. Cell. **3:**579-591.

Appendix A: Buffer composition

Blocking solution for Southern and northern blots with the DIG-eas-hyb system

5 g of blocking reagent

50 mL of maleic acid buffer

heat to 60°C to dissolve and autoclave

store at 4°C

dilute 1:10 in maleic acid buffer to use

Blocking solution for western blots

TBS-T

5% non-fat milk powder

Coomassie staining solution

1.0% (W/V) Coomasie brilliant blue R-250 (Biorad)

10% (V/V) methanol

15% (V/V) glacial acetic acid

complete the volume with distilled water

Destaining solution

10% (V/V) methanol

15% (V/V) glacial acetic acid

0.5% glycerol (V/V)

complete the volume with distilled water

Detection buffer

7.88 g Tris-HCl in 400 mL of H_2O

adjust pH to 9.5

add 2.92 g of NaCl

complete volume to 500 mL with H_2O

Digestion buffer

10 mM Pipes pH 6.8

50 mM NaCl

300 mM sucrose

3 mM $MgCl_2$

1 mM EDTA

0.5 % triton X-100

1.2 mM PMSF

aprotinin 2 μg/mL

leupeptin, 2 μg/mL

pepstatin, 1 μL/mL

6X DNA loading buffer

0.25% (W/V) bromophenol blue

0.25% (W/V) xylene cyanol FF

30% glycerol

2X Laemmli sample buffer

100 mM Tris pH 6.8

200 mM dithiothreitol (DTT)

4% SDS

0.2% bromophenol blue

20% glycerol

LB broth

10 g of tryptone

5 g of yeast extract

10 g of NaCl

complete the volume to1 L with distilled water

Maleic acid buffer

11.61 g of maleic acid

8.77 g of NaCl

H_2O to 1 L, pH 7.5

10X MOPS buffer (DEPC-treated)

25 mL of 1M DEPC-treated sodium acetate

10 mL of 0.5M DEPC-treated EDTA

20.927g of morpholinopropane-sulfonic acid

DEPC-H_2O to 500 mL

1X PBS

8 g NaCl

0.2 g KCl

1.44 g Na_2HPO_4

0.24 g KH_2PO_4

H_2O to 1 L, then adjust pH to 7.4

Resolving gel for SDS-PAGE

10 to 15% acrylamide:bisacrylamide (29:1 ratio)

380 mM Tris pH 8.8

0.1% SDS

0.5 mg/mL APS

0.05% (V/V) TEMED

RNA loading buffer

50% glycerol

1mM EDTA

0.25% bromophenol blue

0.25% xylene cyanol FF

RSB buffer

10 mM NaCl

3 mM $MgCl_2$

10 mM Tris pH 7.5

0.5 mM PMSF

Running buffer for SDS-PAGE

25 mM Tris pH 8.5

0.2 M glycine

5% (V/V) glycerol

0.1% SDS

1X SSC

3M NaCl

0.3M sodium citrate

adjust pH to 7.0

20X SSPE (DEPC-treated)

3.6M NaCl

0.2M NaH_2PO_4

0.02M EDTA pH7.7

Stacking gel for SDS-PAGE

5% acrylamide (W/W)

0.09% bisacrylamide (W/W)

0.1% SDS

145 mM Tris pH 6.8

1 mg/mL ammonium persulfate (APS)

0.05% (V/V) N,N,N',N'-tetramethylethyldiamine (TEMED)

50X TAE

242 g of Tris base

57 mL glacial acetic acid

100 mL of 0.5 M EDTA pH 8.0

complete the volume to a total of 1 L using distilled water

TBS-T

10 mM Tris pH 7.5

0.5% (V/V) Tween 20

150 mM NaCl.

Transfer buffer

800 mL of distilled water

3 g of Tris-Base

14.4 g of glycine

200 mL of methanol

Washing buffer

To 1L of maleic acid buffer, add 3 mL of Tween20